

Investigating a semi-continuous synthetic pathway for the preparation  
of the antiretroviral drugs tenofovir disoproxil and tenofovir  
alafenamide

By

Betty Gabaitsiwe Kwati

Supervisor: Prof. Darren L. Riley

Submitted in partial fulfilment of the requirements for the degree

Master of Science

In the faculty of Natural and Agricultural Sciences

University of Pretoria

Pretoria

(July, 2021)

## ***Declaration***

I, Betty Gabaitsiwe Kwati, declare that the work presented in this dissertation/thesis, which I hereby submit for the degree of Master of Science at the University of Pretoria, Pretoria, is my own work and has not been previously submitted by me for any other degree or examination at this or any other institution.

Signature:.....

Date:.....

## ***Acknowledgements***

The author would like to thank Dr Darren Riley for all of his guidance, support and far-reaching knowledge in the research completed in this thesis/dissertation. The author cannot stress enough how much Dr Darren Riley's patience, compassion and extensive efforts have played a key role in the completion of this thesis/dissertation. The author also wishes to thank Dr Lynne Pilcher for the laboratory space she so generously availed to her and for her moral support and motivation. She also extends her thanks to Dominique Buyens for all the assistance offered in the laboratory and the extensive insight shared on the subject of adenine solubility, and to Ramogale Makuwa for being the best laboratory partner one could ask for. A special thanks to all individuals of the "Riley Group" for all the assistance and support, the unofficial "Africa Group" for all the cultural experiences and all the laughter, and the entire Chemistry Staff from the NMR room all the way down to the GC room.

The author extends a heartfelt thank you to her family and friends, she would not have made it without any of you. To all her CRC family she says thank you (especially to Mel Baloyi who shared the same plight of MSc). To her first true love, Tshediso Keswa, she extends a "massive" thank you for being her true support system through all the tears, doubts, triumphs and restarts. To her beautiful and gentle younger sister, Kgomotso Kwati, she wishes to say thank you for all her support during this life-changing journey. Lastly, to her mother, Neo Kwati, a very heartfelt thank you is extended for all her unwavering support, for never doubting her, for all her patience and for always fighting for her- you're one in a million.

To her God she says: "what a tough journey, I'm not the same as when I started, but I appreciate life more than ever. Thank you for grace, mercy and strength".

It would be amiss for the author to not thank all the sponsors who made this study possible: Pelchem, NRF, University of Pretoria and her employer, the department of chemistry (of the University of Pretoria); Thank you!

## Table of contents

List of figures.....	i
List of schemes.....	iii
List of tables.....	vi
List of abbreviations.....	vii
Abstract.....	x
1. Chapter 1: Human Immunodeficiency Virus (HIV).....	1
1.1) HIV: The statistics.....	1
1.2) HIV: Origin and classification.....	3
1.3) HIV: Transmission and mechanism of infection.....	5
1.4) HIV: Treatment over the years.....	7
1.5) HIV: Treatment (Our focus drugs).....	9
References.....	14
2. Chapter 2: Flow chemistry.....	18
2.1) Chemistry and drug discovery: Room for improvement.....	18
2.2) Flow reactors: Engineering in a chemistry laboratory.....	19
2.3) Immobilized reagents for flow: A match made in "heaven".....	21
2.4) Practical examples of HIV treatment drugs on flow.....	23
Aims and objectives of our project.....	28
References.....	30
3. Chapter 3: Synthesis and isolation of hydroxypropyl adenine (HPA).....	32
The alkylation of adenine: General applications.....	32
A. First step of the synthetic pathway of TD/TA: The alkylation of adenine at the N-9 position.....	33
3.1) Synthesis of HPA: Solubilizing adenine (choosing the right solvent).....	33
3.2a) Synthesis of HPA: The reagents used for the alkylation of adenine to form HPA.....	35
3.2b) Synthesis of HPA: The possible isomers from the alkylation of adenine to form HPA.....	36
3.3a) The experimental alkylation of adenine to form HPA: Assigning the regioisomers of HPA.....	38
3.3b) The experimental alkylation of adenine to form HPA: Regioisomers of HPA in different solvent systems.....	42
B. Post-conversion work-up: Isolation of HPA.....	45
3.4) Triturative work-up and purification.....	45
3.5) Ion-exchange chromatographic work-up and purification.....	46
C. Translation of the alkylation of adenine (step 1) to flow-chemistry.....	50
D. Conclusions on the synthesis and isolation of HPA.....	55
References.....	56
4. Chapter 4: Synthesis of tenofovir.....	58

A. Synthesis and isolation of phosphonate propyl adenine (PPA).....	58
4.1) Previous challenges associated with isolating PPA.....	58
4.2) Validation of the Riley approach.....	60
4.3) Alternative approach to the synthesis of PPA.....	62
4.4) Alternative approach to the isolation of PPA: Resin bound reagent (DESMP).....	67
B. Conclusion for the synthesis of PPA.....	72
C. Hydrolysis of PPA to form the prodrug, tenofovir.....	73
4.5) Literature: The hydrolysis of a dialkyl phosphonate ester to a phosphonic acid.....	73
4.6) Experimental: The hydrolysis of PPA to tenofovir in batch.....	75
D. Conclusion for the synthesis of tenofovir.....	81
References.....	82
5. Chapter 5: The final steps towards the synthesis of TD and TA.....	85
A. Synthesis of prodrug TD.....	86
B. Synthesis of prodrug TA.....	87
C. Final Conclusion towards the synthesis of TD and TA.....	89
References.....	90
6. Chapter 6: Future Work.....	91
6.1) Synthetic Step 1.....	91
6.2) Synthetic Step 2.....	92
6.3) Final synthetic steps.....	95
References.....	96
7. Chapter 7: Experimental descriptions.....	97
General.....	97
Preparation of anhydrous solvents.....	97
Techniques.....	97
Special Instruments.....	97
Spectroscopic data.....	97
Disclaimers.....	97
Experimental for chapter 3: Step 1.....	98
Synthesis of ((R))-9-(2-Hydroxypropyl)adenine (HPA 28).....(Batch).....	98
Synthesis of ((R))-9-(2-Hydroxypropyl)adenine (HPA 28).....(Flow).....	99
Experimental for chapter 4: Step 2a.....	100
Synthesis of ((R))-diethyl (((1-(6-amino-9H-purin-9-yl)propan-2-yl)oxy)methyl)phosphonate (PPA 29) .....(Batch).....	100
Synthesis of Diethyl (tosyloxy) methylphosphonate (DESMP 37).....(Batch).....	100
Synthesis of polymer-supported diethyl (tosyloxy) methylphosphonate (Ps-DESMP, 39).....(Batch).....	101
Synthesis of PPA 29 from Ps-DESMP 39 product.....(Batch).....	102
Synthesis of 9-(((R))-2-(chloromethoxy)propyl)-9H-purin-6-amine (chloromethyl HPA 38) ....(Batch).....	103

Experimental chapter 4: Step 2b .....	103
Synthesis of ((R))-(((Adenin-9-yl)propan-2-oxy)methyl) phosphonic Acid, (PMPA 9) .....	(Batch) ..... 103
Synthesis of ((R))-(((Adenin-9-yl)propan-2-oxy)methyl) phosphonic Acid (PMPA 9) .....	(Flow)..... 104
Experimental for chapter 5: Final steps .....	105
Synthesis of Tenofovir disoproxil (TD 25) .....	(Batch) ..... 105
Synthesis of phenyl hydrogen (((R))-1-(6-amino-9H-purin-9-yl)propan-2-yloxy)methylphosphonate (phenol-PMPA 46) .....	(Batch)..... 106
Synthesis of Tenofovir Alafenamide (TA 26).....	(Batch) ..... 106
APPENDIX A: A summarized collection of the project's NMR spectra .....	108
Experimental chapter 3: Synthesis of HPA .....	108
Experimental chapter 4: Synthesis of PPA.....	109
Experimental chapter 4: Synthesis of tenofovir, PMPA. ....	115
Experimental chapter 5: Synthesis of TD 25.....	116
Experimental chapter 5: Synthesis of phenol-PMPA 46.....	116
Experimental chapter 5: Synthesis of TA 26.....	117

## List of figures

Figure 1.1: Global estimation of people living with HIV reported by World Health Organization (WHO) in 2016. <sup>3</sup> .....	1
Figure 1.2: Global HIV prevalence among adults (15-49 years of age), reported in 2017 by WHO. <sup>3</sup> .....	2
Figure 1.3: HIV prevalence among adults (15-49 years of age) on the African continent, reported by UNAIDS (2016/7). <sup>2</sup> .....	2
Figure 1.4: HIV prevalence statistics in South Africa, reported by UNAIDS (2016/7). <sup>2</sup> .....	3
Figure 1.5: Map with suggested trail of first inter-species infection. <sup>6</sup> .....	3
Figure 1.6: Simplified scheme of how HIV infects a susceptible human cell. <sup>31</sup> .....	6
Figure 1.7: FDA-approved Nucleos(t)ide Reverse Transcriptase Inhibitors (NRTIs) antiretroviral (ARV) drugs from 1987 to 1995.....	7
Figure 1.8: A few of the non-Nucleotide Reverse Transcriptase Inhibitors (NNRTIs) that have been approved by the FDA since 1996.....	8
Figure 1.9: A few of the FDA approved Protease Inhibitors (PIs) from 1995. ....	8
Figure 1.10: Tenofovir.....	10
Figure 1.11: Tenofovir disoproxil fumarate (TDF). ....	10
Figure 1.12: Tenofovir alafenamide fumarate (TAF). ....	11
Figure 1.13: The new FDA-approved Protease Integrase drug, dolutegravir. ....	13
Figure 2.1: Representation of the glass flask over time. <sup>6-8</sup> .....	18
Figure 2.2: A few newspaper articles reporting on pollution in the chemical industry. <sup>12, 19-21</sup> .....	19
Figure 2.3: Standard Uniqsis flow reactor. <sup>23</sup> .....	20
Figure 2.4: Types of immobilization. ....	22
Figure 2.5: General types of continuous flow systems retrieved from Porta et al. <sup>30</sup> .....	23
Figure 3.1: Tautomers of adenine.* .....	32
Figure 3.2: The possible HPA regioisomers: <i>N</i> -9, <i>N</i> -7 and <i>N</i> -3. ....	38
Figure 3.3: Potential target functional groups on HPA, adenine and ( <i>R</i> )-propylene carbonate for resin work-up. .....	46
Figure 3.4: Amberlyst 15® .....	47

Figure 3.5: Flow reactor accessories and consumables clipart. ....	50
Figure 4.1: Proposed coordination of magnesium (II) salts with DESMP, as shown by Riley et al. <sup>4</sup> .....	59
Figure 4.2: Representation of the chloromethylation laboratory set-up.....	66
Figure A1: <sup>1</sup> H NMR spectrum of pure <i>N</i> -9 HPA in DMSO- <i>d</i> <sub>6</sub> . ....	108
Figure A3: <sup>1</sup> H NMR spectrum (aromatic region) of HPA, including allocation of regioisomers. (DMF- reaction solvent and EtOH trituration work-up) in DMSO- <i>d</i> <sub>6</sub> . ....	108
Figure A4: <sup>1</sup> H NMR spectrum (aromatic region) of HPA, including allocation of regioisomers. (reaction solvent - DMSO- and trituration work-up -toluene) in DMSO- <i>d</i> <sub>6</sub> . ....	109
Figure A5: <sup>1</sup> H NMR spectrum of PPA in DMSO- <i>d</i> <sub>6</sub> .....	109
Figure A6: <sup>1</sup> H NMR spectrum of attempt 1 product of chloromethyl HPA in DMSO- <i>d</i> <sub>6</sub> .....	110
Figure A7: <sup>13</sup> C NMR spectrum of HPA in DMSO- <i>d</i> <sub>6</sub> . ....	110
Figure A8: <sup>13</sup> C DEPT 135 NMR spectrum of attempt 1 product of chloromethyl HPA in DMSO- <i>d</i> <sub>6</sub> . ....	111
Figure A9: <sup>1</sup> H NMR spectrum of DMP in DMSO- <i>d</i> <sub>6</sub> . ....	111
Figure A10: <sup>31</sup> P NMR spectrum of DMP in DMSO- <i>d</i> <sub>6</sub> . ....	112
Figure A11: <sup>1</sup> H NMR spectra of DESMP synthesized using Et <sub>3</sub> N, in DMSO- <i>d</i> <sub>6</sub> . ....	112
Figure A12: <sup>1</sup> H NMR spectrum of Ps-TsCl in DMSO- <i>d</i> <sub>6</sub> .....	113
Figure A13: <sup>1</sup> H NMR spectrum of attempt 4 polymer of Ps-DESMP in DMSO- <i>d</i> <sub>6</sub> . ....	113
Figure A14: <sup>31</sup> P NMR spectra of attempt 4 polymer of Ps-DESMP in DMSO- <i>d</i> <sub>6</sub> .....	114
Figure A15: <sup>1</sup> H NMR spectra of attempt 3 polymer of Ps-DESMP in DMSO- <i>d</i> <sub>6</sub> . ....	114
Figure A16: <sup>31</sup> P NMR spectra of attempt 3 polymer of Ps-DESMP in DMSO- <i>d</i> <sub>6</sub> .....	115
Figure A17: <sup>1</sup> H NMR spectrum of tenofovir, PMPA in DMSO- <i>d</i> <sub>6</sub> . ....	115
Figure A18: <sup>1</sup> H NMR spectrum of TD in DMSO- <i>d</i> <sub>6</sub> .....	116
Figure A19: <sup>1</sup> H NMR spectrum of phenol-PMPA in DMSO- <i>d</i> <sub>6</sub> . ....	116
Figure A.20: <sup>1</sup> H NMR spectrum of TA attempt product in DMSO- <i>d</i> <sub>6</sub> . ....	117



## List of schemes

Scheme 1.1: TD and TA are both metabolized to tenofovir-diphosphate, however, TD is first metabolized in the plasma to tenofovir while the complete metabolism of TA occurs in the target cell. ....	12
Scheme 2.1: The flow reactor step for the synthesis of HIV NNRTI, doravirine; a semi-continuous synthetic pathway. Gauthier, D.R. et al reported a retention time of 1-60 seconds. <sup>42</sup> .....	24
Scheme 2.2: The final flow step synthesis of HIV Integrase inhibitor, dolutegravir as reported by Ziegler, (R). et al. The step gave an 89% yield of dolutegravir,ii within 31 minutes. <sup>43</sup> .....	24
Scheme 2.3: A continuous flow synthesis of an $\alpha$ - chloro ketone- a building block of HIV protease inhibitor. An 87% maximum yield reported by Pinho V. et al . <sup>44</sup> .....	26
Scheme 2.4: A summary of the synthetic pathway of adenine to prodrugs TD and TA. ....	28
Scheme 3.1: A generic example of the alkylation of adenine to afford <i>N</i> -9-alkylated adenine. X is a halide leaving group. ....	33
Scheme 3.2: Initial step of the synthetic pathway of both TD /TA (formation of HPA via the alkylation of adenine).....	33
Scheme 3.3: S <sub>N</sub> 2 mechanism involved in the alkylation of adenine with ( <i>R</i> )-propylene carbonate, using catalytic amounts of base ( <sup>-</sup> OH). ....	35
Scheme 3.4: Isomerization of the <i>N</i> 10- adenine anion to <i>N</i> -9- adenine anion. <sup>28</sup> .....	37
Scheme 3.5: Illustration of the possible resonance structures of <i>N</i> -9 HPA.....	41
Scheme 3.6: Illustration of the possible resonance structures of <i>N</i> -3 HPA.....	41
Scheme 3.7: Illustration of the possible resonance structures of <i>N</i> -7 HPA.....	42
Scheme 3.8: Amberlyst 15®and HPA interactions on a molecular level. ....	47
Scheme 3.9: A simplified representation of the flow reactor set-up for the synthesis of HPA* .....	51
Scheme 3.10: A representation of the flow reactor set-up with an added glass chip. ....	52
Scheme 3.11: A representation of the flow reactor set-up with an added glass chip and packed-bed reactor containing Amberlyst 15®. ....	53
Scheme 3.12: The final flow system set-up for the synthesis of HPA using anhydrous DMSO as a solvent. ....	54
Scheme 4.1: Addition of the phosphonate ester to HPA and the hydrolysis thereof to form tenofovir. ....	58
Scheme 4.2: Proposed reaction mechanism for the formation of PPA from HPA.....	59

Scheme 4.3: Formation of PPA from HPA using the Grignard and <sup>t</sup> BuOH. ....	60
Scheme 4.4: The work-up process for the isolation of PPA from the magnesium salt cake. ....	61
Scheme 4.5: An alternative retrospective approach to the synthesis of PPA. ....	62
Scheme 4.6: A generic representation of an Arbuzov reaction.....	62
Scheme 4.7: Mechanistic synthesis of PPA from chloromethyl HPA via the Arbuzov route. ....	63
Scheme 4.8: Proposed reaction for the chloromethylation of HPA to form chloromethyl HPA. ....	64
Scheme 4.9: The mechanistic chloromethylation of HPA to form chloromethyl HPA. ....	64
Scheme 4.10: Proposed synthesis of PPA using polymer-supported DESMP. ....	67
Scheme 4.11: Formation of DESMP from TsCl in the presence of a base. ....	68
Scheme 4.12: Reaction mechanism for the tosylation of DMP to form DESMP in the presence of a base. ....	69
Scheme 4.13: Hydrolysis of the phosphonate esters of to form tenofovir. ....	73
Scheme 4.14: The Mechanism of the hydrolysis of phosphonate ester of PPA, using TMSX. X represents a halide. ....	74
Scheme 4.15: Flow set-up for trials attempting to convert PPA to PMPA; with PPA and TMSCl intercepting at the T-piece and mixing at the mixing chip. ....	76
Scheme 4.16: Flow set-up for trials attempting to convert PPA to tenofovir; with PPA and TMSCl pre-mixed before entering the flow system.....	78
Scheme 4.17: Flow set-up for trials attempting to convert PPA to tenofovir; with PPA and TMSCl pre-mixed before entering the flow system and flowing through a column bed of NaBr.....	79
Scheme 5.1: Translation of tenofovir to ARV drugs, TD and TA. ....	85
Scheme 5.2: Synthesis of TDF from tenofovir. ....	86
Scheme 5.3: Synthesis of TAF from tenofovir. ....	87
Scheme 5.4: Summary of the synthetic pathway for the synthesis of TD and TA. ....	89
Scheme 6.1: Proposed in-line work-up with Amberlyst 15® in glass column fitted with alternative, DMSO-compatible material, fittings.....	91
Scheme 6.2: Proposed employment of the flow synthesis of ( <i>R</i> )-propylene carbonate using Suveges et al <sup>1</sup> method to our flow synthesis of HPA, including our proposed in-line workup. ....	92
Scheme 6.3: A simplified representation of a flow set-up for the synthesis of Ps-DESMP from Ps-TsCl and conversion of HPA to PPA with a spectroscopy detector included. ....	93

Scheme 6.4: Summary of a prospective synthetic pathway for the synthesis of TA and TD, with continuous flow reaching the up to the synthesis of tenofovir.....94

Scheme 6.5: Summary of a prospective fully continuous (at least 5 stages) synthetic pathway for the synthesis of TA and TD.....95

## List of tables

Table 3.1: Yields obtained for HPA in the different solvent systems.....	37
Table 3.2: <sup>1</sup> H NMR spectrum chemical shifts (ppm) of HPA from the respective literature sources.....	39
Table 3.3: Trituration work-up yields of HPA with the different reaction solvents.....	45
Table 3.4: Summary of the yields and regioisomer distribution of HPA when using a tritulative vs. ion exchange work-up and purification. ....	48
Table 3.5: The main flow parameters used for the initial flow trials.....	51
Table 3.6: Flow parameters used with addition of a mixing chip to the system.....	53
Table 4.1: The reaction parameters used for the halide methylation of HPA.....	65
Table 4.2: Reaction parameters used in the trials of formation of Ps-DESMP from Ps-TsCl.....	70
Table 4.3: Reagents used for the hydrolysis of PPA to tenofovir, performed under pressure.....	75
Table 4.4: Parameters used for the trials performed under flow as shown in scheme 4.15, in attempt to convert PPA to tenofovir, using both a mixing chip and coil reactor. ....	77
Table 4.5: Parameters used for the trials performed under flow in attempt to convert PPA to tenofovir, using both a column and coil reactor. ....	79

## *List of abbreviations*

<b>3TC</b>	Lamivudine
<b>AIDS</b>	Acquired Immunodeficiency Syndrome
<b>ARV</b>	Antiretroviral
<b>AZT</b>	Azidothymidine
<b>BPR</b>	Back Pressure Regulator
<b>CDI</b>	1,1'-Carbonyldiimidazole
<b>CMIC</b>	Chloromethyl isopropylcarbonate
<b>d4T</b>	Stavudine
<b>d<sub>6</sub>-DMSO</b>	Deuterated Dimethyl Sulfoxide
<b>DABU</b>	1,4-diazabicyclo[2,2,2]octane
<b>DCC</b>	Dicyclohexyl Carbodiimide
<b>DCM</b>	Dichloromethane
<b>ddC</b>	Zalcitabine
<b>ddI</b>	Didanosine
<b>DESMP</b>	Diethyl (tosyloxy) Methylphosphonate
<b>DMAP</b>	4-Dimethylaminopyridine
<b>DMF</b>	Dimethylformamide
<b>DMP</b>	Diethyl (hydroxymethyl) Phosphonate
<b>DMSO</b>	Dimethyl Sulfoxide
<b>DNA</b>	Deoxyribonucleic Acid
<b>FDA</b>	Food and Drug Administration
<b>FTIR</b>	Fourier-transform Infrared
<b>GC</b>	Gas Chromatography
<b>HAART</b>	Highly Active Antiretroviral Therapy
<b>HBV</b>	Hepatitis B
<b>HIV</b>	Human Immunodeficiency Virus
<b>HMBC</b>	Heteronuclear Multiple Bond Correlation
<b>HPA</b>	Hydroxypropyl Adenine / ((R))-9-(2-Hydroxypropyl)adenine
<b>HPLC</b>	High Performance Liquid Chromatography
<b>HT</b>	High Temperature
<b>HTLV</b>	Human T-Lymphotropic Virus
<b>HTS</b>	High-Throughput Screening

<b>IR</b>	Infrared
<b>LC</b>	Liquid Chromatography
<b>mRNA</b>	Messenger Ribonucleic Acid
<b>MTB</b>	Magnesium <i>tert</i> -Butoxide
<b>NMP</b>	<i>N</i> -Methyl-2-Pyrrolidone
<b>NMR</b>	Nuclear Magnetic Resonance
<b>NNRTI</b>	Non-Nucleoside Reverse Transcriptase Inhibitor
<b>NRTI</b>	Nucleoside Reverse Transcriptase Inhibitor
<b>PDE</b>	Phosphodiesterase
<b>PEEK</b>	Polyether Ether Ketone
<b>phenol-PMPA</b>	Phenol tenofovir
<b>PI</b>	Protease Inhibitor
<b>PMPA</b>	Tenofovir
<b>PPA</b>	Phosphonatepropyl Adenine
<b>PrEP</b>	Pre-Exposure Prophylaxis
<b>Ps</b>	Polymer-supported
<b>PTFE</b>	Polytetrafluoroethylene
<b>RBF</b>	Round-bottom Flask
<b>RM</b>	Reaction Mixture
<b>RNA</b>	Ribonucleic Acid
<b>RT</b>	Room Temperature
<b>SIV</b>	Simian Virus
<b>STI</b>	Sexually Transmitted Infection
<b>TA</b>	Tenofovir Alafenamide
<b>TAC</b>	Treatment Action Campaign
<b>TAF</b>	Tenofovir Alafenamide Fumarate
<b>TB</b>	Tuberculosis
<b>TD</b>	Tenofovir Disoproxil
<b>TDF</b>	Tenofovir Disoproxil Fumarate
<b>THF</b>	Tetrahydrofuran
<b>TLC</b>	Thin Layer Chromatography
<b>TMS</b>	Trimethylsilyl
<b>TMSBr</b>	Trimethylsilyl Bromide
<b>TMSCI</b>	Trimethylsilyl Chloride

<b>UN</b>	United Nations
<b>UV</b>	Ultraviolet
<b>ZDV</b>	Zidovudine

## *Abstract*

This dissertation details the investigation of the synthetic pathway of the antiretroviral drug, tenofovir, and its prodrug forms tenofovir disoproxil and tenofovir alafenamide, in attempt to develop a more efficient route by exploring both batch and flow-chemistry avenues for each synthetic step.

The initial step of the synthesis was an *N*-9 alkylation of adenine which, due to its solubility challenges, limited our reaction solvent options to only polar aprotic solvents (dimethylformamide, dimethyl sulfoxide and *N*-methyl-2-pyrrolidone) under basic conditions. The results showed that the presence of water in the solvent system produced both *N*-9 hydroxypropyl adenine and minor hydroxypropyl adenine regioisomers (*N*-7 and *N*-3).

Hydroxypropyl adenine was isolated in one of two ways: trituration or newly implemented “catch-and-release” resin work-up. Trituration with ethanol or a mixture of <sup>1</sup>propanol/methanol (1:1) produced the purest product while the ion-exchange work-up with Amberlyst 15<sup>®</sup> resin gave the highest yields and required less solvent.

The translation of step 1 to a flow reactor required an addition of a glass mixing chip and a steel coil as accessories before we could obtain any conversion of adenine to hydroxypropyl adenine. The conversion to hydroxypropyl adenine was 50% faster than that obtained in batch, however, we were unable to pursue an in-line resin work-up because the glass Omnifit<sup>™</sup> column accessory was incompatible with our reaction solvent, dimethyl sulfoxide.

The second step of the synthetic pathway was split into two sub-steps: a) the addition of a phosphonate ester to produce phosphonatepropyl adenine and b) the hydrolysis of the ester, producing active antiretroviral drug tenofovir. We managed to successfully synthesize and isolate phosphonatepropyl adenine by replicating the method employed by Riley *et al.* This method was particularly problematic in terms of its work-up because of the sticky salt cake that made it difficult to extract our product. We, therefore, attempted to solve the problem in one of two ways: i) an alternative synthetic route for the synthesis of phosphonatepropyl adenine which involved an Arbuzov reaction. We were unsuccessful in this approach and so moved on in attempt to ii) develop a polymer-supported reagent (Polymer-supported diethyl (tosyloxy) methyl phosphonate) that we believed would allow us to isolate phosphonatepropyl adenine from the sticky cake while trapping the troublesome magnesium salts on the spent solid support. The results on the formation of polymer-supported diethyl (tosyloxy) methylphosphonate were inconclusive, leaving step 2a as a batch reaction.



Step 2b involved hydrolysis of the phosphate ester using classical reagents, trimethylsilyl bromide and trimethylsilyl chloride under high pressure in order to produce the phosphonic acid. The reaction worked best with trimethylsilyl bromide but the cost effective alternative trimethylsilyl chloride produced satisfactory results, especially in the presence of NaBr. This step, although unoptimized, was successfully translated to flow with the addition of a glass Omnifit™ column and coil reactor accessories.

The final steps of the synthetic pathway diverged into the synthesis of prodrugs tenofovir disoproxil and tenofovir alafenamide. Alkylative esterification of tenofovir (using chloromethyl isopropylcarbonate) successfully afforded tenofovir disoproxil using the batch method reported by Ripin *et al.*

The synthesis of tenofovir alafenamide was more challenging, requiring two separate steps as reported by Chapman *et al.*: the first being esterification of tenofovir using phenol to afford phenol-tenofovir, and the second was the addition of isopropyl L-alanine to form tenofovir alafenamide. We successfully synthesized phenol-tenofovir in batch but unfortunately were unsuccessful in the synthesis of tenofovir alafenamide.

In entirety we managed to establish a semi-continuous synthetic pathway for the synthesis of antiretroviral active drug, tenofovir and its prodrug tenofovir disoproxil as well as precursor to tenofovir alafenamide, phenol-tenofovir. This success provides a useful stepping stone towards future research for a proficient and elegant pathway for the synthesis of antiretroviral prodrugs tenofovir disoproxil and tenofovir alafenamide which might include coupling of an already-existing flow synthesis of essential reagent, (*R*)-propylene carbonate.

# *Introductory Chapters*

*HIV Treatment and Flow Chemistry*

# Chapter 1: Human Immunodeficiency Virus (HIV).

## 1.1) HIV: The statistics

In 1981 the first case of Human Immunodeficiency Virus (HIV) was reported in the United States of America<sup>1</sup>. Thirty-five years later in 2016, more than 77 million people had been infected by the virus and an estimated 35 million had died worldwide as a consequence of the virus, bearing in mind that this only reflects the reported cases<sup>2</sup>. In 2016 it was reported that the world sits with at least 36.7 million people, of the 7 billion population, living with HIV<sup>3</sup> (figure 1.1).

### Global estimates by WHO region

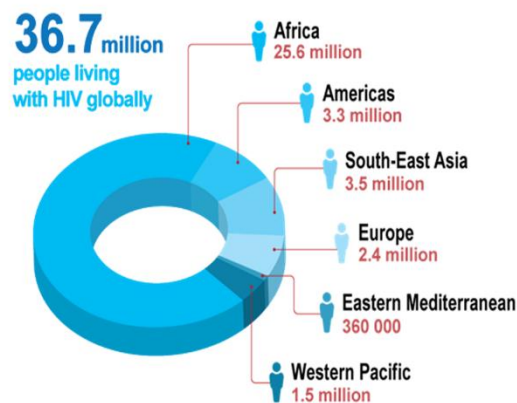


Figure 1.1: Global estimation of people living with HIV reported by World Health Organization (WHO) in 2016.<sup>3</sup>

Statistics show Africa to be the continent having suffered the most devastating impact from the HIV and AIDS epidemic, accounting for almost 70% of the global estimate of people living with HIV (figure 1.2).

In 2000, the then Secretary General of the United Nations (UN), Kofi Annan, made a statement mentioning the devastating effects AIDS was having on the African continent on a social, political and economic level. He mentioned that more people had died of AIDS in the “past year” (1999-2000) in Africa, than in all the wars on the continent,<sup>4</sup> giving context of a grim reality that had hit Africa.

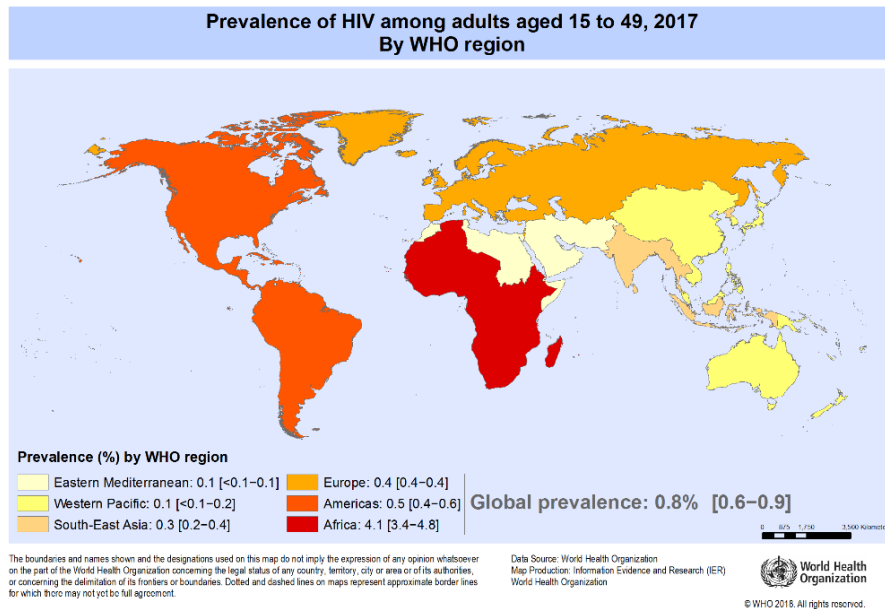


Figure 1.2: Global HIV prevalence among adults (15-49 years of age), reported in 2017 by WHO.<sup>3</sup>

Sub-Saharan Africa was recorded as the region worst affected by the virus in 2016 (figure 1.2; 1.3), with statistics showing that it contributed roughly 51% to the 36.7 million living with HIV globally.<sup>3</sup>

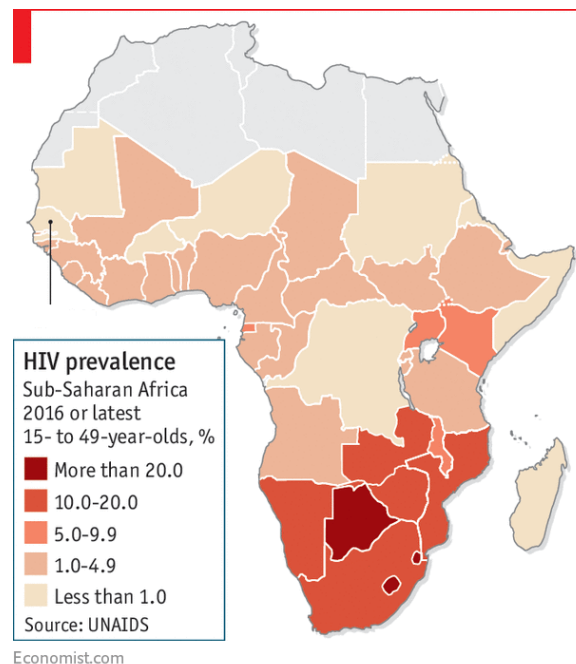


Figure 1.3: HIV prevalence among adults (15-49 years of age) on the African continent, reported by UNAIDS (2016/7).<sup>2</sup>

South Africa in particular has one of the highest prevalence rates of HIV positive individuals on the continent, having 18.9% adult prevalence (figure 1.4) in its population reported in 2016 and Swaziland having the highest prevalence at 28%.<sup>2,5</sup>

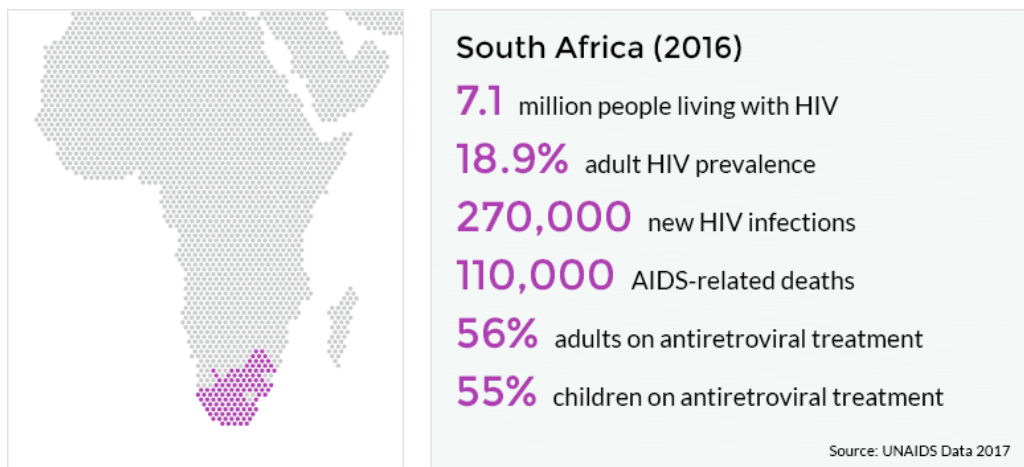


Figure 1.4: HIV prevalence statistics in South Africa, reported by UNAIDS (2016/7).<sup>2</sup>

## 1.2) HIV: Origin and classification

Researchers report that HIV originated in Central Africa in the Democratic Republic of Congo (figure 1.5), specifically in its capital, Kinshasa, in the early twentieth century, 1920.<sup>6</sup>

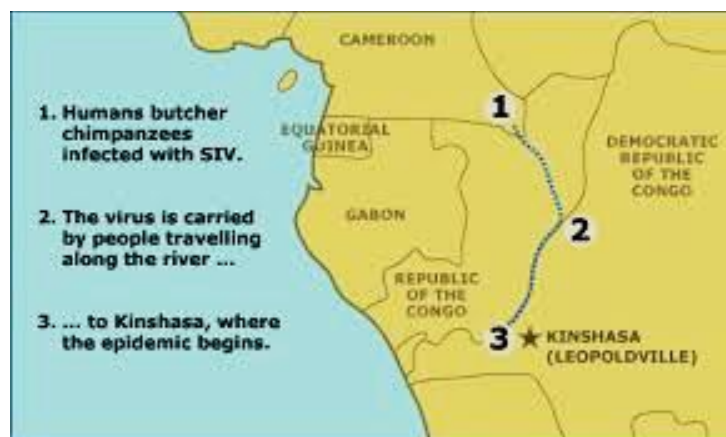


Figure 1.5: Map with suggested trail of first inter-species infection.<sup>6</sup>

It was only in 1981, however, that an Acquired Immune Deficiency Syndrome (AIDS) was recognized when an increasing number of American males “succumbed to unusual opportunistic infections and rare malignancies” such as pneumonia and Kaposi sarcoma (a type of cancer).<sup>5,7</sup> It came to light that the underlying cause of these infections was a result of the inefficiency of the body’s defence system to prevent infection from otherwise common pathogens that it was exposed to. Although a weak

defence system was not unprecedented, AIDS was unique in a sense that it affected a particular group of men (homosexuals), indicating that it was infectious, and also because it had resulted in a 100% mortality rate.<sup>8</sup> Not long after this it was discovered that blood transfusion recipients, haemophiliacs, drug-injecting individuals as well as individuals involved in heterosexual intercourse were also susceptible to infection. European countries also reported cases of AIDS and Uganda reported a few cases of a disease called “slim” which it described as a “fatal wasting disease” (with symptoms like weight loss, diarrhoea and eventual death, which are strongly associated with HIV) and in 1982 South Africa reported its first case of HIV.<sup>9,10</sup>

In the year of 1983, the AIDS causing agent was isolated<sup>11</sup> and surprisingly bore similar features to an already known virus, the T-cell leukemia virus (HTLV-I and HTLV-II).<sup>12</sup> Closer evaluation of this AIDS virus revealed that it had close genetic similarities to retroviruses that caused multiple chronic infections in animals (e.g. maedi-visna in sheep) and are collectively called lentiviruses. This AIDS virus was then coined as the Human Immunodeficiency Virus (HIV) in the year 1986 by the International Committee on the Taxonomy of viruses, because of its detrimental effect on the human immune defence system.<sup>13</sup>

HIV is believed to be a result of cross-species transmission between humans and primates and two main strains of the virus exist, HIV-1 and HIV-2. The predominant strain is HIV-1, which is responsible for the epidemic, while HIV-2 is found in a small group of individuals in West Africa, or of Western African origin.<sup>5,6</sup> Interestingly, HIV-1 and HIV-2 strains were found to have a highly significant phylogenetic distance between them and more closely related to simian viruses (SIVs) that caused immunodeficiency in different primates. HIV-1 was found to closely relate to a SIV found in chimpanzees (SIV<sub>cpz</sub>) and HIV-2 to an SIV found in sooty mangabeys (SIV<sub>smm</sub>), confirming the suspicion that HIV was a consequence of cross-species infections. Knowledge as to exactly when and how the virus crossed over is still a matter of speculation.<sup>5,6</sup>

After isolation of HIV-1, it was later discovered that the strain comprises four different lineages: M, N, O and P. The main group, group M, is the one responsible for the pandemic form of HIV-1 and has been discovered worldwide. Group M is further classified into different clades (subtypes) that phylogenetically associate with one other, i.e. A<sub>1</sub>, A<sub>2</sub>, B, C, D, F<sub>1</sub>, F<sub>2</sub>, G, H and K.<sup>14</sup> Group O (“outlier” group) is the second most prevalent form and has been found in individuals from West Africa together with Group N which is less prevalent.<sup>14</sup> The least prevalent group is P, which has only been found in 2009 in one individual from Cameroon, living in France.<sup>6</sup> In 1986, a different genomic strain of HIV was identified and named HIV-2 to differentiate it from the first isolate, HIV-1, and it has been found to be less infectious than HIV-1, with patients able to suppress it better than those infected with HIV-1. Research has shown that patients with HIV-2 tend to live longer without treatment (with progress to

AIDS extremely rare) and the rate of spread is much lower than with HIV-1. From here onwards HIV-1 will be referred to as HIV, unless stated otherwise.<sup>5,14,15</sup>

### **1.3) HIV: Transmission and mechanism of infection**

Transmission of the retrovirus requires bodily contact with an infected individual via sexual contact across mucosal surfaces, by maternal-infant exposure, and by percutaneous inoculation.<sup>16</sup> In laymen terms, transmission can occur through unprotected sex, any form of blood exchange; injection, mother-to-unborn child and breast feeding. This does not include saliva, sweat and/or tears because the concentration of the virus in these fluids is minimal.<sup>17,18</sup> There are extremely rare cases of individuals who have been exposed to the virus but maintain high CD4<sup>+</sup> cell count and low viral load in the absence of treatment, referred to as “elite controllers”.<sup>19</sup> The mechanism behind this phenomenon is not yet understood and it thought to be a potential door towards an HIV/AIDS cure and eradication. HIV/AIDS suppresses the immune system of an individual and so infected patients are vulnerable to other diseases.<sup>17</sup> In South Africa, other sexually transmitted infections (STIs) and tuberculosis (TB) are common co-infections in people living with HIV/AIDS and many programmes have been developed to manage these diseases both individually and in combination with the virus.<sup>20,21</sup>

As with most concepts/theories/models etc., there were some scientists and authorities who were opposing the notion that HIV is the causative agent of AIDS in its early discovery stages. Unfortunately, this was the case with the then President of South Africa, Thabo Mbeki, who together with his entourage of scientists and advisers, claimed adamantly that HIV was *not* the causative agent of AIDS.<sup>22</sup> This caused a huge perturbation globally as many established scientists claimed that there wasn't strong scientific basis for that claim. Needless to say, because of this many lives in South Africa were lost from the year 2000 to 2005 because no antiretroviral (ARV) treatment was offered to HIV infected individuals. It is estimated that over 300'000 lives were lost that could likely have been saved had the government allowed for the necessary treatment.<sup>22-24</sup> In 2002 the Treatment Action Campaign (TAC) won a case against the state to allow antiretroviral (ARV) treatment for pregnant women and also wanted the then Minister of Health, Manto Tshabalala-Msimang and former state President, Thabo Mbeki to account for for all the HIV/AIDS-related deaths from the years 1998 to 2008 before a commission of enquiry.<sup>25</sup> Much more evidence to support the notion that HIV is a causative agent of AIDS has emerged throughout the years and so has a better understanding of the virus and its mode of action.

The HI virus is simple in structure, containing only proteins necessary for invasion, replication and repetition. Its outer core consists of proteins that allow it to recognize and bind to host cells, assisting as an entry pass into the cell.<sup>14</sup> The inner core, the most important layer, consists of a reverse

transcriptase enzyme which enables the virus to transcribe its RNA into DNA (the reverse of the natural process of DNA being transcribed into RNA, hence the name “retrovirus”). It also has the integrase and protease enzymes, which assist in inserting the viral DNA into the host DNA and cleaves proteins to form fully functional virions, respectively.<sup>14,19</sup>

Once the retrovirus enters the body, it targets host cells that bear CD4+ receptors such as T-lymphocytes and macrophages. HIV binds to the CD4+ receptors (or the co-receptors; chemokine-receptors such as CCR<sub>5</sub> and CXCR<sub>4</sub>) on the cell membrane via gp120 protein found on its outer layer, resulting in a fusion between the HIV envelope and the host cell membrane, allowing the virus entry into the cell.<sup>14</sup> The virus then sheds its protein coat upon entry, activating its reverse transcriptase enzyme to transcribe its RNA into complementary DNA, which is integrated into the host’s DNA by the integrase to form a “provirus”. The provirus is transcribed into mRNA which eventually steer the synthesis of viral proteins. The viral proteins assemble and eventually bud out of the cell and the protease enzyme releases a mature virion which can infect the next host cell to repeat the cycle. The fatality of the virus is that it causes the body’s T-cells (both infected and uninfected) to self destruct, via apoptosis.<sup>26–28</sup> The T-cells form part of the body’s white blood cells which are essential for the defence of the host from foreign antigens, and their destruction makes the body vulnerable to all types of diseases.<sup>29,30</sup> Drugs targeting each step of the HI viral infection (figure 1.6) have since been developed.<sup>31</sup>

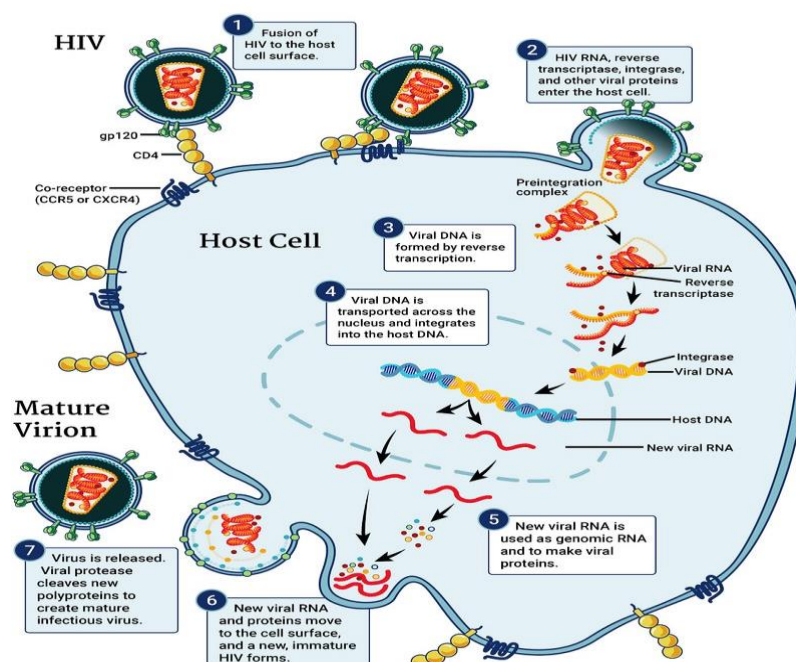


Figure 1.6: Simplified scheme of how HIV infects a susceptible human cell.<sup>31</sup>



#### 1.4) HIV: Treatment over the years

It has been over three decades and a cure to HIV and AIDS has not yet been found, however, this is not to take away from the extensive progress in the treatment of the disease since its inception. By 1987, a drug that acted as a direct nucleoside reverse transcriptase inhibitor (NRTI), azidothymidine (AZT) later known as zidovudine (ZDV) **1** (figure 1.7), was approved as treatment for patients with advanced HIV, despite having short lived benefits and multiple side effects.<sup>32,33</sup> Three more NRTIs were approved from 1991 to 1994 which had their own toxicities, and the effects could not be improved by having the patients alternate between the therapies. In pursuit of a solution, combinatory therapy was attempted with ZDV taken with one of the other NRTIs, zalcitabine (ddC) **2** or didanosine (ddI) **3** (figure 1.7), however, the benefits were short lived as the tolerability and safety factors were low even though there was an improvement in the CD4<sup>+</sup> lymphocyte count.<sup>19,34</sup>

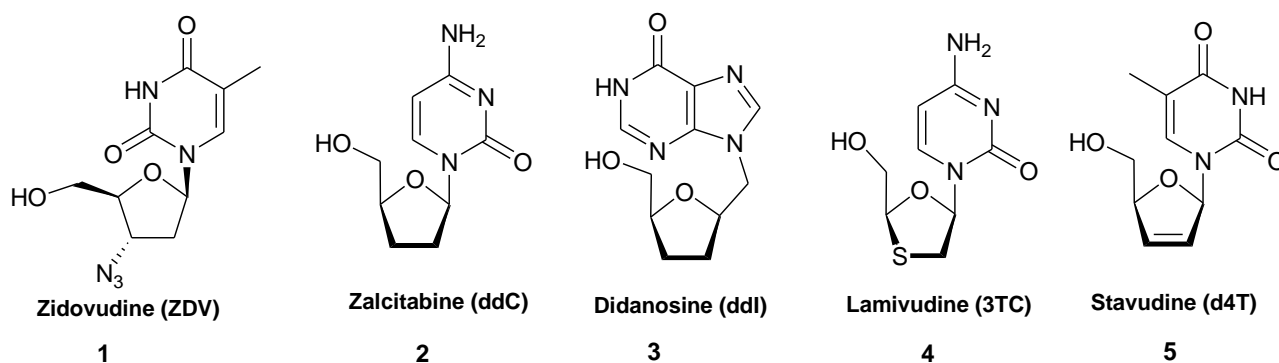


Figure 1.7: FDA-approved Nucleos(t)ide Reverse Transcriptase Inhibitors (NRTIs) antiretroviral (ARV) drugs from 1987 to 1995.

In 1994 a new NRTI cytidine analogue drug, lamivudine (3TC) **4** (figure 1.7), was approved by the FDA (Food and Drug Administration) after most thymidine analogue drugs were rejected because of their high toxicity levels. Monotherapy had been written off as ineffective, resulting in rapid drug resistance and short-lived benefits, and so 3TC **4** was administered with either ZDV **1** or stavudine (d4T) **5** (figure 1.7), together with a third drug, to effectively stabilize the infection.<sup>35</sup>

ARV treatment had not yet reached a satisfactory level of effectiveness until the emergence of new classes of drugs, non-nucleoside reverse transcriptase (NNRTI) (figure 1.8) and protease inhibitors (PI) (figure 1.9).

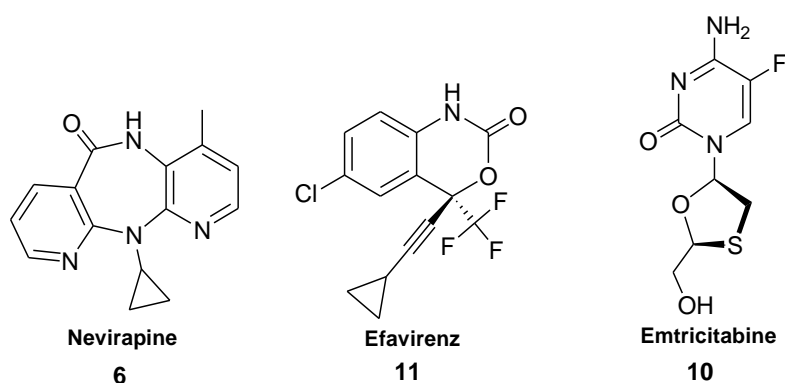


Figure 1.8: A few of the non-Nucleotide Reverse Transcriptase Inhibitors (NNRTIs) that have been approved by the FDA since 1996.

The first NNRTI drug to be approved by the FDA was nevirapine **6** (figure 1.8) in 1996 and it is still used across most of the globe today. Saquinavir **7** (figure 1.9) was the first PI to be approved by the FDA in 1995, but its effectiveness could not overcome its poor tolerability and was replaced by a PI released to the market in 1996, indinavir **8** (figure 1.9).<sup>34</sup>

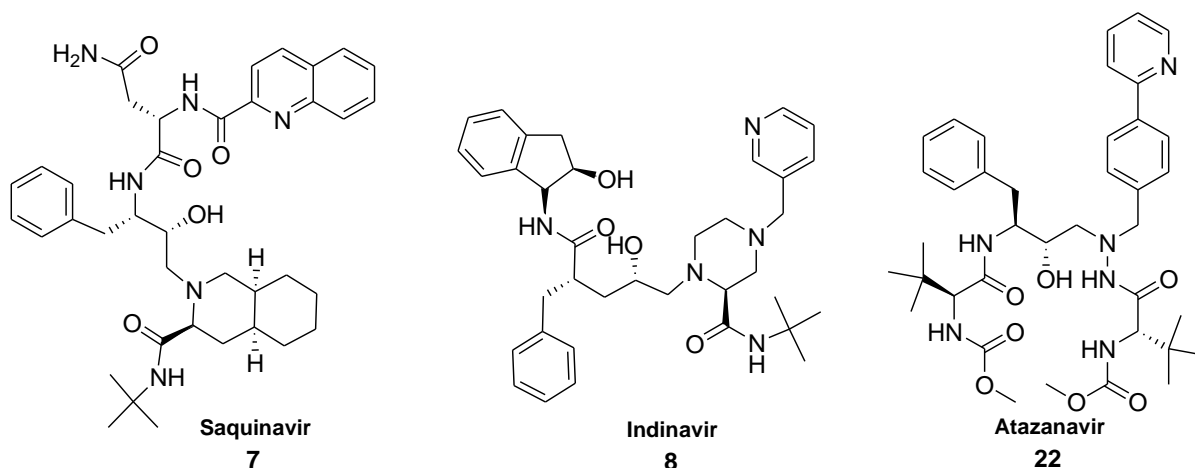


Figure 1.9: A few of the FDA approved Protease Inhibitors (PIs) from 1995.

Indinavir **8** had a quick entry into the market because of the huge success of the clinical trials which had the patients on a triple combination therapy with ZDV **1**, lamivudine **4** and indinavir **8**. The study showed a huge suppression of the viral load in the patients both during the study and beyond.<sup>36</sup> There was unfortunately a substantial disadvantage to this treatment because indinavir **8** required being taken three times daily without any food and had quite severe side effects as well as a complex

synthetic route. For these reasons, the use of indinavir **8** has reduced over recent years and new PIs (e.g. ritonavir in 1996) have overtaken it in the market.

A breakthrough was reached with the introduction of these new classes of drugs and the use of triple-combination therapy, bringing about a highly active antiretroviral therapy (HAART) in 1995 (the same year United Nations programme of AIDS, UNAIDS was created) that would help move HIV from a terminal disease into a manageable chronic illness.<sup>37</sup> The typical HAART regimen comprises of taking three different ARV drugs daily and the reason it is effective is because it reduces the risk of drug-resistance and decreases the mortality and morbidity rates of HIV-infected individuals.<sup>37</sup>

The therapy has seen improvement since its inception in 1996, with new approved drugs reducing the severity of the side effects of the treatment (figure 1.9). Some studies attempted to introduce a fourth drug to the dosage but found that it resulted in increased toxic effects rather than therapeutic effect.<sup>34</sup> The next big question of the treatment was “when to start the treatment”. The uncertainty of early treatment was initiated in the first trials of an ARV, where ZDV **1** was given to patients either immediately or deferred.<sup>38</sup> The results showed no difference in the two groups, as the immediate group showed no superior advantage to the group that had deferred treatment, and in fact it seemed as though the immediate group was at a disadvantage because it was more likely to become resistant to the drug. After years of polarized opinions, only in 2015 was there enough evidence collected to safely conclude that immediate treatment is the best option for better viral control and that all patients living with HIV should receive ARV treatment. South Africa effectively started following these guidelines from September 2016.<sup>39</sup>

### **1.5) HIV: Treatment (Our focus drugs)**

In the 21<sup>st</sup> century, more advances were made in both the drug design and drug classes and there are currently twenty-eight FDA approved ARV drugs on the market. Recently, there have been improvements in the therapy, with two and four drug dosage regimens also underway.

Tenofovir **9** (figure 1.10), a NRTI, made its way into the market in 2001, after a long period since its pharmacological discovery in 1993,<sup>19,34</sup> which was delayed because a suitable prodrug was challenging to find. It has replaced thymidine analogues, and has not been superseded by any other NRTI until present.

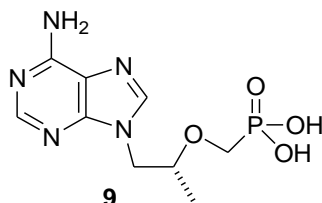


Figure 1.10: Tenofovir.

Tenofovir **9** has been recognized as a major player,<sup>31,40</sup> in both combination ARV treatment and pre-exposure prophylaxis (PrEP).<sup>40</sup> WHO treatment guidelines suggested in 2015 that as a first line treatment, adult patients should take NRTI tenofovir **9** in combination with lamivudine **4**/emtricitabine **10** and a NNRTI efavirenz **11** (figure 1.8).

The first-generation prodrug of tenofovir **9** approved in 2001 was tenofovir disoproxil fumarate **12** (TDF) (figure 1.11) which is metabolized into tenofovir **9** in the plasma after oral consumption before being distributed intracellularly.

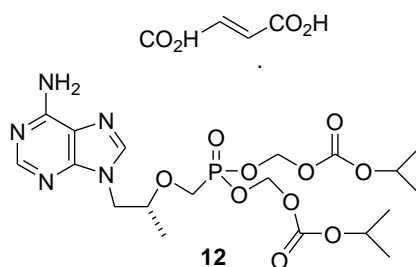


Figure 1.11: Tenofovir disoproxil fumarate (TDF).

TDF **12** has quite a few challenging side effects, despite its favourable safety and tolerability, such as renal failure, reduced bone mineral density and tubular wasting syndrome.<sup>31</sup> Seeing that ARV treatment is currently a lifetime-treatment plan it is crucial that the drugs taken don't only have a high efficacy but that they also have a reduced pill burden and a long term adherence factor to them. For these reasons, next generation drugs have been looked at for tenofovir **9**, to obtain a prodrug that might reduce the side effects (especially its nephrotoxicity) without having a major change in the efficacy of the NRTI drug on disease control.

An alternative analogue (adenosine /adenine 5' monophosphate analogue) of TDF **12**, tenofovir alafenamide fumarate **13** (TAF) (figure 1.12) received FDA approval in 2011. Studies performed in human clinical trials have indicated that there is a relationship between tenofovir **9** levels in the plasma and renal toxicity.<sup>41</sup> Unlike TDF **12**, TAF **13** is metabolized to tenofovir **9** intracellularly because it is stable in plasma and this results in about 90% reduction in tenofovir **9** levels compared to TDF.<sup>42</sup>

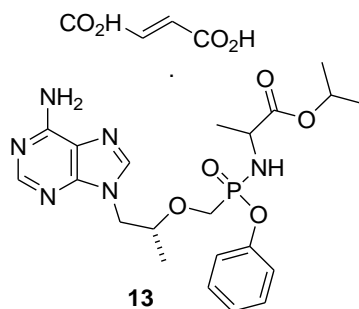
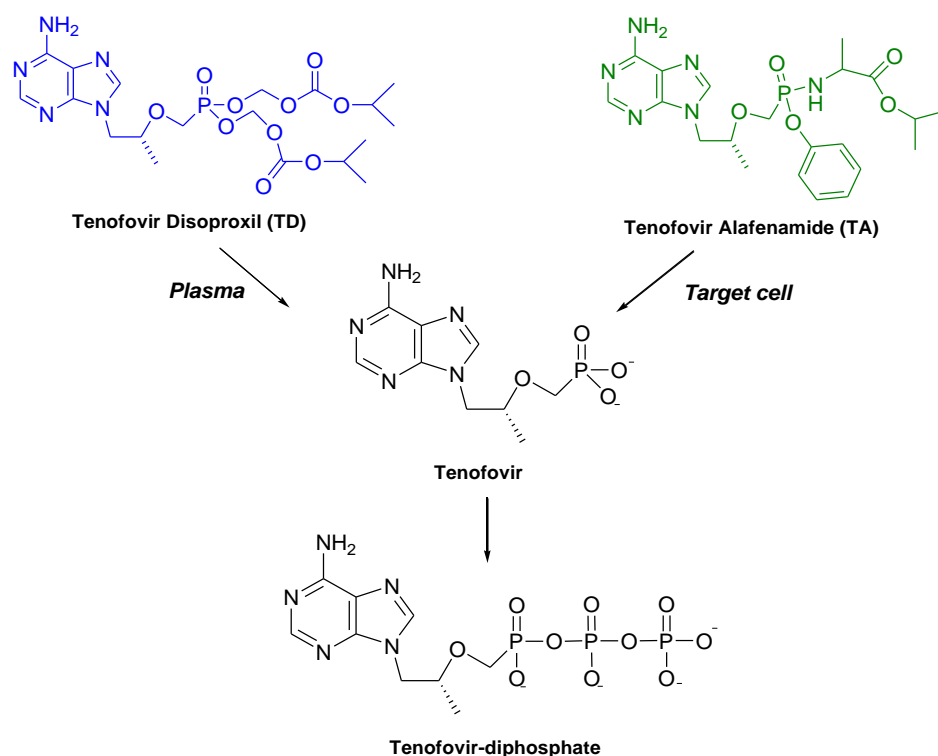


Figure 1.12: Tenofovir alafenamide fumarate (TAF).

This reduction in the off-target tissue distribution/exposure, may be the cause of the reduction of nephrotoxicity and bone density effects in patients that are on TAF **13** as opposed to TDF **12**.

Another advantage of TAF **13** is that the intracellular metabolism results in higher concentrations of tenofovir **9** intracellularly relative to TDF **12** (scheme 1.1), permitting a much lower dose of TAF **13** for the same efficiency of TDF **12** (300 mg TDF vs. 25 mg TAF).<sup>42,43</sup> These advantages apply to both patients who take TAF **13** as their first-line treatment and those patients who are already on a TDF-based treatment but switch to a TAF-based one.



*Scheme 1.1: TD and TA are both metabolized to tenofovir-diphosphate, however, TD is first metabolized in the plasma to tenofovir while the complete metabolism of TA occurs in the target cell.*

Although HAART has been very effective, reducing the number of HIV-related deaths by about 60% globally, the treatment has been costly and demand continues to increase because the treatment has seen a surge in the survival rates of HIV-infected individuals and so the number of people living with the disease is rapidly accumulating. Also, since treatment is now subject to everyone who is infected with the virus and no longer restricted to the CD4<sup>+</sup> count, the number of individuals on treatment has increased substantially since 2015. The cost burden is felt more by developing countries as international funding is not being raised to match the new costs and so countries such as South Africa have to rely heavily on their own domestic funding.<sup>39</sup> South Africa already has the largest antiretroviral

(ARV) programme globally, with its domestic funding covering about 75% of its overall HIV expenditures, most of it going towards first-line treatment.<sup>44</sup>

The need to find drugs that are less susceptible to resistance (because of the extended period of treatment since life expectancy has increased) and also that are of low cost have been on the rise.<sup>39</sup> In recent developments, efavirenz **11** (figure 1.8) has been replaced by dolutegravir **14** (figure 1.13), as announced by the UNAIDS in September 2017, in FDC therapy (3-in one pill). This was agreed upon at an affordable rate and dolutegravir has been found to have less side effects than efavirenz and a higher efficiency.<sup>25</sup>

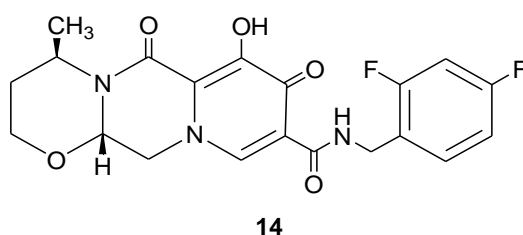


*Figure 1.13: The new FDA-approved Protease Integrase drug, dolutegravir.*

The tenofovir **9** second generation prodrug, TAF **13**, has another advantage to it compared to TDF **12**. It has been reported that TAF **13** has lower manufacturing costs to TDF and it is more compatible with the new integrase drug, dolutegravir **14**.<sup>44</sup> The two have also been reported to be potential second-line treatment drugs.<sup>45</sup>

In the research reported in this dissertation we focus on the synthetic pathway leading to tenofovir **9** which in turn can be used to access both TD **25** and TA **26**, attempting to improve the pathway with the incorporation of flow chemistry.

## References

1. Pneumocystis Pneumonia — Los Angeles. Morbidity and Mortality Weekly Report. 1981;30(21):250–2.
2. UNAIDS. Fact sheet - Latest statistics on the status of the AIDS epidemic [Internet]. Vol. 2018. 2017. Available from: <http://www.unaids.org/en/resources/fact-sheet>
3. World Health Organization. HIV/AIDS Data and Statistics [Internet]. Vol. 2018. 2018. Available from: <http://origin.who.int/hiv/data/en/>
4. The Guardian. More die of Aids than war in Africa says Kofi Annan [Internet]. Vol. 2018. 2000. Available from: <https://www.theguardian.com/world/2000/mar/14/unitednations>
5. Holmes EC. On the origin and evolution of the human immunodeficiency virus (HIV). Biol Rev. 2001;76(2):239–54.
6. Sharp PM, Hahn BH. Origins of HIV and the AIDS Pandemic. Cold Spring Harb Perspect Med. 2011;1(1):a006841.
7. Quagliarello V. The Acquired Immunodeficiency Syndrome: current status. Yale J Biol Med. 1982;55(5–6):443–52.
8. Castro KG, Ward JW, Slutsker L, Buehler JW, Jaffe HW, Berkelman RL, et al. 1993 revised classification system for HIV infection and expanded surveillance case definition for AIDS among adolescents and adults. Clin Infect Dis. 1993;17(4):802–10.
9. Karim QA, Karim SSA. The evolving HIV epidemic in South Africa. Int J Epidemiol. 2002 Jan;31(1):37–40.
10. Sher (R). Acquired immune deficiency syndrome (AIDS) in the RSA. South African Med J. 1986;70(4):23–6.
11. Barré-Sinoussi F, Chermann JC, Rey F, Nugeyre MT, Chamaret S, Gruest J, et al. Isolation of a T-Lymphotropic Retrovirus from a Patient at Risk for Acquired Immune Deficiency Syndrome (AIDS). Science (80- ). 1983;220(4599):868–71.
12. Sarngadharan MG, Popovic M, Bruch L, Schupbach J, Gallo RC. Antibodies reactive with human T-lymphotropic retroviruses (HTLV-III) in the serum of patients with AIDS. Science. 1984 May 4;224(4648):506–8.
13. Melhuish A, Lewthwaite P. Natural history of HIV and AIDS. Medicine (Baltimore). 2018;46(6):356–61.
14. Al-Jabri A. How does HIV-1 infect a susceptible human cell?: Current thinking. J Sci Res Sci / Sultan Qaboos Univ. 2003;5(1–2):31–44.
15. Campbell-Yesufu O, Gandhi RT. Update on Human Immunodeficiency Virus (HIV)-2 Infection. Clin Infect Dis An Off Publ Infect Dis Soc Am. 2010;52(6):780–7.
16. Shaw GM, Hunter E. HIV Transmission. Cold Spring Harb Perspect Med. 2012;2(11):a006965.



17. Wilton J. From Exposure to Infection: The Biology of HIV Transmission [Internet]. Vol. 2016. 2011. Available from: <http://www.catie.ca/en/pif/fall-2011/exposure-infection-biology-hiv-transmission>
18. Centers for Disease Control and Prevention. HIV Transmission [Internet]. Vol. 2018. 2018. Available from: <https://www.cdc.gov/hiv/basics/transmission.html>
19. Palmisano L, Vella S. A brief history of antiretroviral therapy of HIV infection: success and challenges. *Ann Ist Super Sanita*. 2011;47:44–8.
20. Abdool Karim S. S, Churchyard GJ, Abdool Karim Q, Lawn SD. HIV infection and tuberculosis in South Africa: an urgent need to escalate the public health response. *Lancet*. 2009;374(9693):921–33.
21. Mntlangula MN, Khuzwayo N, Taylor M. Nurses perceptions about their behavioural counselling for HIV/AIDS, STIs and TB in eThekweni Municipality clinics KwAZulu-Natal, South Africa. *Health SA Gesondheid*. 2017;22:52–60.
22. Simelela NP, Venter WDF. A brief history of South Africa’s response to AIDS. *SAMJ South African Med J*. 2014;104(3):249–51.
23. Fassin D, Schneider H. The politics of AIDS in South Africa: beyond the controversies. *BMJ Br Med J*. 2002 May;326(7387):495–7.
24. The Guardian. Mbeki Aids Denial Caused 300 000 Deaths [Internet]. Vol. 2018. 2008. Available from: <https://www.theguardian.com/world/2008/nov/26/aids-south-africa>
25. Nair N, Swart W. Mbeki Must Account for 330 000 Deaths [Internet]. Vol. 2018. 2009. Available from: <https://www.timeslive.co.za/sunday-times/lifestyle/2009-09-01-mbeki-must-account-for-330000-deaths/>
26. Okoye AA, Picker LJ. CD4(+) T cell depletion in HIV infection: mechanisms of immunological failure. *Immunol Rev*. 2013;254(1):54–64.
27. Doitsh G, Greene WC. Dissecting How CD4 T Cells Are Lost During HIV Infection. *Cell Host Microbe*. 2016 Sep;19(3):280–91.
28. Famularo G, De Simone C, Marcellini S. Apoptosis: mechanisms and relation to AIDS. *Med Hypotheses*. 1997 May;48(5):423–9.
29. Weiss RA. How does HIV cause AIDS? *Science*. 1993 May 28;260(5112):1273–9.
30. Selliah N, Finkel TH. Biochemical mechanisms of HIV induced T cell apoptosis. *Cell Death Differ*. 2001;8(2):127.
31. Meintjes Moorhouse, M., Carmona, S., Davies, N., Dlamini, S., van Vuuren, C., Manzini, T., Mathe, M., Moosa, Y., Nash, J., Nel, J., Pakade, Y., Woods, J., van Zyl, G., Conradie, F., Venter, F. G. Adult antiretroviral therapy guidelines 2017. *South Afr J HIV Med*. 2017;18(1).

32. St Clair MH, Richards CA, Spector T, Weinhold KJ, Miller WH, Langlois AJ, et al. 3'-Azido-3'-deoxythymidine triphosphate as an inhibitor and substrate of purified human immunodeficiency virus reverse transcriptase. *Antimicrob Agents Chemother.* 1987 Dec;31(12):1972–7.
33. Fischl MA, Richman DD, Grieco MH, Gottlieb MS, Volberding PA, Laskin OL, et al. The efficacy of azidothymidine (AZT) in the treatment of patients with AIDS and AIDS-related complex. *N Engl J Med.* 1987;317(4):185–91.
34. Vella S, Schwartzländer B, Sow P, Paul Eholie S, L Murphy Robert. The history of antiretroviral therapy and of its implementation in resource-limited areas of the world. *AIDS.* 2012;26(10):1231–41.
35. Cihlar T, Fordyce M. Current status and prospects of HIV treatment. *Curr Opin Virol.* 2016;18:50–6.
36. Hammer SM, Squires KE, Hughes MD, Grimes JM, Demeter LM, Currier JS, et al. A controlled trial of two nucleoside analogues plus indinavir in persons with human immunodeficiency virus infection and CD4 cell counts of 200 per cubic millimeter or less. *N Engl J Med.* 1997;337(11):725–33.
37. Torres TS, Cardoso SW, Velasque LS, Veloso VG, Grinsztejn B. Incidence rate of modifying or discontinuing first combined antiretroviral therapy regimen due to toxicity during the first year of treatment stratified by age. *Brazilian J Infect Dis.* 2014;18(1):34–41.
38. Geffen Low, M. N. When to start antiretroviral treatment? A history and analysis of a scientific controversy. *South Afr J HIV Med.* 2017;18(1):8.
39. Meyer-Rath G, Johnson LF, Pillay Y, Blecher M, Brennan AT, Long L, et al. Changing the South African national antiretroviral therapy guidelines: The role of cost modelling. Lima VD, editor. *PLoS One.* 2017 Feb;12(10):e0186557.
40. Gregson J, Tang M, Ndembu N, Hamers RL, Rhee S-Y, Marconi VC, et al. Global epidemiology of drug resistance after failure of WHO recommended first-line regimens for adult HIV-1 infection: a multicentre retrospective cohort study. *Lancet Infect Dis.* 2016;16(5):565–75.
41. Sax PE, Zolopa A, Brar I, Elion (R), Ortiz (R), Post F, et al. Tenofovir Alafenamide Vs. Tenofovir Disoproxil Fumarate in Single Tablet Regimens for Initial HIV-1 Therapy: A Randomized Phase 2 Study. *JAIDS J Acquir Immune Defic Syndr.* 2014;67(1).
42. Ray AS, Fordyce MW, Hitchcock MJM. Tenofovir alafenamide: A novel prodrug of tenofovir for the treatment of Human Immunodeficiency Virus. *Antiviral Res.* 2016;125:63–70.
43. Mills A, Arribas JR, Andrade-Villanueva J, DiPerri G, Van Lunzen J, Koenig E, et al. Switching from tenofovir disoproxil fumarate to tenofovir alafenamide in antiretroviral regimens for

- virologically suppressed adults with HIV-1 infection: a randomised, active-controlled, multicentre, open-label, phase 3, non-inferiority study. *Lancet Infect Dis*. 2016;16(1):43–52.
44. Venter Kaiser, B., Pillay, Y., Conradie, F., Gomez, G., Clayden, P., Matsolo, M., Amole, C., Rutter, L., Abdullah, F., Abrams, E., Casas, C., Barnhart, M., Pillay, A., Pozniak, A., Hill, A., Fairlie, L., Boffito, M., Moorhouse, M., Chersich, M., Serenata, C., Quevedo, J., Loots, G. W. Cutting the cost of South African antiretroviral therapy using newer, safer drugs. *South African Med J*. 2016;107(1).
45. Barnhart M, Shelton JD. ARVs: The Next Generation. Going Boldly Together to New Frontiers of HIV Treatment. *Glob Heal Sci Pract*. 2015 Feb;3(1):1–11.

## Chapter 2: Flow chemistry

### 2.1) Chemistry and drug discovery: Room for improvement

In 2016 *The Business Times* wrote an article where the founder and chief executive of The Future Agency, Gerd Leonhard, declared that the next 20 years will likely “bring more change to humanity than the past 300 years”.<sup>1</sup> He attributed this to the new age of digital “ations”- “digitisation, screenification, automation, visualisation, etc.” The reality is that the world has become one gigantic globe with the population increasing at an all-time high, sitting at almost 8 billion people. Consequently, this has come with considerable pressure for all fields to not only conform to the new-found demands of society, but also to do so at an exaggerated speed.

In the field of chemistry research it’s interesting to see how over the past 200 years of chemistry, change and progression is witnessed by the vast expansion of knowledge and understanding of reactions on the molecular level as well as the enhancements and improvements made to both apparatus and equipment together with techniques to improve and better controlled chemical reaction conditions and parameters,<sup>2-4</sup> (for example, from manual stirring and heating over a flame, to the laboratory today using magnetic stirrers and heating mantles as basic laboratory equipment).<sup>5</sup> It is quite ironic, however, to witness some classical tools in the field; a classic example of this being the glass round bottom flask (RBF), which is a concept as old as alchemy (figure 2.1).<sup>6-8</sup> This does, however, not completely undermine the effectiveness of the ‘oldies’, but rather can affirm their usefulness.



Glass flask, Roman, 151-300AD



Pyrex company boiling flask, released after 1916



Typical glass RBF today



Figure 2.1: Representation of the glass flask over time.<sup>6-8</sup>

In the field of drug discovery, there has been huge progress since advances in genomics and proteomics, as well as in high-throughput screening (HTS)<sup>9</sup> which can be traced back to work done by

Merrifield,(R).B.<sup>10</sup> Steve Ley and co-workers, however, make mention that these advances seem to be “increasing research and development expenditure with fewer new drugs actually making it to the market place”.<sup>11</sup> For this reason there seems to be a gap that needs to be filled that will allow for the fast process with consideration to cost, safety and the environment.<sup>12</sup>

In the late 1990s, S. Ley and I Baxendale, both respected chemists, initiated a futuristic project determined to claim a spot for organic chemistry in the modern world.<sup>13–17</sup> They introduced the idea of having flow micro reactors in a typical research synthetic laboratory, with essentially two objectives in mind:

1. To increase the rate of drug discovery by increasing the rate at which libraries are built-up. The need for speed is not only from the increase in demand based on the large number of the population and rapid rate of consumption, but also because of the heightened rate of drug-efficiency decay/resistance. Hence the need for liberal drug diversity.<sup>12,18</sup>

2. To move towards greener chemistry; for the sake of future generations. In the past and present years chemistry has received a notorious reputation for being an environment-harming science and has at many times been blamed for much of the environmental problems the world faces right now, with the big one being global warming (figure 2.2). It is so imperative for the survival of the field to bring solutions that move towards cleaner processes.<sup>12,19–21</sup>



Figure 2.2: A few newspaper articles reporting on pollution in the chemical industry.<sup>12, 19–21</sup>

The task would require “much cleaner, strategically important reaction processes that lead to the assembly of molecules free from waste products and which proceed with high atom efficiencies”.<sup>18</sup>

## 2.2) Flow reactors: Engineering in a chemistry laboratory

Flow reactors (figure 2.3) have been used by chemical engineers for the past century and have only been recently condensed to fit the use of an organic chemist.<sup>22</sup> Flow chemistry allows the chemist to let go of the traditional reaction vessel, such as the round-bottomed flask, for cartridges, loops, chips and columns. Currently, there are two types of flow reactors based on size. The first is a micro reactor, which typically has tubes with an inner diameter between 10  $\mu\text{m}$  to 500  $\mu\text{m}$ . The second type is a *meso*

reactor, which has tubes of inner diameters ranging from 500  $\mu\text{m}$  to several millilitres. Anything larger is typically dealt with by engineers.

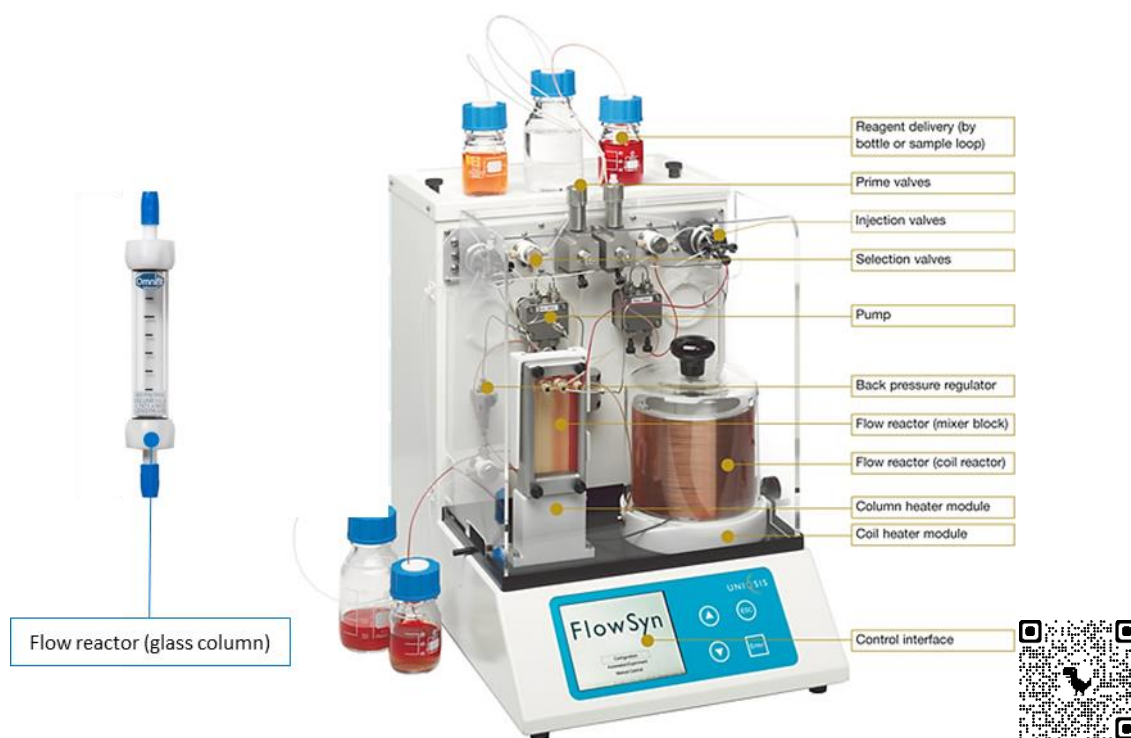


Figure 2.3: Standard UniQsis flow reactor.<sup>23</sup>

The size of the flow reactor is responsible for many of the advantages associated with using flow. One of these advantages is the high heat transfer capacity. Heat transfer is highly dependent on the area size and so the small channels of both micro and meso reactors achieve high heat transfer per unit volume, with values ranging from 5000 to 50 000  $\text{m}^2\text{m}^{-3}$  for *micro* and 100- 10 000  $\text{m}^2\text{m}^{-3}$  for *meso* reactors.<sup>24</sup>

Not only is the capacity for heat transfer high, but the small dimensions of the micro reactor also permit precise monitoring of heat exchange (easily controlled heat application and removal).<sup>25</sup> This excellent heat and mass transfer makes micro reactors exceptional mediums for unstable, exothermic reactions. It is easier to carry out reactions with hazardous reagents or highly reactive intermediates, as already done by multiple research groups, e.g. McPhake C. and Stanford G.<sup>26,27</sup> who performed fluorinations using flow.

Flow offers more precise control of not only temperature, but also of mixing and pressure, as compared to batch synthesis.<sup>25</sup> The high pressures allow reactions to occur at temperatures higher than the boiling point of the solvent used (super-critical conditions can even be reached) and this has

proved to be a very useful advantage as some reactions have been optimized in this manner, such as esterifications by *Kappe et al.*<sup>28</sup>

Reaction monitoring has proved more convenient when using flow because the reactor can easily be connected to characterization devices such as IR machines, HPLC, LC/GC as well as UV.<sup>12</sup>

Micro reactors are in no way the “be all, end all” for organic chemists for they too come bearing disadvantages. The small dimensions of a micro reactor may be the reason of many of its advantages, but concurrently it brings about challenges such as easy blockage (hence only solution based reactions are possible, with no precipitates), high pressure drops and a limited flow capacity.<sup>22,24</sup> The cost associated with reactors and their integrated features/monitors is also another point to consider. The pros are, however, impressive enough to consider flow chemistry as a great compliment of batch synthesis.

For a long time industrial chemistry obtained information regarding a synthetic route based on the laboratory batch process, which formed a disconnect that required extra optimizations and/or remodelling of the synthesis process and needless to say, costing much more time and money. This brings us to another advantage of flow chemistry because reaction parameters of a micro reactor can easily be translated onto larger flow systems, without exhaustive optimization steps.<sup>29</sup> There are three steps of scale-up mentioned by Porta and co-workers;<sup>30</sup> the first is the most common which is “scaling out”. This is done by running the process for longer in the micro reactor. The second option is “numbering up”, which is using multiple reactors in parallel, however, Wegner and co-workers<sup>24</sup> do mention that this is less preferred because of the “complex online monitoring”. The third option is “scaling up” which is just the use of reactors that are larger in size.<sup>25</sup>

### ***2.3) Immobilized reagents for flow: A match made in “heaven”***

As mentioned previously, continuous reactors have been around for a while, dating back as early as 1932 when the first use of heterogeneous reagents under flow was reported,<sup>31</sup> however, they have gained the spotlight ever since immobilized reagents have exploded into the commercial market.<sup>32-34</sup>

As with continuous reactors, immobilized reagents are not a new concept, with the first recorded use being as early as 1946.<sup>35</sup> Recent advances and increased commercial availability of immobilized molecules including (1) immobilized enzymes/ catalysts, (2) immobilized scavengers, (3) catch-and-release agents to a variety of (4) immobilized reactants have made immobilized reagents a powerful tool of interest.<sup>12,18,36,37</sup>

The idea behind immobilized reagents is having a molecule attached to an unreactive polymer resin.<sup>38</sup> The most commonly used polymer is polystyrene because it is inexpensive, easy to handle and inert to most chemical changes.<sup>39</sup> The use of solid-supported reagents has received attention because of the possible applications: Reactions can be driven towards completion because the solid-supported reagents can be used in excess and work-up is further simplified by just removing the supported reagent/s by manual filtration, and if the reagent was a catalyst it can be regenerated- a clean and economical process.<sup>37</sup> The use of solid-supported (phase) reagents (figure 2.4) for work-up takes precedence over typical work-up such as water-quenching, solvent extraction, solvent evaporation, distillation, crystallization and chromatography<sup>11,18,40</sup> This in turn saves much time and material resources.

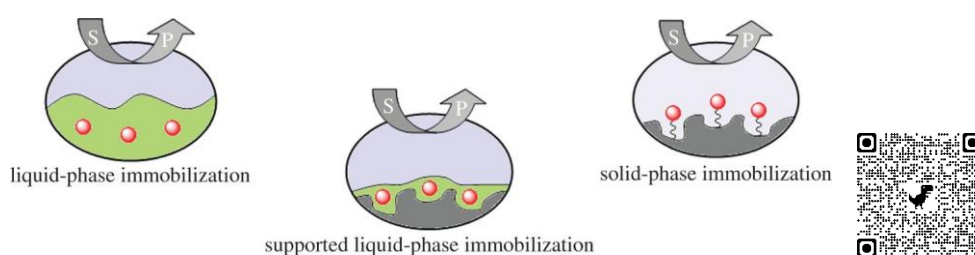


Figure 2.4: Types of immobilization.

Another environmental advantage with solid support reagents is that hazardous reagents or intermediates can be immobilized and thus provide a much safer route of production of certain species. Many reactions produce undesired by-products, impurities and/or use excess reagents so this is where the use of scavengers and catch-and release agents come in to either remove the undesired material or selectively isolate the product from the reaction mixture.<sup>11</sup>

It is no surprise that the use of solid supported reagents is attractive to the continuous flow process because its sophistication allows for work-up to take place without any interruptions of batch product isolation, ultimately allowing for continuous multi-step synthesis.

The solid-supported reagents can be loaded into cartridges and/or columns available for each reactor and the parameters, temperature and flow rate and mixing can be controlled in such a way as to give optimal conversion and isolation of product.



Tsubogo and co-workers illustrated the different approaches to using solid-supported reagents and catalysts in flow (figure 2.5).<sup>41</sup> For multistep synthesis a combination of these can be employed to best fit the synthetic pathway.

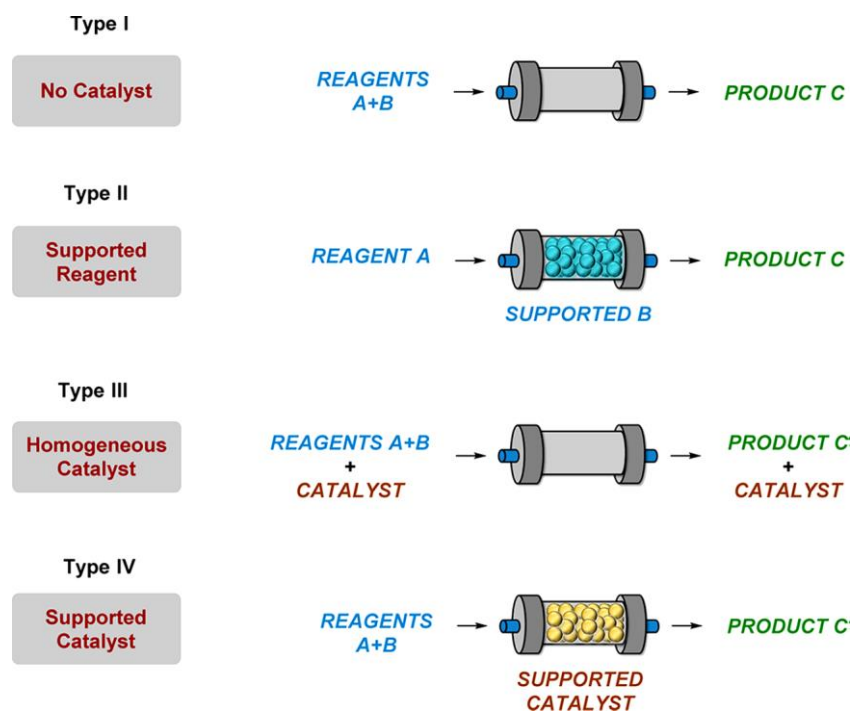


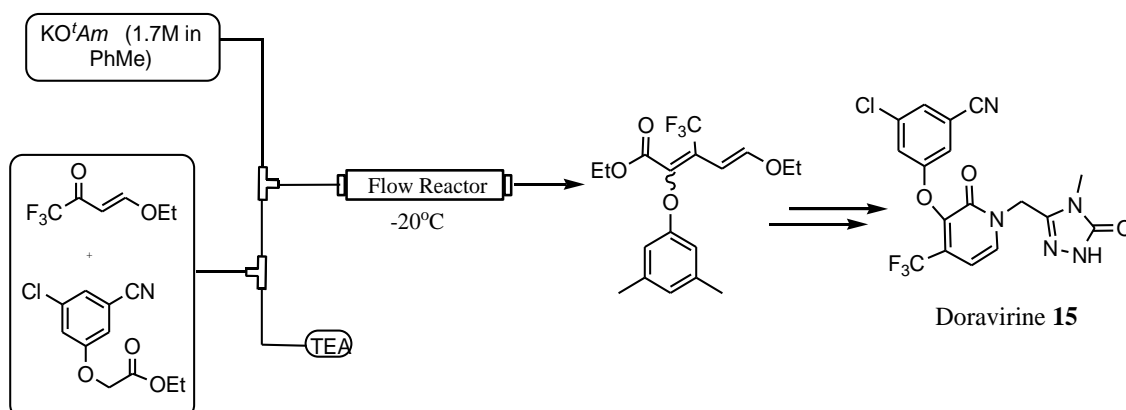
Figure 2.5: General types of continuous flow systems retrieved from Porta et al.<sup>30</sup>

#### 2.4) Practical examples of HIV treatment drugs on flow

Some examples of successful syntheses on flow of HIV-treatment drugs mentioned in the previous introductory chapter 1 are described in the following section.

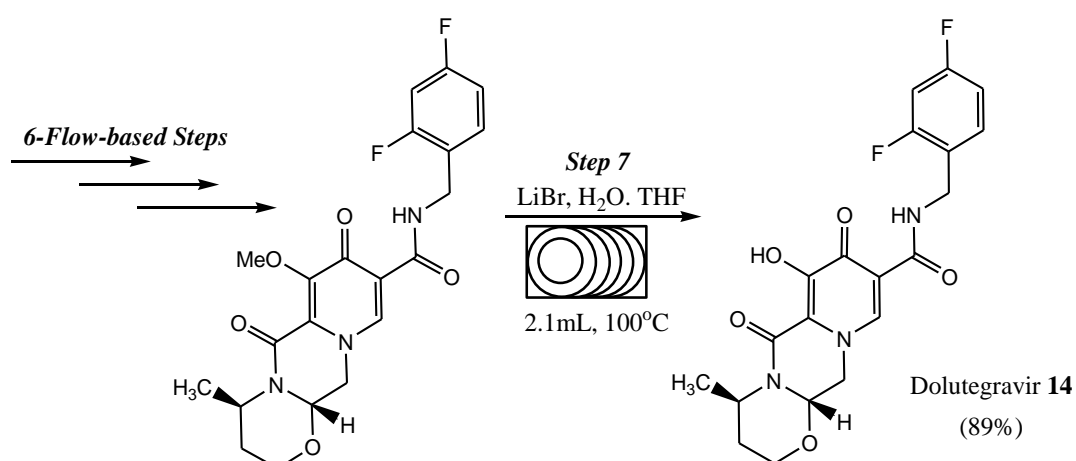
Gauthier and co-workers<sup>42</sup> developed a synthetic pathway for doravirine **15** that incorporated a flow step for the aldol reaction (scheme 2.1). The initial step of the synthesis was performed on a flow reactor where one feed that contained the ethyl ester and the vinylogous ester in toluene was combined (via a T-mixer) into one stream with a second feed that contained potassium *tert*-amyloxide in toluene. The aldol adduct was formed in the reactor coil at -20 °C and the rest of the synthetic route took place in batch to eventually afford a 52% overall yield of doravirine **15**.<sup>42</sup> This step was purposefully translated to flow in order to address enolate instability problems faced when dealing

with these particular esters in batch. The flow synthesis showed an improved yield for the aldol adduct from the optimized batch synthesis (assay yield of 65 – 77%) of 85%.<sup>42</sup>



*Scheme 2.1: The flow reactor step for the synthesis of HIV NNRTI, doravirine; a semi-continuous synthetic pathway. Gauthier et al reported a retention time of 1-60 seconds.<sup>42</sup>*

A seven-step flow synthesis of dolutegravir **14** was developed by Ziegler and co-workers (scheme 2.2).<sup>43</sup> The initial step had feed A which contained methyl 4-methoxyacetoacetate and feed B containing dimethylformamide dimethylacetal (DMF-DMA) combined into one stream via a T-mixer and heated in a reactor coil at 85 °C for ten minutes. Five more flow-based reactions took place and finally step 7 included a demethylation reaction using LiBr, at 100 °C, for thirty-one minutes residence time, resulting in an 89% yield for dolutegravir **14**. Overall, the flow-based synthesis took seven steps in three separate flow operations, giving an overall yield of 24%.

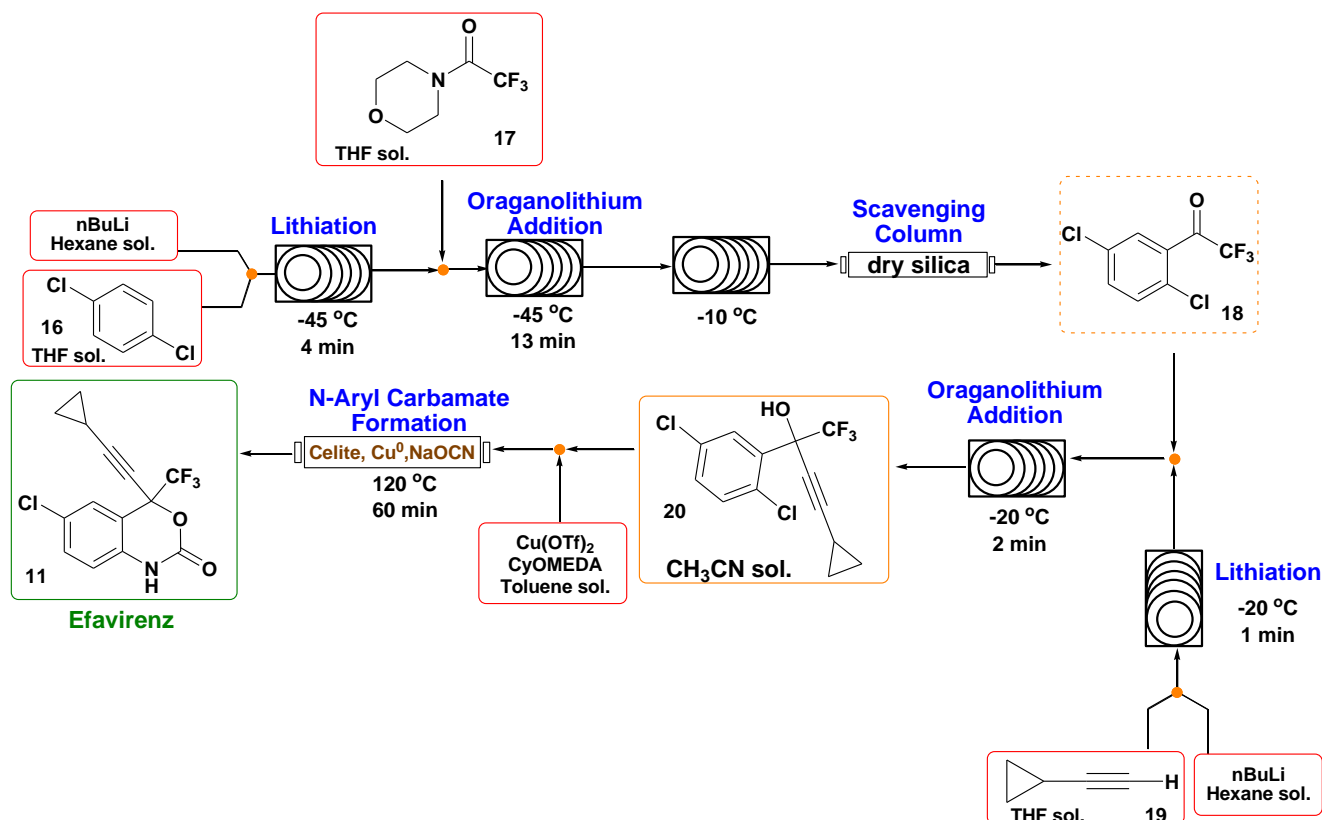


*Scheme 2.2: The final flow step synthesis of HIV Integrase inhibitor, dolutegravir as reported by Ziegler et al. The step gave an 89% yield of dolutegravir,ii within 31 minutes.<sup>43</sup>*

Ziegler and co-workers<sup>43</sup> mentioned the key benefits of their established flow synthetic route as follows: i) rapid manufacturing time, direct amidation of ester to reduce the step count, and separation

of the acetal deprotection/oxazine formation ii) flow reactors attain high reactivity and selectivity for tricyclic product DTG-OMe, and iii) synthesis should be adaptable to both cabotegravir and bictegravir (which are both integrase inhibitors)

Porta and co-workers reported on a flow-based synthesis of efavirenz **11** an HIV NNRTI (scheme 2.3)<sup>30</sup>.

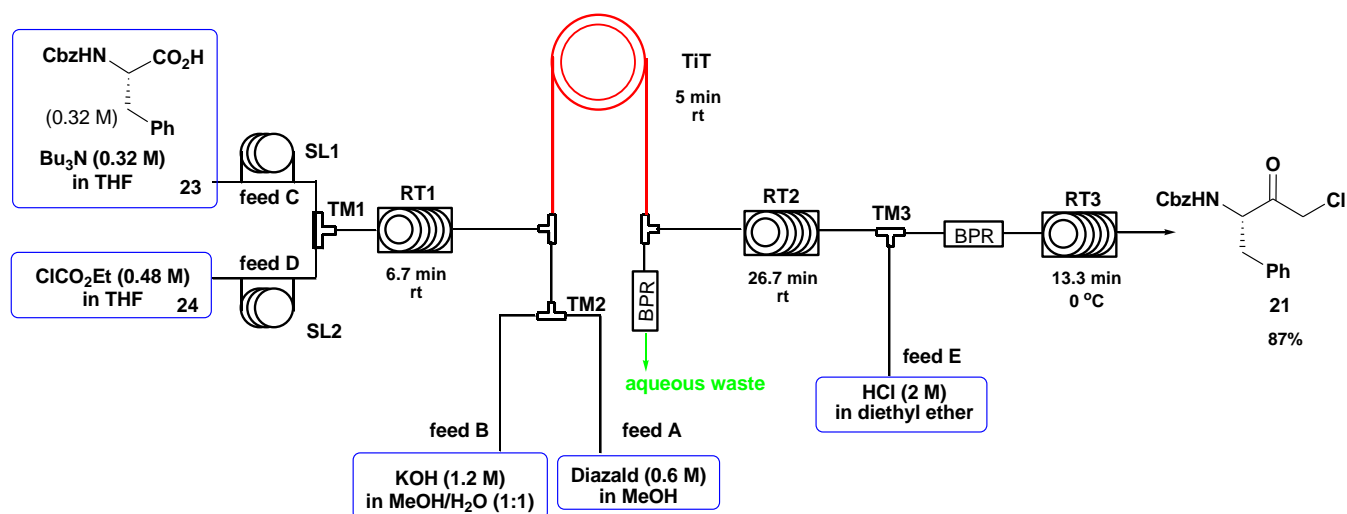


Scheme 2.1.: Continuous flow synthesis of efavirenz **11**- An HIV NNRTI. 42% overall yield reported by Porta et al.<sup>30</sup>

The approach starts with the lithiation of 1,4-dichlorobenzene **16** in a reactor coil at -45 °C. This is then quenched by THF solution of morpholine **17** in a second reactor coil at the same temperature. The reaction mixture is then warmed up to -10 °C in a third reaction coil and the by-products are scavenged in silica embedded in a glass column, resulting in the ketone product **18**. In parallel, lithiation of the alkyne **19** took place in a separate reactor coil at -20 °C and the product stream was combined with the ketone **18** in a fourth reactor coil to form alcohol **20**. The crude product was purified using brine and chromatography, and an acetonitrile solution of the pure alcohol was re-added to flow and combined with Cu(OTf)<sub>2</sub> and *trans*-*N,N'*-dimethyl-1,2-cyclohexanediamine (CyDMEDA). This was passed through a cartridge containing Cu<sup>0</sup>, NaOCN and Celite at 120 °C. The copper-catalyzed *N*-aryl carbamate formation gave efavirenz **11** in 62% yield after extraction and purification of the crude mixture.

According to Porta and co-workers,<sup>30</sup> this translation to flow gave an overall yield of 45% and had a total reaction time that was less than two hours- which is the shortest existing route for the synthesis of efavirenz **11**.

Pinho and co-workers<sup>44</sup> reported the synthesis of an  $\alpha$ -chloro ketone **21** (scheme 2.4), which is a building block for an HIV anti-protease such as atazanavir **22** (figure 1.9). The synthesis of an  $\alpha$ -chloro ketone on flow required three successive reactions (RTs): firstly the activation of an amino acid **23** to a mixed anhydride **24**. Secondly, the condensation of the mixed anhydride and diazomethane to form a  $\alpha$ -diazo ketone, and lastly hydrohalogenation of the diazo ketone to an  $\alpha$ -halo ketone.



Scheme 2.3: A continuous flow synthesis of an  $\alpha$ -chloro ketone- a building block of HIV protease inhibitor. An 87% maximum yield reported by Pinho et al.<sup>44</sup>

Scheme 2.4 illustrates the flow set-up employed by Pinho and co-workers: Solution 1 and 2 (SL1 and SL2) were pumped (feed C and D) and merged into one stream via the T-mixer (TM1) at 75  $\mu$ L/min, which went through the reactor/coil (RT1) at room temperature for seven minutes to form the mixed anhydride. The solution then passed through the “outer chamber of the tube-in-tube device” (TiT) in which the solution was saturated with diazomethane (from feed A and B), into the reactor/coil (RT2) at room temperature for twenty-seven minutes. Feed C was then pumped into the system at 80  $\mu$ L/min to combine with the product stream from RT2, in a T-mixer (RM3) at 0 °C and the resultant stream went through the final reactor/coil (RT3) at 0 °C. The final product was collected in a flask at 0 °C and after collection and purification by flash chromatography, 87% yield was obtained of an  $\alpha$ -chloro ketone, (*S*)-benzyl (4-Chloro-3-oxo-1-phenylbutan-2-yl)carbamate **21**.

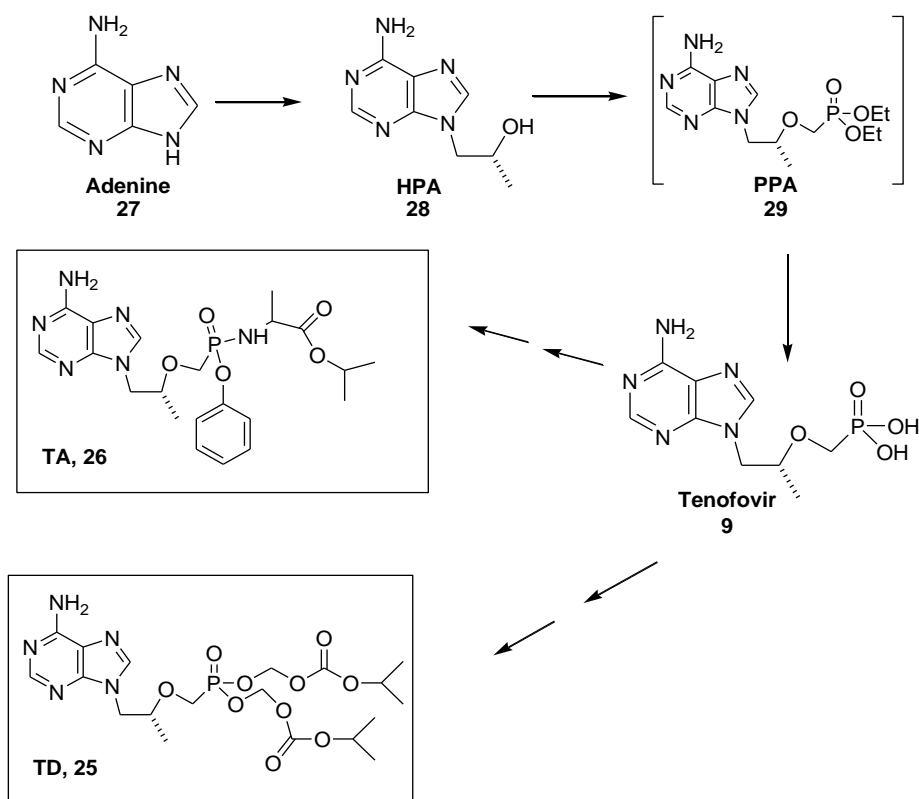
This flow translation allowed for the use of diazomethane, which although extremely useful as C1 building block and usually results in very fast and mild condition reactions, is severely limited in the

laboratory because of its hazardous nature. In the process described, diazomethane is formed in the inner tube of the TiT and diffuses through the gas-permeable inner tube to react with the mixed anhydride; furthermore any excess was destroyed with either HCl or HBr – No storage or handling of the toxic reagent was necessary and the reaction proceeded successfully with this “continuous robust set-up” in an 87% yield.

The success of the previous examples (scheme 2.1-2.4) make it apparent that flow chemistry is a great contender in the field of drug discovery and research for even pre-existing batch synthetic routes.

## Aims and objectives of our project.

We wanted to investigate the possible translation of the synthetic pathway of active HIV NNRTI drug, tenofovir **9** (scheme 2.5), to flow with possible extension of the translation to the prodrugs TD **25** and TA **26**.



Scheme 2.4: A summary of the synthetic pathway of adenine to prodrugs TD **25** and TA **26**.

This dissertation is therefore broken down into three main parts each dedicated to a particular step towards the synthesis of the prodrugs TD **25** and TA **26**

1. The *third chapter* will focus on the first step of the synthesis: the alkylation of adenine **27** (to form hydroxyl propyl adenine, HPA **28**) and its translation to flow.
  - a. We will attempt to find an alternative reaction solvent that will be suitable for the adenine **27** for both batch and the flow conditions.
  - b. We will investigate different work-up systems, including polymer supported reagents.
  - c. We will attempt translation of the synthesis and work-up on flow.
2. The *fourth chapter* will focus on the formation of the active drug, tenofovir **9**.
  - a. We will attempt to replicate the method reported by Riley *et al*, in order to isolate intermediate ester product, phosphonate propyl adenine, PPA **29**.

- b. We will attempt alternative work-up systems for the intermediate step (formation of PPA **29**), including polymer supported reagents.
  - c. We will investigate at least one alternative route for the synthesis of PPA **29**.
  - d. We will attempt the hydrolysis of PPA **29** to form tenofovir **9** as reported by Riley *et al.*
  - e. We will attempt to translate the entire step to flow (dependent on the success of point a-e).
3. The *final chapter* will address the last stages towards the synthesis of TD **25** and TA **26**.
- a. We will attempt to synthesize TD **25** and TA **26** in batch.
  - b. Dependent on time, we will attempt to translate the final steps to flow.

By performing these objectives we believe that we could develop a synthetic pathway for HIV prodrugs TD **25** and TA **26** that would be more time, economical, and environmentally savvy and would be a good contribution to both the chemistry and drug discovery fields.

## References

1. Choudhury AR. Futurist: More changes in next 20 years than last 300 [Internet]. Business Times. 2016 [cited 2019 May 27]. Available from: <https://www.businesstimes.com.sg/government-economy/futurist-more-changes-in-next-20-years-than-last-300>
2. Brock WH. The History of Chemistry: A Very Short Introduction. Oxford University Press; 2016. (Very short introductions).
3. Meyer M. Chemistry began the moment our ancestors became human. UNESCO. 2011 Jun;
4. Bagley M. History of Chemistry | Famous Chemists. LiveScience. 2014 Jun;
5. Buie J. Evolution of Biological Shakers and Stirrers [Internet]. 2011 [cited 2019 Jun 26]. Available from: <https://www.labmanager.com/lab-product/evolution-of-biological-shakers-and-stirrers-18253>
6. Glass flask, Roman, 151-300AD [Internet]. Science Museum Group Collection. [cited 2019 Jun 26]. Available from: <https://collection.sciencemuseumgroup.org.uk/objects/co89916/glass-flask-roman-151-300ad-flask-bottle>
7. Boiling flask [Internet]. National Museum of American History. [cited 2019 Jun 26]. Available from: [https://americanhistory.si.edu/collections/search/object/nmah\\_1154](https://americanhistory.si.edu/collections/search/object/nmah_1154)
8. No Title [Internet]. [cited 2019 Jun 26]. Available from: [https://www.google.com/search?q=round+bottom+flask&sxsrf=ALeKk01R8dxJpijXP4fXwAAoKQAK8CFmGQ:1613145465060&source=lnms&tbnm=shop&sa=X&ved=2ahUKewjFo6mT2-TuAhVRuXEKHYYCCyEQ\\_AUoAnoECA8QBA&biw=1366&bih=638#spd=6011060367209202454](https://www.google.com/search?q=round+bottom+flask&sxsrf=ALeKk01R8dxJpijXP4fXwAAoKQAK8CFmGQ:1613145465060&source=lnms&tbnm=shop&sa=X&ved=2ahUKewjFo6mT2-TuAhVRuXEKHYYCCyEQ_AUoAnoECA8QBA&biw=1366&bih=638#spd=6011060367209202454)
9. Kenny BA, Bushfield M, Parry-Smith DJ, Fogarty S, Treherne JM. The application of high-throughput screening to novel lead discovery BT - Progress in Drug Research. In: Ren S, Lien EJ, Turner NC, Clapham JC, Prokai L, Wagey RTE, et al., editors. Progress in Drug Research. Basel: Birkhäuser Basel; 1998. p. 245–69.
10. Merrifield RB. Solid Phase Peptide Synthesis. I. The Synthesis of a Tetrapeptide. J Am Chem Soc. 1963 Jul 1;85(14):2149–54.
11. Ley S, Baxendale I, Myers (R). EVOLUTION OR REVOLUTION : THE CHALLENGE TO TODAY'S MEDICINAL CHEMIST. In Beilstein-Institut; 2005. p. 1–32.
12. Baxendale, IR Hayward, JJ Lanners, S Ley, SV Smith C. Microreactors in Organic Synthesis and Catalysis. Wirth T, editor. 2008. 84–122 p.
13. Hinzen B, V. Ley S. Polymer supported perruthenate (PSP): a new oxidant for clean organic synthesis. J Chem Soc Perkin Trans 1. 1997;(13):1907–8.
14. Hinzen B, Lenz (R), Ley S V. Polymer Supported Perruthenate (PSP): Clean Oxidation of Primary Alcohols to Carbonyl Compounds Using Oxygen as Cooxidant. Synthesis (Stuttg). 1998;1998(07):977–9.
15. Green L, Hinzen B, Ince SJ, Langer P, Ley S V, Warriner SL. One-pot Synthesis of Penta- and Hepta-saccharides from Monomeric Mannose Building Blocks Using the Principles of Orthogonality and Reactivity Tuning. Synlett. 1998;1998(04):440–2.
16. V. Ley S, H. Bolli M, Hinzen B, Gervois A-G, J. Hall B. Use of polymer supported reagents for clean multi-step organic synthesis: preparation of amines and amine derivatives from alcohols for use in compound library generation. J Chem Soc Perkin Trans 1. 1998;(15):2239–



- 42.
17. Ley S V, Baxendale IR, Bream RN, Jackson PS, Leach AG, Longbottom DA, et al. Multi-step organic synthesis using solid-supported reagents and scavengers: a new paradigm in chemical library generation. *J Chem Soc Perkin Trans 1*. 2000;(23):3815–4195.
  18. Ley S. Chemistry in a changing world: new tools for the modern molecule maker. Archer, MD Haley C, editor. Cambridge University Press; 2005. 283–303 p.
  19. Saleh HE-DM, Koller M. Introductory Chapter: Principles of Green Chemistry. In: Koller MKE-HE-DMSE-M, editor. Rijeka: IntechOpen; 2018. p. Ch. 1.
  20. Royal Society of Chemistry. Campaigning and outreach: Environment. *RSC Advances*. 2016 Feb;
  21. No Title [Internet]. Available from: [https://www.google.com/search?q=chemistry+is+a+polluter&tbn=nws&sxsrf=ALeKk02X-6my-c9zL7urHF0DztCt2jdCRg:1613463827580&source=Int&tbs=ar:1&sa=X&ved=0OahUKEwjK07OS\\_e3uAhVkrXUIHXWoBgUQpwUIKQ&biw=1366&bih=638&dpr=1](https://www.google.com/search?q=chemistry+is+a+polluter&tbn=nws&sxsrf=ALeKk02X-6my-c9zL7urHF0DztCt2jdCRg:1613463827580&source=Int&tbs=ar:1&sa=X&ved=0OahUKEwjK07OS_e3uAhVkrXUIHXWoBgUQpwUIKQ&biw=1366&bih=638&dpr=1)
  22. Mcquade DT, Seeberger PH. Applying Flow Chemistry: Methods, Materials, and Multistep Synthesis. *J Org Chem*. 2013;78:6384–9.
  23. Uniqsis Ltd. The FlowSyn System [Internet]. [cited 2019 Jun 25]. Available from: <https://www.uniqsis.com/paFlowSystem.aspx>
  24. Wegner J, Ceylan S, Kirschning A. Ten key issues in modern flow chemistry. *Chem Commun*. 2011;47:4583–92.
  25. Sharma UK, der Eycken E V. Flow Chemistry for the Synthesis of Heterocycles. Springer International Publishing; 2018. 12–13 p. (Topics in Heterocyclic Chemistry).
  26. McPake CB, Sandford G. Selective Continuous Flow Processes Using Fluorine Gas. *Org Process Res Dev*. 2012 May 18;16(5):844–51.
  27. Sandford G. 12 - Continuous Flow Selective Direct Fluorination Using Fluorine Gas. In: Groult H, Leroux FR, Tressaud ABT-MSP and (R) of FC, editors. Elsevier; 2017. p. 339–48.
  28. Kappe CO, Dallinger D. Controlled microwave heating in modern organic synthesis: highlights from the 2004–2008 literature. *Mol Divers*. 2009;13(2):71.
  29. Hessel V. RSC/SCI: Continuous Processing and Flow Chemistry Symposium. 2010.
  30. Porta (R), Benaglia M, Puglisi A. Flow Chemistry : Recent Developments in the Synthesis of Pharmaceutical Products. *Org Process Res Dev*. 2016;20(1):2–5.
  31. Karnatz FA, Whitmore FC. DEHYDRATION OF DIETHYLCARBINOL. *J Am Chem Soc*. 1932 Aug 1;54(8):3461.
  32. Akelah A. Heterogeneous Organic Synthesis using Functionalised Polymers. *Synthesis (Stuttg)*. 1981;1981(06):413–38.
  33. Kirschning A, Monenschein H, Wittenberg (R). Functionalized Polymers—Emerging Versatile Tools for Solution-Phase Chemistry and Automated Parallel Synthesis. *Angew Chemie Int Ed*. 2001 Feb 16;40(4):650–79.
  34. Jaunzems J, Kashin D, Schönberger A, Kirschning A. Polymer-Bound Diphenylphosphane Hydrobromide, a Mild Acid for the Activation of Enol Ethers: Applications in Polymer-Assisted

- Glycosidations. *European J Org Chem*. 2004 Aug 1;2004(16):3435–46.
35. Sussman S. Catalysis by Acid-Regenerated Cation Exchangers. *Ind Eng Chem*. 1946 Dec 1;38(12):1228–30.
  36. Ley S V, Ladlow M, Vickerstaffe E. The Use of Polymer-Assisted Solution-Phase Synthesis and Automation for the High-Throughput Preparation of Biologically Active Compounds. In: Bartlett P, Entzeroth M, editors. *Exploiting Chemical Diversity for Drug Discover*. Royal Society of Chemistry; 2007. p. 1–31.
  37. Baxendale IR, Ley S V. Solid Supported Reagents in Multi-Step Flow Synthesis. In Springer International Publishing; 2007. p. 151–85.
  38. Blossey EC, Ford WT. 3 - Polymeric Reagents. In: Allen G, Bevington JCBT-CPS and S, editors. *Amsterdam: Pergamon; 1998. p. 81–114.*
  39. Naka K. Polymer Reagents BT - Encyclopedia of Polymeric Nanomaterials. In: Kobayashi S, Müllen K, editors. *Berlin, Heidelberg: Springer Berlin Heidelberg; 2014. p. 1–5.*
  40. Baxendale IR, Ley S V, Mansfield AC, Smith CD. Multistep Synthesis Using Modular Flow Reactors : Bestmann – Ohira Reagent for the Formation of Alkynes and Triazoles. *Angew Chemie*. 2009;121(22):4017–21.
  41. Tsubogo T, Oyamada H, Kobayashi S. Multistep continuous-flow synthesis of ((*R*))- and (*S*)-rolipram using heterogeneous catalysts. *Nature*. 2015;520(7547):329–32.
  42. Gauthier DRJ, Sherry BD, Cao Y, Journet M, Humphrey G, Itoh T, et al. Highly efficient synthesis of HIV NNRTI doravirine. *Org Lett*. 2015 Mar;17(6):1353–6.
  43. Ziegler RE, Desai BK, Jee J-A, Gupton BF, Roper TD, Jamison TF. Corrigendum: 7-Step Flow Synthesis of the HIV Integrase Inhibitor Dolutegravir. *Angew Chem Int Ed Engl*. 2018 Nov;57(46):14969.
  44. Pinho VD, Gutmann B, Miranda LSM, de Souza RO, Kappe CO. Continuous Flow Synthesis of  $\alpha$  - Halo Ketones: Essential Building Blocks of Antiretroviral Agents. *J Org Chem*. 2014;79(4):1555–62.

# *Results and Discussion*

*The synthetic pathway taken for the project; the synthesis of tenofovir and its prodrugs, TD and TA.*

## Chapter 3: Synthesis and isolation of hydroxypropyl adenine (HPA)

### The alkylation of adenine: General applications

Alkylated adenine derivatives have been extensively studied over the years because of interest in their important biological roles.<sup>1</sup> The *N*-9 substituted adenine derivatives in particular, have been shown to have potent biological activity against several targets, and as a result are arguably the most commonly encountered derivatives of adenine. They have been widely reported to have antiviral activities against targets like HIV and hepatitis B, HBV, (see introductory chapter 1).<sup>2,3</sup> In addition, they also act as phosphodiesterase (PDE) isozyme inhibitors (specifically PDE-4),<sup>4</sup> with anti-inflammatory activity, that helps combat asthma, atopic dermatitis, rheumatoid arthritis, multiple sclerosis and autoimmune diseases,<sup>2,5-7,16-18</sup> and several *N*-9-alkyladenines have also been shown to act as cytotoxic agents.<sup>8</sup>

Adenine **27** forms part of the four biological nucleic acid bases (nucleobases). Nucleobases can exist, theoretically, as different tautomers when considering the different positions that the hydrogen atom can take (figure 3.1). Biologically, this might lead to different biochemical reactions, such as point mutations during DNA replication, however, tautomerization is a rare event and the nucleobases tend to be predominantly present in the form of the most stable tautomer. Studies have been conducted that show that 9-*H*-adenine (**27**) is the predominant tautomer in both solution and gas phase, however, in the presence of water the relative stability of the tautomers can change due to water assisted/promoted proton transfers<sup>9-11</sup>

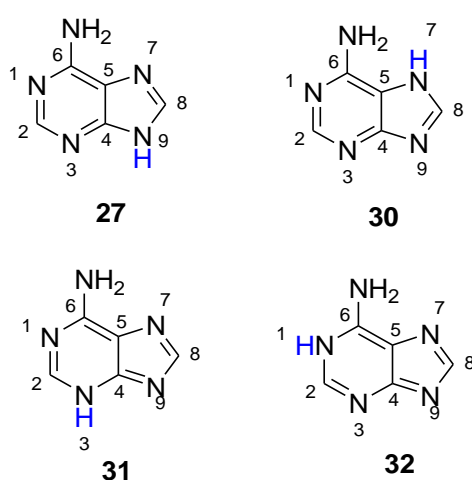
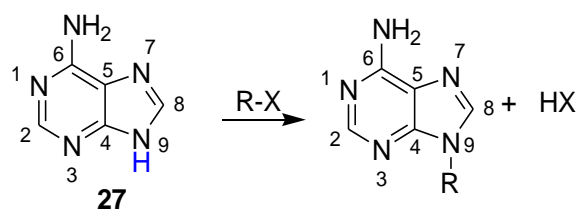


Figure 3.1: Tautomers of adenine.\*

\*Please note that "adenine" could refer to any/all tautomer(s) unless specified in text or using the compound number (i.e. 27, 30, 31 or 32).

The 9-*H* adenine tautomer (**27**) is reported to have the lowest energy when compared to the other tautomeric forms, however, both 7-*H* (**30**) and 9-*H* (**27**) tautomers can co-exist in polar solutions, in varying ratios according studies by Salter *et al.*<sup>10</sup> They also reported that the formation of the 3-*H* tautomer (**31**) may take place in a polar solution upon electronic excitation (also that the 1-*H* tautomer (**32**) energy is also lowered in the excited state). The general consensus between the computational studies is that the tautomers should exist as follows 9-*H*<7-*H*<3-*H*<1-*H* in moving from the lowest to highest ground state energy.<sup>10</sup>

As a result, the alkylation of **27** through an S<sub>N</sub>2 type reaction, should result in the formation of an *N*-9 alkylated product (scheme 3.1).

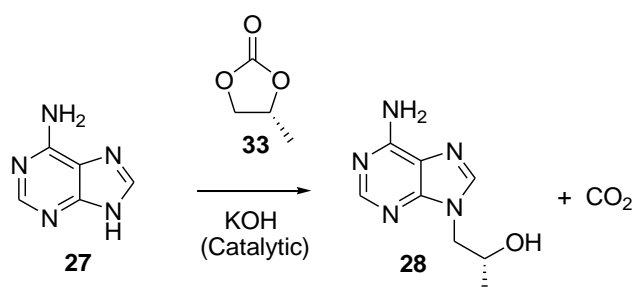


Scheme 3.1: A generic example of the alkylation of adenine to afford *N*-9-alkylated adenine. *X* is a halide leaving group.

#### A. First step of the synthetic pathway of TD/TA: The alkylation of adenine at the *N*-9 position.

##### 3.1) Synthesis of HPA: Solubilizing adenine (choosing the right solvent).

The common initial step towards the synthesis of TD **25**/TA **26** is an *N*-9 alkylation of **27** using a chiral carbonate (as opposed to the more commonly reported alkyl halides) in the presence of catalytic base (scheme 3.2).<sup>20-22</sup>



Scheme 3.2: Initial step of the synthetic pathway of both TD /TA (formation of HPA via the alkylation of adenine).

One of the major issues with realising an efficient flow (synthesis) translation of this step is the solubility of adenine **27**. Nucleobases are well known to be challenging to work with, with regard to solubility, with adenine being the least soluble in water, followed by guanine, thymine and then cytosine.<sup>12</sup> The solubility is not just an issue in water, but also in organic solvents.<sup>13</sup> Nucleobases are highly polar molecules with multiple proton-donating and accepting capabilities. Zielenkiewicz *et al* performed studies that indicated the polar interactions with these nucleobases are the key to their solubilities,<sup>14</sup> and so it is reasonable to expect polar media to be the most solubilizing of these molecules.

Attempts have been made to increase the solubility of nucleobases in aqueous solutions,<sup>12,15 16</sup> and in most cases the goal was to increase solubility by the increasing the ionic strength of the aqueous solvent to better dissolve the polar nucleobases. Studies by Hart and co-workers<sup>15</sup> as well and Hirano *et al*,<sup>17</sup> reported on the addition of inorganic salts like KOH and HCl, respectively, but these only led to marginal improvements in solubility. Hirano and co-workers also attempted to use the amino acid, arginine, as an additive to improve the solubility, with positive results for all the nucleobases at pH 7.<sup>17</sup> Currently, what has gained popular interest, because of their solvation properties, are the use of ionic liquids. Ionic liquids contain both charged and (variable) hydrophobic regions that allow them to dissolve a wide array of molecules and a study by Ghoshdastidar *et al* showed that the solubility of adenine **27** and some amino acids could be increased through the use of ionic liquids in an aqueous system.<sup>18</sup>

Although the findings are arguably a step forward, the advance is still limited as it is based only in an aqueous environment, which is important in biochemical research, but it is practically limiting in a chemical laboratory where manipulating nucleobases often requires anhydrous conditions and the use of organic solvents. As a result, the solubilization of nucleobases in non-aqueous solvents needs further exploration.

Thus far, the most commonly reported solubilizing organic solvents for nucleobases, particularly adenine **27**, have been aprotic polar solvents such as dimethylformamide (DMF), dimethyl sulfoxide (DMSO), *N*-methyl-2-pyrrolidone (NMP), and the toxic hexamethylphosphoramide.<sup>16</sup> A closer look at adenine **27** reveals that the interactions it has with aprotic solvents require activation by heat, because at room temperature adenine **27** remains insoluble in all these solvents. A further observation is that adenine **27** tends to be better dissolved in the presence of a base.<sup>12,15</sup>

As part of this study we aimed to assess the use of several polar organic solvents including dimethyl sulfoxide, glycerol, dimethylformamide, *N*-methyl-2-pyrrolidone and ethoxy ethanol for the *N*-9

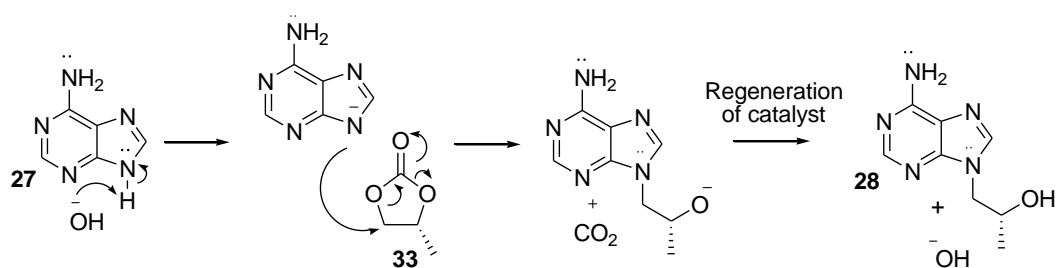
alkylation of **27** in the presence of base. The solvents chosen presented attractive qualities that could possibly accommodate an adenine-based reaction mixture.

Dimethyl sulfoxide is a high boiling point polar aprotic solvent (189 °C) that characteristically is highly solubilising. For example, bases are easily solubilized because dimethyl sulfoxide is only weakly acidic and it can readily accommodate strong bases. Dimethyl sulfoxide is also well suited to dissolve cations because of its highly polarized oxygen.<sup>19</sup> In addition, dimethyl sulfoxide readily dissolves both polar and nonpolar molecules because of its amphipathic character, arising due to the presence of a highly polar sulfonyl group that is flanked by two nonpolar methyl groups. Both dimethylformamide and *N*-methyl-2-pyrrolidone are also high boiling point polar aprotic solvents (153 °C and 202 °C, respectively) that are commonly used for similar reactions to dimethyl sulfoxide. Dimethyl sulfoxide, however, is regarded as the safer alternative for both these solvents, presenting less toxic effects.<sup>20,21</sup>

Ethoxy ethanol, unlike the other solvents investigated, is protic in nature, has a lower boiling point (135.6 °C) than dimethyl sulfoxide and is attractive as it can be more readily removed post-reaction. Glycerol was also attractive as it is considered a green solvent that is relatively polar and is able to dissolve both organic and inorganic compounds. For this project, all these solvents were investigated for this first stage.

### 3.2a) Synthesis of HPA: The reagents used for the alkylation of adenine to form HPA.

This first stage (scheme 3.2) in the synthesis of TD **25** /TA **26** is an S<sub>N</sub>2 alkylation reaction using either sodium or potassium hydroxide to facilitate a nucleophilic attack of the least sterically hindered electron-deficient carbon of (*R*)-propylene carbonate **33**, by adenine **27**. The process is driven by the release of gaseous carbon dioxide, affording an anion, followed by protonation of the anion resulting in the regeneration of the base and formation of HPA **28** (Scheme 3.3).



Scheme 3.3: S<sub>N</sub>2 mechanism involved in the alkylation of adenine with (*R*)-propylene carbonate, using catalytic amounts of base (OH<sup>-</sup>).

In literature there have been several attempts to deprotonate adenine **27** at the *N*-9 position using bases of differing size and alkalinity. *Riley et al*<sup>22</sup> tested different bases catalytically, including NaOH, KOH, K<sub>2</sub>CO<sub>3</sub> and LiOH. The size of the metal ion seemed to influence the efficiency of the deprotonation, with conversion increasing with increasing size of the metal cation (K<sub>2</sub>CO<sub>3</sub>>KOH>NaOH>LiOH). These results suggest potential stabilization of the anionic intermediate by the metal cation.

The potassium ion being larger in size than the sodium ion seemed to better stabilize the *N*-9 intermediate, potentially by allowing greater contact time of the nucleophile with the electrophilic carbonate, hence the faster conversion of adenine **27** into HPA **28**, given the same reaction conditions. The nucleophilic attack favours the C4 position of the carbonate as it is less sterically hindered than the C3 position. As such, the desired secondary alcohol is formed with retention of stereochemistry, this has previously been evidenced in literature by crystal structures.<sup>23</sup>

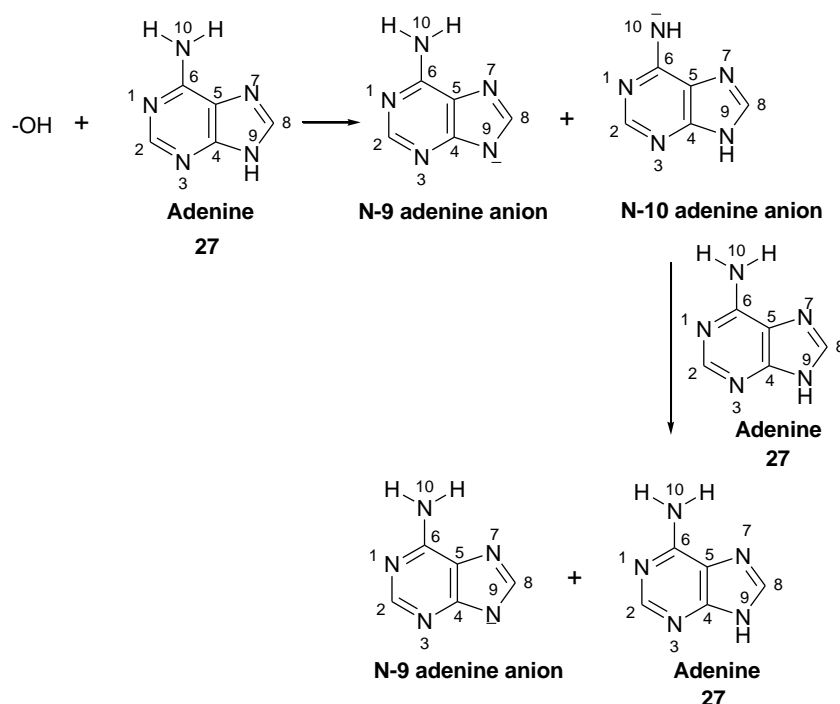
### **3.2b) Synthesis of HPA: The possible isomers from the alkylation of adenine to form HPA.**

The deprotonation of adenine has been shown experimentally to produce differing ratios of the: *N*-9, *N*-7 and *N*-3 isomers,<sup>24,25</sup> depending on the base used as well as the reaction parameters. Research has shown that deprotonation of the *N*-9 position is favoured under inert conditions while *N*-7 is most commonly obtained when using hydrous solvents/conditions,<sup>10</sup> accompanied by trace amounts of the *N*-3 product as well. *Rejnek et al.*<sup>26</sup> concluded from their findings, having studied the free energies of the tautomers in both micro and bulk hydration states, that the presence of water reduces the free energy state of both *N*-7 and *N*-3. The calculated energy states in bulk hydration were as such that the *N*-9 tautomer remained the most stable and both *N*-7 and *N*-3 had comparable free energies, supporting their co-existence in bulk hydration state.<sup>26</sup> Gu J. and Leszczynski J<sup>11</sup> conducted a DFT study on the effect water has on the tautomerization and found that the water molecules assist in the proton transfer from one tautomer to the other by lowering the activation energy associated with intramolecular proton transfer. Their computational studies also investigated the *N*-9/*N*-7 selectivity in the presence and absence of water<sup>11</sup> and concluded that although *N*-7 regioisomer in a hydrated environment has reduced activation energy, it is still not more stable than the *N*-9 regioisomer under the same conditions.

Another isomer that is occasionally observed involves alkylation at the exocyclic amine with Ripin *et al* noting that when they formed HPA, the main impurity observed was the exocyclic isomer.<sup>27</sup> They did not, however, provide any corroborations to their claim and it is still unclear why they did not consider the other possible isomers mentioned above.



Sharma S. and Lee J.K. reported that deprotonation at the exocyclic amine and *N*-9 position, using a strong base, does occur, however, the *N*-10 anion isomerizes to the *N*-9 anion, in the presence of neutral adenine **27** (scheme 3.4).<sup>28</sup>



Scheme 3.4: Isomerization of the *N*10- adenine anion to *N*-9- adenine anion.<sup>28</sup>

### 3.3) First step of the synthetic pathway: The experimental alkylation of adenine to form HPA.

As mentioned before, in an effort to identify an appropriate solubilising solvent system for flow translation of this step we investigated the use of several polar protic and aprotic solvents including dimethyl sulfoxide, dimethylformamide, *N*-methyl-2-pyrrolidone, glycerol and ethoxy ethanol, under standard batch conditions (table 3.1).

Table 3.1: Yields obtained for HPA in the different solvent systems.

Reaction Solvent	Reaction Time (hours)	Work-up Solvent	Yield (%)		Ratio of Isolated HPA Regioisomers ( <i>N</i> -9: <i>N</i> -7/ <i>N</i> -3: <i>N</i> -7/ <i>N</i> -3) <sup>a</sup>	
			Dry <sup>b</sup>	Wet <sup>b</sup>	Dry <sup>b</sup>	Wet <sup>b</sup>
DMSO	2.5	EtOH	54	60	1:0:0	10:1:1
DMF	3.0	EtOH	51	54	7:1:0	10:1:1
NMP	3.5	EtOH	54	58	7:1:0	10:1:1
Ethoxy EtOH	16	EtOH	0		N/A	
Glycerol	16	N/A	0		N/A	

<sup>a</sup> The first digit in the ratio represents the *N*-9 regioisomer, the second and third could not be conclusively determined and so for the purpose of the table, the second digit in the ratio could represent either *N*-7 or *N*-3, and the same applies with the third digit of the ratio. Please note that the

second and third digit cannot represent the same regioisomer concurrently.<sup>b</sup> “Dry” refers to anhydrous solvent use and “Wet” refers to hydrous solvent use.

Standard conditions: **27** (1 equiv), KOH (0.1 equiv), solvent (1.5 M), **33** (1.3 equiv), 120 °C. Work-up, trituration with EtOH

Dimethyl sulfoxide, dimethylformamide and *N*-methyl-2-pyrrolidone all afforded HPA **28** in moderate yields of 51-54% under anhydrous conditions and 54-60% under hydrous conditions with reasonably short reaction times ranging from two-and-a-half to three-and-a-half hours (Table 3.1). Unfortunately, both ethoxy ethanol and glycerol afforded no conversion to HPA **28**. In the case of ethoxy ethanol the reaction mixture was readily solubilised, however, no HPA **28** was detected even after sixteen hours of heating. Glycerol, on the other hand, did not solubilize the reaction mixture at all. These solvent systems failed even with manipulation of temperature (maximum 150 °C), equivalence of base (as high as 1:1), reaction time and concentration (as much as 3 M). The solvent systems were concluded as unsuccessful and as such only the three solvents (dimethyl sulfoxide, dimethylformamide and *N*-methyl-2-pyrrolidone) that were successful were subjected to additional testing.

### 3.3a) The experimental alkylation of adenine to form HPA: Assigning the regioisomers of HPA.

Although **28** was the expected major product, we still had the possibility of forming both **34** and **35** (figure 3.2). For this reason, we had to be able to distinguish between the regioisomers using spectral analysis (table 3.2).

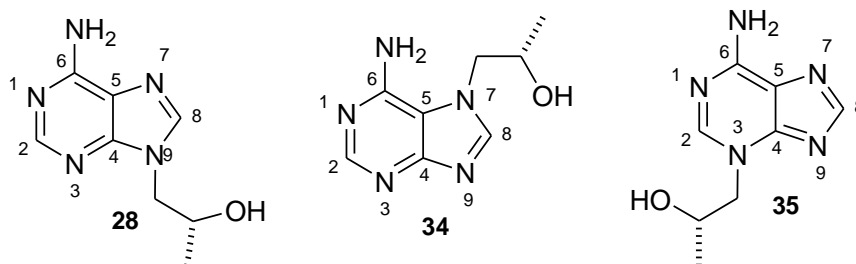


Figure 3.2: The possible HPA regioisomers: N-9, N-7 and N-3.

\*Please note that “HPA” could refer to any/all regioisomer(s) unless specified in text or using the compound number (i.e. 28, 34 or 35).

Table 3.2: <sup>1</sup>H NMR spectrum chemical shifts (ppm) of HPA from the respective literature sources.

HPA Regiomers	Reference	2-H	8-H	N-H	(CH <sub>2</sub> CH)-H	Solvent
<b>N-9 (28)</b>	Gao et al. <sup>23</sup>	8.13 (s)	8.03 (s)	7.06 (s)	4.10 + 3.99 (m)	DMSO-d <sub>6</sub>
	Chavakula et al. <sup>29</sup>	8.14 (s)	8.05 (s)	7.19 (br,s)	4.06 (m)	DMSO-d <sub>6</sub>
	Lambertucci et al. <sup>30</sup>	8.13 (s)	8.05 (s)	7.21 (br, s)	4.06 (m)	DMSO-d <sub>6</sub>
<b>N-7 (34)</b>	Lambertucci et al. <sup>30</sup>	7.74 (s)	8.20 (s)	7.85 (br,s)	4.05 + 4.33 (m)	DMSO-d <sub>6</sub>
<b>N-3 (35)</b>	Gao et al. <sup>23</sup>	8.20 (s)	7.74 (s)	7.86 (br,s)	4.35 + 4.13 (m)	DMSO-d <sub>6</sub>

s= singlet; m= multiplet; br=broad peak

From the information gathered in table 3.2 we can note the following:

- Gao *et al.*<sup>23</sup>, Lambertucci *et al.*<sup>30</sup> and Chavakula *et al.*<sup>29</sup> all agree with the 2-H and 8-H chemical shift being at 8.1 and 8.0 ppm, respectively, for the N-9 regioisomer of HPA (**28**).
- Lambertucci *et al.*<sup>30</sup> places 2-H of the N-7 regioisomer (**34**) upfield of the 2-H of the N-9 regioisomer (**28**) at 7.7 ppm.
- Lambertucci *et al.*<sup>30</sup> also differs in their placement of the 8-H of the N-7 regioisomer (**34**) (from the N-9 regioisomer) placing it downfield to the 8-H of the N-9 regioisomer (**28**), at 8.2 ppm.
- Gao *et al.*<sup>23</sup> reported that the 2-H of the N-3 regioisomer had a chemical shift of 8.2 ppm, which is downfield to both that of the N-9 and N-7 regioisomers.

- e. Gao *et al.*<sup>23</sup> also reported 8-H at 7.7 ppm, upfield from both the reported 8-H of *N*-9 and *N*-7 regioisomers. These would imply that both *N*-7 and *N*-9's 2-H and 8-H peaks would lie in between the peaks of *N*-3's 2-H and 8-H respectively.

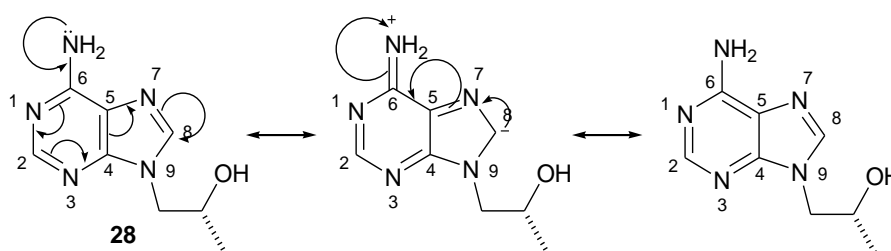
Oddly enough, Gao *et al.*<sup>23</sup> and Lambertucci *et al.*<sup>30</sup> both recorded the exact same chemical shift readings for the aromatic protons (8.20 and 7.74 ppm) but assigned them oppositely (for *N*-7, 8-H is 8.20 and 2-H is 7.74 ppm, while the opposite applies for *N*-3).

The regioisomers can be identified using NMR spectroscopy by looking at the relative chemical shifts of the 8-H and 2-H protons. In the <sup>1</sup>H NMR, however, the 8-H and 2-H proton of *N*-7 (**34**) and *N*-3 (**35**) have similar shifts (table 3.2) and so to distinguish between them 2D NMR, such as HMBC, would be necessary (Gao and his group<sup>23</sup> have studied this previously). For our research, our main focus was on the major product, *N*-9 (**28**), and since its 8-H and 2-H <sup>1</sup>H NMR shifts were easily distinguishable from both those of **34** and **35**, we decided to merely use <sup>1</sup>H NMR for analysis. This would mean that we could not confirm if any of the minor regioisomer isolated belonged to *N*-7 or *N*-3, and so we have reported the ratios as belonging to either.

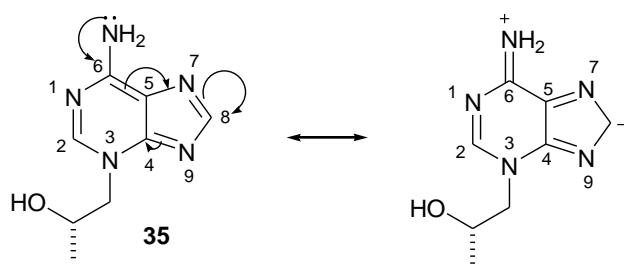
### Chemical shifts from table 3.2.

In the case of both **28** and **35** the 8-H proton is more shielded than the 2-H proton as each of the regioisomers have a resonance structure that has a negative charge on 8-H (scheme 3.5 and 3.6).

The 8-H resonance structure is, however, slightly more shielded (7.7 ppm) on **35** than **28** (8.03 ppm) probably due to its limited aromaticity compared to **28**. The 2-H of **35** is slightly more deshielded (8.20ppm) compared to the **27** (8.13ppm). This can be attributed to the additional resonance structures of the **28** that includes both *N*-7 and *N*-8 atoms, having a slightly greater push of electron density into the 5-membered ring (increase shielding) and hence a slight deshielding effect in the 6-membered ring.

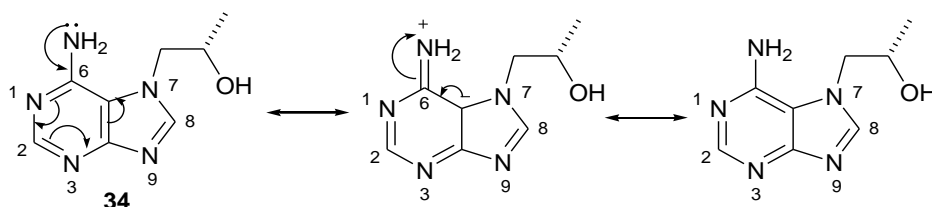


Scheme 3.5: Illustration of the possible resonance structures of *N*-9 HPA.



Scheme 3.6: Illustration of the possible resonance structures of *N*-3 HPA.

For **34**, the chemical shifts (table 3.2) show 8-H is more deshielded than its 2-H counterpart. The resonance structures (scheme 3.7) show that the five-membered ring does not take part in the aromaticity of the structure while the six-membered ring does, which goes to explain why 2-H would experience more electron density than 8-H, hence it is more upfield. The resonance structures for *N*-7 and *N*-3 are also shown in schemes 3.7 and 3.6, respectively.



Scheme 3.7: Illustration of the possible resonance structures of *N*-7 HPA.

Based on the literature reports on the chemical shifts of 2-H and 8-H of **28**, **34** and **35** (7.74 ppm – 8.20 ppm), we allocated the  $^1\text{H}$  NMR chemical shifts of our experimentally obtained crude HPA product. From this, the integrals of the shifts were taken to determine the ratio (*N*-9:*N*-7/*N*-3) of regioisomers present in the isolated product.

### 3.3b) The experimental alkylation of adenine to form HPA: Regioisomers of HPA in different solvent systems.

Going back to the results in table 3.1, we can see that in addition to having an influence on the yield of HPA, the presence/absence of water also had an effect on the regioselectivity of the process. In hydrous systems, all three possible regioisomers were observed in a fixed 10:1:1 ratio, whereas, in anhydrous solvents, only one or two regioisomers (*N*-9 and/or *N*-7 or *N*-3) were observed. For anhydrous dimethyl sulfoxide, only *N*-9 was obtained while both anhydrous *N*-methyl-2-pyrrolidone and dimethylformamide resulted in a 7:1:0 ratio of *N*-9: *N*-7 (or *N*-3).

As discussed previously, the presence of water stabilizes some tautomers in solution with the water molecules assisting in the transfer of protons.<sup>18</sup> That being said, although the presence of water results in more tautomers found in solution, the rate of tautomerization appears to significantly favour the *N*-9 tautomer in a 10:1 ratio as evidenced through the analysis of the integral traces from the obtained NMR spectra. This contrasts with literature which suggests that water can *drastically* affect the stability of tautomers.<sup>9</sup> In computational studies conducted by Hanus *et al.*<sup>26</sup> the extent of hydration in the system seemed to have a link to the level of tautomerization in the system. The group performed computational studies which they described as “micro” (one to two water molecules) and “bulk” (continuous) hydration systems of **27**. The studies suggested that tautomerization was more rapid in

bulk hydration states than in microstates. Hanus *et al.*<sup>23</sup> stated that dehydration offers slightly increased stability to the tautomers as compared to monohydration. In contrast, Shukla *et al.*<sup>21</sup> in an overview concluded that nucleic bases do not tautomerize in bulk water solutions and exist in their respective canonical forms.<sup>24</sup> Singh *et al.*<sup>26</sup> supported this claim, stating that one of the challenges faced in aqueous conditions is the low abundance of minor tautomers, owed to the fast rate of tautomeric equilibria.<sup>31</sup>

Our experimental results tend to support the claims of Singh *et al.*<sup>26</sup> and Shukla *et al.*<sup>21</sup> seeing that in hydrated solvent systems, there was an overwhelming presence of one regioisomer, *N*-9, indicating that tautomerization was not significantly at play. We could not confidently attribute the contradiction of our results to the conclusions of Hanus *et al.*<sup>26</sup> to the level of hydration in our systems (which we could not analytically quantify) but perhaps we could assume that the duration that the nucleobase (**27**) was left exposed to the solvent might have also played a role in the level of tautomerization that took place. Possibly further studies that accurately control the amount of water in the system as well as the time of exposure of adenine to the solvent system might reveal different results in terms of isomeric ratios obtained. This, however, fell beyond the scope of this project.

In anhydrous dimethyl sulfoxide, only the *N*-9 regioisomer was present after isolation, while dimethylformamide and *N*-methyl-2-pyrrolidone afforded the *N*-9 and *N*-7 (*N*-3) regioisomers, with the *N*-9 being favoured in a ratio of 7:1. A possible explanation for the presence of the minor regioisomer, in both dimethylformamide and *N*-methyl-2-pyrrolidone systems could be linked to the time taken to fully dissolve adenine. The time of dissolution in the dimethylformamide and *N*-methyl-2-pyrrolidone systems typically required 30 minutes additional heating compared to that of the dimethyl sulfoxide system; and one could argue that when using dimethylformamide and *N*-methyl-2-pyrrolidone, adenine **27** could have had more time to tautomerize than when dissolved in dimethyl sulfoxide. The identity of the solvent may also play a role, however, that in itself is still intrinsically linked to the rate of dissolution.

As expected, the high boiling point aprotic solvents (dimethyl sulfoxide, dimethylformamide and *N*-methyl-2-pyrrolidone) acted similarly in a sense that they all were able to successfully dissolve the reaction mixture, albeit at high temperatures, with two-and-a-half to three-and-a-half hours reaction times affording optimal conversion. Dimethyl sulfoxide was most attractive in the sense that it was the safest and greenest of the three polar aprotic solvents (has low toxicity, is recyclable and environmentally friendly).<sup>21</sup> In comparison, *N*-methyl-2-pyrrolidone and dimethylformamide have associated toxicities and are both not classified as green solvents.

The question did arise as to why dimethyl sulfoxide was the better solvating solvent for this reaction. As mentioned previously, studies have shown that the key to the solubility of nucleobases is in the polar interactions with the solvent and in this instance, dimethyl sulfoxide has the highest dielectric constant (47) of the three polar aprotic solvents, implying that it would more readily dissociate KOH into its respective ions than dimethylformamide or *N*-methyl-2-pyrrolidone. This avails the  $\text{OH}^-$  ions to more rapidly deprotonate the most acidic proton of **27** (9-H), and hence drives the formation of HPA in a shorter reaction time. This argument provides further insight as to why adenine **27** dissolves better in the presence of a base.

Still on the topic of solubility, it is also worth noting that when hydrous solvents were used, the reactions took about 20 minutes longer to dissolve adenine **27** than the anhydrous solvents counterparts. Water seemed to interrupt the interactions between adenine **27** and the anion (base) because of its strong hydrogen-bond-forming nature, hence the increase in time for dissolution. Overall, nevertheless, dimethyl sulfoxide was still best at solubilizing the inorganic salts / adenine combination.



## B. Post-conversion work-up: Isolation of HPA

### 3.4) Triturative work-up and purification.

The solubility issues associated with adenine **27** posed further problems with the downstream work-up and processing. The high boiling point aprotic solvents that are required to ensure the solubilisation of adenine **27** (dimethyl sulfoxide, dimethylformamide or *N*-methyl-2-pyrrolidone) could not be readily removed under standard evaporative conditions and furthermore, these solvents are miscible with water and most other organic solvents, inhibiting the use of solvent-extraction for the isolation of HPA.

As a result, a triturative work-up technique was employed to allow for the isolation of pure HPA. Trituration was chosen because it would take advantage of the difference in solubility of HPA in different solvents. For the polar aprotic solvents (dimethyl sulfoxide, dimethylformamide and *N*-methyl-2-pyrrolidone), polar protic or non-polar solvents would be good anti-solvents for the trituration. With that in mind, ethanol, *iso*-propanol, methanol (polar protic) and toluene (non-polar aprotic) were the solvents investigated for this process.

Table 3.3 shows the average yields of HPA **28** isolated from trituration with three different triturating solvent systems in the respective reaction solvents used. About five times the volume of reaction solvents had to be used for the triturative solvents in order to effectively change the environment of the target compound (HPA **28**) before it would precipitate out of solution. Also worth noting is that the yield of HPA **28** varied depending on the temperature in which the trituration solvent was added and also the amount of HPA **28** produced in the reaction, hence why average percentage yields are reported in table 3.3.

Table 3.3: Trituration work-up yields of HPA with the different reaction solvents.

Trituration Solvent	Reaction solvent Average yield (%)		
	DMSO	DMF	NMP
Ethanol	54	51	54
<sup>i</sup> Propanol/Methanol (1:1)	51	50	N/A
Toluene	70	60	N/A

Trituration in toluene gave the highest yield in both dimethyl sulfoxide and dimethylformamide, 70% and 60% respectively. Ethanol followed with a yield of 54% for both dimethyl sulfoxide and *N*-methyl-

2-pyrrolidone, and 51% for dimethylformamide. The mixture of *iso*-propanol/methanol (1:1) gave the lowest yield from the trituration technique. Overall, it seemed as though dimethyl sulfoxide coupled better with the solvents selected for trituration because it gave higher yields in all instances in comparison to dimethylformamide and *N*-methyl-2-pyrrolidone.

### 3.5) Ion-exchange chromatographic work-up and purification.

With the tritulative work-up being tedious, non-economical (copious amounts of solvents were required) and producing below 80% yields of HPA **28**, we decided to explore an alternative work-up technique. The use of solid-supported resins which are functionalised to act as scavengers represented an attractive alternative post-conversion work-up option because it would allow for the selective isolation of a compound depending on its functional groups. In the case of HPA **28**, the exocyclic amino group as well as the hydroxyl group are both suitable targets for a work-up utilising acid/base ion exchange resins. These functional group targets were potentially good handles for the selective removal of the product HPA **28** from the reaction matrix. Adenine **27** (the starting material and limiting reagent) has the exocyclic amine group in common with the target product HPA **28**, but because of the high conversion rates of the reaction (up to 97%) we believed that at best would only have a limited influence on the purity of the product if we were to use a resin that would target the exocyclic amine.

The other starting material (*R*)-propylene carbonate **33** which was used in excess, has free lone pairs of electrons on the oxygen atom which can interact with an acidic resin, however, the pKa of the oxygen (3.9) is much lower than that of the amine nitrogen (17) and so cation exchange is favoured between the proton donor and the amine group. The aprotic solvent used also poses no competitive interference with an acidic resin (figure 3.3).

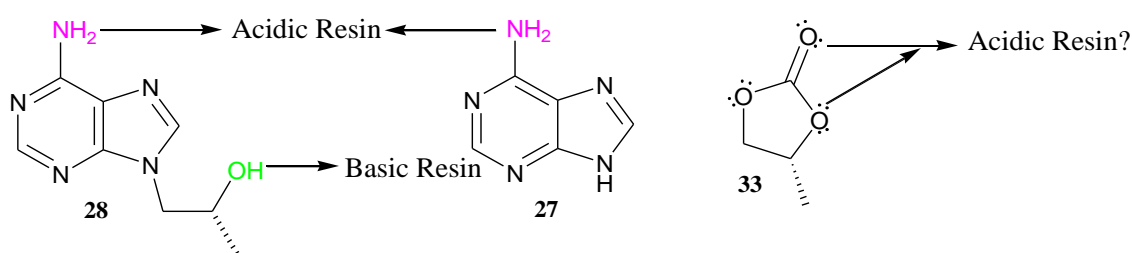


Figure 3.3: Potential target functional groups on HPA, adenine and (*R*)-propylene carbonate for resin work-up.

We chose to begin the resin work-up trials with an acidic / cation exchange resin, which was already readily available in the laboratory, to determine if we could isolate HPA **28** from the reaction mixture successfully in higher yields than when employing the tritulative work-up technique.

A rigid, macro porous resin, Amberlyst 15<sup>®</sup> **36** was selected for investigation (figure 3.4). Amberlyst 15<sup>®</sup> **36** is a safe to use and commercially available solid supported resin which was selected as it acts as a strong cation exchanger (an acidic resin) when immersed in a solvent.

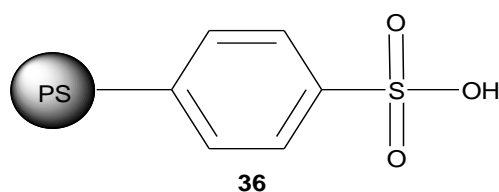
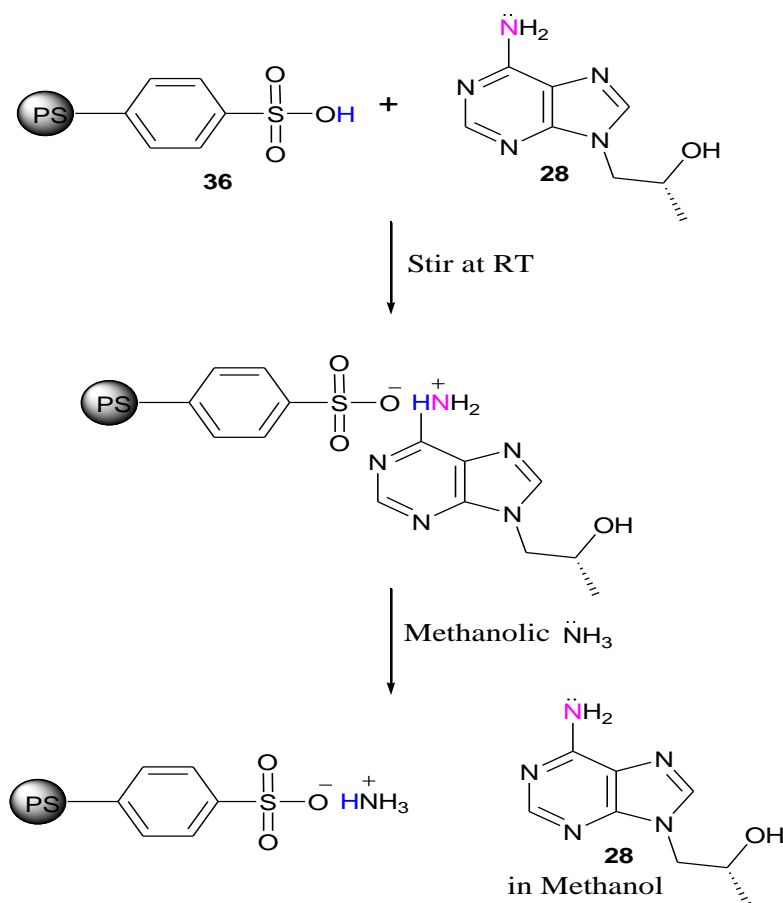


Figure 3.4: Amberlyst 15<sup>®</sup>

Amberlyst 15<sup>®</sup> **36** is a macro reticular polystyrene (styrene-divinylbenzene copolymer) based ion exchange resin that contains a sulfonic acid group which acts as a strong proton donor, as such the group will readily protonate the primary amine in our target product, HPA **28**.

As we mentioned, the use of Amberlyst 15<sup>®</sup> **36** as an ion-exchange resin allowed us to target the primary amine group found of HPA **28** (scheme 3.8).



Scheme 3.8: Amberlyst 15<sup>®</sup> and HPA interactions on a molecular level.

The acid-base exchange (ionic interaction) between the resin and HPA **28** (and residual adenine **27**) effectively removes the product from the reaction mixture, leaving behind impurities, primarily unreacted (*R*)-propylene carbonate**33**, in the liquor. The progress was monitored by TLC and deemed complete once HPA **28** was no longer visible under UV light. The ionic interaction between the functional groups (amine and sulfonic acid) could then be disrupted by either the addition of a stronger base or acid. If a stronger acid was used it would interact with the amine of HPA **28**, releasing it into the solution, however, this approach would then require an additional neutralization step to release HPA **28** as a neutral species into the organic solvent. The alternative was the use of a strong base which would interact with the resin, releasing HPA **28** into solution. We decided to make use of ethanolic ammonia, which allowed for the convenient release of HPA **28** as a neutral species into the solution, which was thereafter followed by simple removal of the solvent *in vacuo*.

The drawback to this approach was that it was more time consuming than the trituration and there was no selectivity between HPA and unreacted adenine **27**. The advantages as mentioned in the introductory chapter regarding resins, was that it was a simplified, selective and green (in terms of the amount of solvent that was required) alternative work-up. The results obtained using resin work-up compared to trituration are shown in table 3.4:

Table 3.4: Summary of the yields and regioisomer distribution of HPA when using a tritulative vs. ion exchange work-up and purification.

Work-up Method	Work-up Compound	DMF		DMSO	
		Yield (%)	Regioisomer Ratio <i>N</i> -9: <i>N</i> -7/3: <i>N</i> -3/7 <sup>a</sup>	Yield (%)	Regioisomer Ratio <i>N</i> -9: <i>N</i> -7/3: <i>N</i> -3/7 <sup>a</sup>
Trituration	<b>Propanol/Methanol (1:1)</b>	50	1:0:0	51	1:0:0
	<b>Toluene</b>	60	4:1:0	70	4:1:0
	<b>Ethyl acetate</b>	N/A	N/A	58	7:1:0
	<b>Ethanol</b>	51	7:1:0	54	1:0:0
<b>Ion-exchange resin</b>	<b>Amberlyst 15<sup>®</sup></b>	73	20:10:1	77	20:10:1

<sup>a</sup> The first digit in the ratio represents the *N*-9 regioisomer, the second and third could not be conclusively determined and so for the purpose of the table, the second digit in the ratio could represent either *N*-7 or *N*-3, and the same applies with the third digit of the ratio. Please note that the second and third digit cannot represent the same regioisomer concurrently.

Under both tritulative and ion-exchange conditions the isolated yields tended to be higher when the reaction was performed in dimethyl sulfoxide as opposed to dimethylformamide. Toluene afforded the highest yields when the reaction was performed in both dimethyl sulfoxide and

dimethylformamide, giving an average of 70 and 60% respectively, however, it also resulted in the isolation of the highest relative proportions of the minor regioisomers (*N*-7/*N*-3) with about 20% in trituration and 35% in resin based on NMR integrals. In comparison, the *iso*-propanol/methanol (1:1) mixture was arguably more attractive for the trituration work-up because only the *N*-9 isomer was isolated in both dimethyl sulfoxide and dimethylformamide, albeit with lower isolated yields (50-51%). Ethanol afford a slightly better yield of 54% of the pure *N*-9 regioisomer when using dimethyl sulfoxide, oddly when the reaction was performed in dimethylformamide followed by ethanol mediated trituration, the *N*-7 or *N*-3 regioisomer were again observed, in this case accounting for 12.5% of the material isolated. Ethyl acetate was also tested with dimethyl sulfoxide as the reaction solvent affording 58% yield with an *N*-9: *N*-7/3: *N*-3/7 distribution ratio of 7:1:0. The resin work up worked more effeciently in dimethyl sulfoxide, with a yield of 77%, but the regioisomeric ratios remained identical to those in dimethylformamide.

The ion-exchange chromatographic work-up (discussed in *chapter 2, page 20*) and purification seemed to isolate more of the minor regioisomers than trituration. The principles used for both techniques differ, for trituration, just like crystallization, the quantity of the compound plays a crucial role in determining which product is isolated (crashes out of solution).

Although the resin workup isolated higher yields than tritulative work-up, the impurity of the product (about 30%, based on <sup>1</sup>H NMR) made it the less preferred method, even when we consider its economic and environmental advantages. However, for the sake of a simplified continuous flow system synthesis and isolation of HPA, the flow trials would include the resin work-up.

### C. Translation of the alkylation of adenine (step 1) to flow-chemistry.

The translation of the synthesis of HPA **28** to flow would be beneficial if i) the reaction time could be reduced from that in batch, ii) the temperature required for the reaction could be reduced and/or iii) the reaction work-up could be included in an effective, continuous fashion.

We planned on having, initially, a simple set up for the flow reactor (figure 3.5 shows the clipart used for the accessories and consumables of the reactor) that would use HPLC pumps to combine a solubilized stock solution of 0.5 M adenine **27** with 10% KOH and merge it at a T-piece mixer with a stock solution of 1.5 M (*R*)-propylene carbonate **33**.

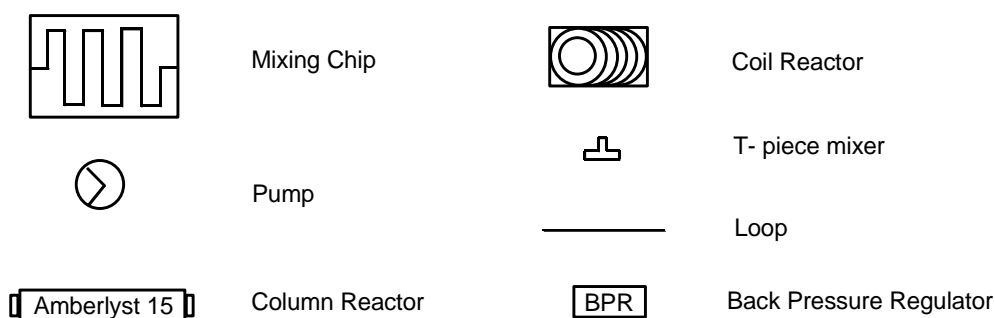
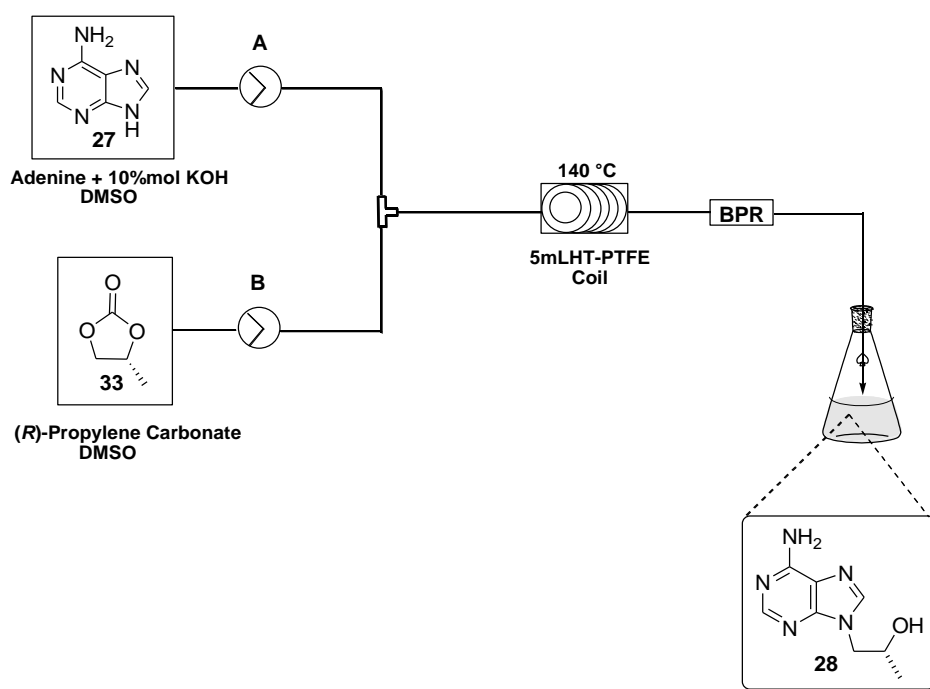


Figure 3.5: Flow reactor accessories and consumables clipart.

The mixture would thereafter be allowed to heat in an HT-PTFE coil reactor followed by passage of the expected product, HPA **28**, through a BPR (back pressure regulator) before collection (scheme 3.9). The coil reactor serves as the main temperature control agent (for heating and cooling of the reaction) in the system; it can be likened to the oil/ice bath in a batch system.<sup>32</sup>

Scheme 3.9 illustrates the flow set-up described using clipart from figure 3.5.



Scheme 3.9: A simplified representation of the flow reactor set-up for the synthesis of HPA\*

\* In order to ensure homogeneity in the system prior to entry into the flow reactor, the stock solution of adenine **27** and 10% KOH in DMSO were pre-heated at 140 °C for 20 min prior to entry into the flow reactor to ensure complete dissolution.

The entire flow system, including the heating coil, had an HT-PTFE tubing flow-path, but unfortunately the PTFE showed poor compatibility with dimethyl sulfoxide, resulting in dimethyl sulfoxide sweating through the tubing walls throughout the system. As such, we elected to replace the HT-PTFE with a stainless steel flow path, including the coil reactor. Thereafter the entire flow system remained sealed and no leakage problems were experienced. Trial runs were then performed as depicted in scheme 3.9 assessing the impact of residence time in the coil reactor, table 3.5.

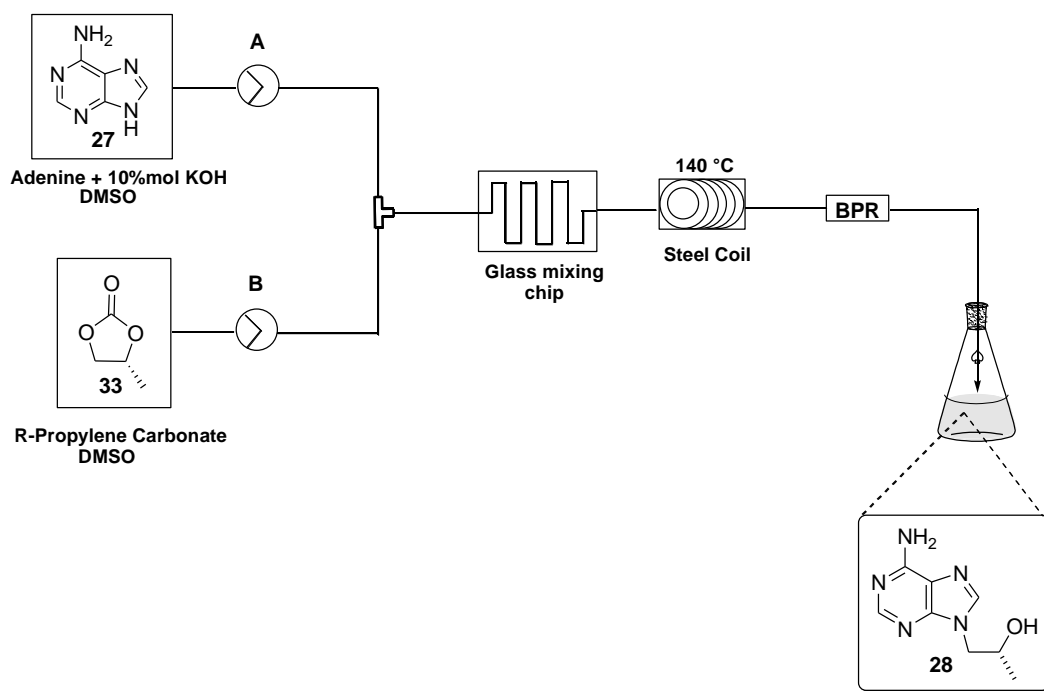
Table 3.5: The main flow parameters used for the initial flow trials.

Entry	Flow Rate (mL/min)	Temperature (°C)	Coil Volume <sup>a</sup> (mL)	Residence Time (hours:minutes:seconds)
1	0.1	140	5	04:27:54
2	0.2	140	5	02:18:16
3	0.4	140	5	00:58:52
4	0.6	140	5	00:53:26
5	0.8	140	5	00:42:34
6	1.0	140	5	00:35:58

<sup>a</sup> Stainless Steel

Unfortunately, using this setup no product formation was detected when screened with residence times ranging from thirty-six minutes to four-and-a-half hours. We suspected that on the relatively small test scale there was significant dispersion between the two reagent solutions preventing efficient mixing at the desired stoichiometric ratios.

As such we inserted a heated (120 °C) glass mixing chip into the reactor. The purpose of the mixing chip was to afford rapid turbulent mixing (Scheme 3.10).<sup>32</sup> In this instance we noted the immediate formation of HPA **28**.



*Scheme 3.10: A representation of the flow reactor set-up with an added glass chip.*

We then proceeded to screen a range of residence times (table 3.6) and an optimal residence time was found to be one hour and fifty-five minutes (0.2 mL.min<sup>-1</sup> flow rate), and at flow rates above 0.4 mL/min (one hour residence time) yields dropped off significantly.



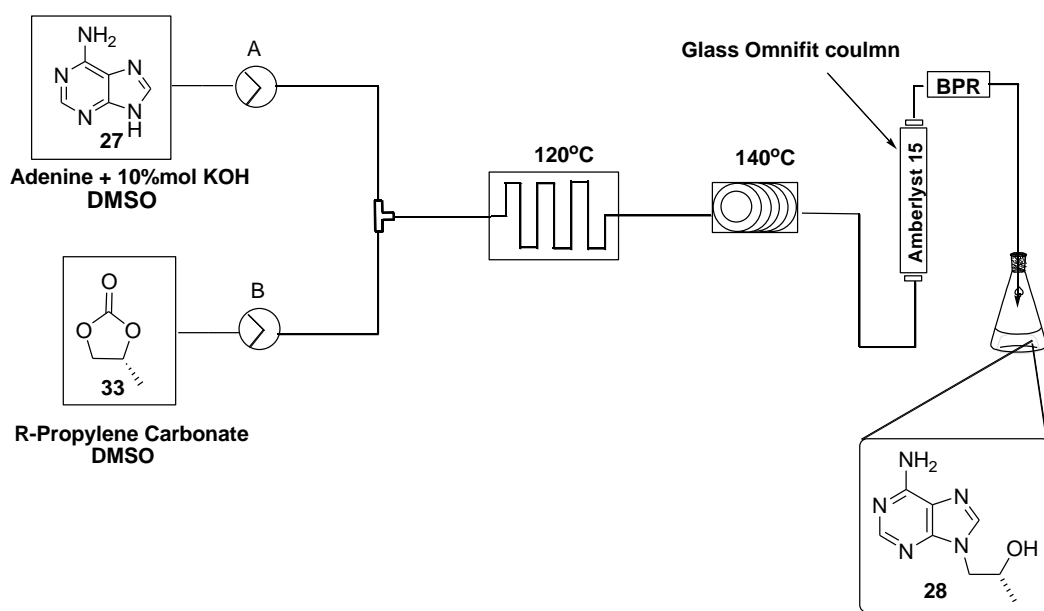
The conversions at 0.8 and 1.0 mL/min were not determined as TLC analysis suggested that unreacted adenine **27** was the overwhelmingly major component in those solutions.

Table 3.6: Flow parameters used with addition of a mixing chip to the system.

Entry	Flow Rate (mL/min)	Steel Coil		Glass Chip		Post Collect + Final Wash Vol. (mL)	Residence Time (hours:minutes:seconds)	Conversion (%)
		Temp (°C)	Coil Vol. (mL)	Temp. (°C)	Chip Vol. (mL)			
1	0.1	140	5	120	2	16	03:44:27	62
2	0.2	140	5	120	2	16	01:54:52	70
3	0.4	140	5	120	2	16	00:59:52	50
4	0.6	140	5	120	2	16	00:55:33	30
5	0.8	140	5	120	2	16	00:30:03	N/A
6	1.0	140	5	120	2	16	00:27:26	N/A

7 mL 1.3 M (R)-propylene carbonate **33** and 7 mL 1.0 M adenine **27** in 10% KOH were (both pre-heated at 140 °C). The product liquor was collected into the gently stirring Amberlyst 15<sup>®</sup> **36** solution and the same procedure mentioned in batch was implemented thereafter.

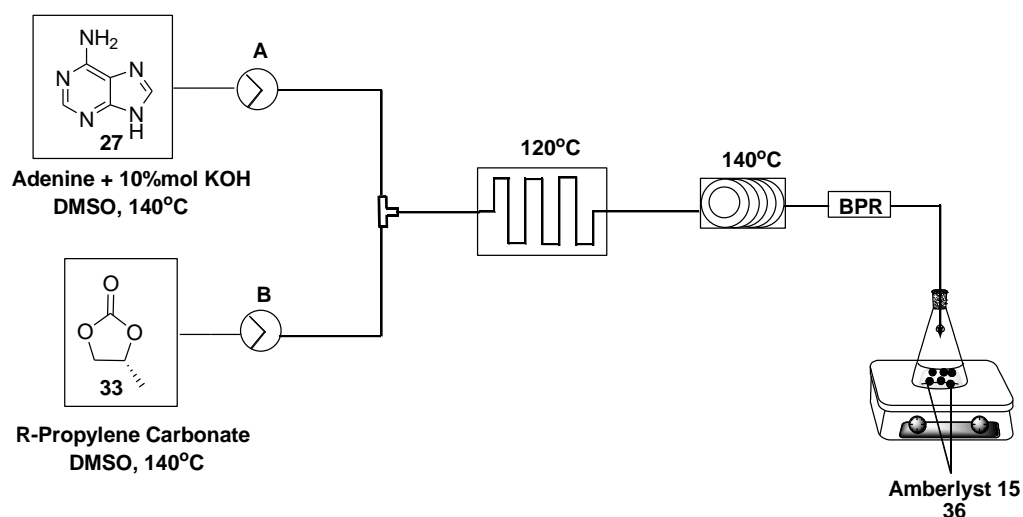
Using these optimised conditions and set-up, a post-conversion work-up point was added to test if pure HPA would be collected in a continuous flow fashion. To facilitate the inline purification a 10 mL glass Omnifit<sup>™</sup> packed-bed reactor (an accessory used to pack solids such as catalysts, scavengers, etc.)<sup>32</sup> housing Amberlyst 15<sup>®</sup> **36** resin was inserted between the coil reactor and the back pressure regulator (scheme 3.11).



Scheme 3.11: A representation of the flow reactor set-up with an added glass chip and packed-bed reactor containing Amberlyst 15<sup>®</sup>.

The Amberlyst 15<sup>®</sup> **36** resin was packed to the half-way calibration mark of the column and anhydrous dimethyl sulfoxide was allowed to flow into the column, causing the resin beads to swell, once swelling was deemed to be complete the column was sealed and the reaction was commenced. Unfortunately, after about an hour the column showed signs of leakage at its terminals, again the issue was found to be the use of dimethyl sulfoxide which was degrading the PTFE and PEEK end fittings of the column.

As we did not have access to alternative packed-bed reactor housing we ran several trials using both dimethylformamide/*N*-methyl-2-pyrrolidone as alternative solvents, however, these proved to be unsuccessful as both of these solvents failed to solubilize adenine **27** and KOH in the absence of (*R*)-propylene carbonate **33**. We then elected to perform the work-up/purification offline by allowing the reactor run-off to drip into a stirred flask housing Amberlyst 15<sup>®</sup> **36** (scheme 3.12). We managed to achieve conversions of 90% at a flow rate of 0.067 mL/min (with a residence time of one hour and fifty-five minutes) using this set up.



Scheme 3.12: The final flow system set-up for the synthesis of HPA using anhydrous DMSO as a solvent.

#### ***D. Conclusions on the synthesis and isolation of HPA.***

To conclude from the results obtained, we can affirm that polar aprotic solvents are still the best solvents to solubilize adenine **27** under basic conditions, particularly dimethyl sulfoxide. We have also observed that the presence of water in the solvent system does indeed influence the formation of minor regioisomers of HPA. We can, however, state that *N*-9 HPA, **28**, was the major product that was formed (based on NMR data and literature reference) when adenine **27** was alkylated with (*R*)-propylene carbonate **33**, regardless of the solvent used or the presence/absence of water in the system.

We successfully isolated HPA **28** using two different techniques: trituration and “catch-release” resin work-up. Trituration produced the purest product and the ion-exchange work-up with Amberlyst 15® **36** gave the highest yields and used less solvent, but that being said, this approach resulted in the isolation of more of the unwanted regioisomers.

Translation of the synthesis of HPA **28** to flow required addition of accessories (mixing chip and coil) and also required the same temperature (as batch) of 140 °C. The attempt of integrating the work-up stage into the flow system failed because dimethyl sulfoxide was not compatible with the glass Omnifit™ column that was required to contain the resin and as a result we had to perform the work-up externally from the flow system.

Ultimately, the flow synthesis of HPA showed high conversions of 90%. This was achieved in one hour and fifteen minutes, which was about 50% faster than in batch, a significant benefit of the flow synthesis. Flow also had the benefit of safety as the entire process was performed with little handling of material. The closed system of flow was also better at energy conservation than that of batch which easily loses heat to the atmosphere.

Although the work-up (ion exchange using Amberlyst-15®**36**) was identical in both flow and batch synthesis, flow is still at an advantageous position as it has a greater prospect of optimizing the work-up inline, provided that suitable materials are made available. All this led us to believe that the synthesis of HPA was better in a flow system.

## References

1. Dinesh S, Shikha G, Bhavana G, Nidhi S, Dileep S. Biological activities of purine analogues: a review. *J Pharm Sci Innov.* 2012;1(2):29–34.
2. Bielekova B, Lincoln A, McFarland H, Martin (R). Therapeutic Potential of Phosphodiesterase-4 and -3 Inhibitors in Th1-Mediated Autoimmune Diseases. *J Immunol.* 2014;164(2):1117–24.
3. Phadtare S, Zemlicka J, Kessel D, Corbett TH, Zemlicka J, Kessel D, et al. Unsaturated and Carbocyclic Nucleoside Analogues: Synthesis, Antitumor, and Antiviral Activity. *J Med Chem.* 1991;34(1):421–9.
4. Raboisson P, Lugnier C, Muller C, Reimund J-M, Schultz D, Pinna G, et al. Design, synthesis and structure-activity relationships of a series of 9-substituted adenine derivatives as selective phosphodiesterase type-4 inhibitors. *Eur J Med Chem.* 2003 Feb;38(2):199–214.
5. Torphy TJ. State of the Art Molecular Targets for Novel Antiasthma Agents. *Am J Respir Crit Care Med.* 1998;157(16):351–70.
6. Doherty MA. Phosphodiesterase 4 inhibitors as novel anti-inflammatory agents. *Chem Biol.* 1999;3(4):466–73.
7. Boichot E, Wallace JL, Germain N, Corbel M, Lugnier C, Lagente V, et al. Anti-inflammatory activities of a new series of selective phosphodiesterase 4 inhibitors derived from 9-benzyladenine. *J Pharmacol Exp Ther.* 2000;292(2):647–53.
8. Johnson F, Pillai KMR, Grollman AP, Tseng L, Takeshita M. Synthesis and Biological Activity of a New Class of Cytotoxic Agents: N-(3-Oxoprop-1-enyl)-Substituted Pyrimidines and Purines. *J Med Chem.* 1984;27(8):954–8.
9. Hanus M, Kabela M, Rejnek J, Ryja F, Hobza P, Heyro J V. Correlated ab Initio Study of Nucleic Acid Bases and Their Tautomers in the Gas Phase , in a Microhydrated Environment , and in Aqueous Solution . Part 3 . Adenine. *J Phys Chem B.* 2004;108(6):2087–97.
10. Salter LM, Chaban GM. Theoretical study of gas phase tautomerization reactions for the ground and first excited electronic states of adenine. *J Phys Chem A.* 2002;106(16):4251–6.
11. Gu J, Leszczynski J. A DFT Study of the Water-Assisted Intramolecular Proton Transfer in the Tautomers of Adenine. *J Phys Chem A.* 1999;103(15):2744–50.
12. Herskovits TT, Harrington JP. Solution studies of the nucleic acid bases and related model compounds. Solubility in aqueous alcohol and glycol solutions. *Biochemistry.* 1972;11(25):4800–11.
13. Chakraborty P. Design, Synthesis and Structural Investigation of Nucleobase Functionalized B-Peptides [beta-Peptides]. Cuvillier Verlag; 2005. 32–36 p.
14. W. Zielenkiewicz, J. Poznariski AZ. Partial Molar Volumes of Alkylated Uracils--Insight into the Solvation Shell? Part II. *J Solution Chem.* 1998;27(6):543–51.
15. Hart DS, Keightley A, Sappington D, Nguyen PTM, Chritton C, Seckinger GR, et al. Stability of adenine-based cytokinins in aqueous solution. *Vitr Cell Dev Biol.* 2016;52(1):1–9.
16. Yamazaki Y, Science I. A New Method of Chemical Modification of N6-Amino Group in Adenine Nucleotides with Formaldehyde and a Thiol and Its Application to Preparing Immobilized ADP and ATP. *Eur J Biochem.* 1978;92(1):197–207.
17. Hirano A, Tokunaga H, Tokunaga M, Arakawa T, Shiraki K. The solubility of nucleobases in aqueous arginine solutions. *Arch Biochem Biophys.* 2010;497(1–2):90–6.

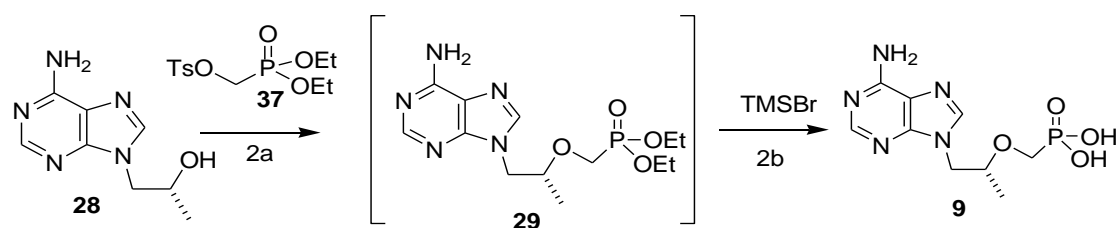
18. Ghoshdastidar D, Ghosh D, Senapati S. High Nucleobase-Solubilizing Ability of Low-Viscous Ionic Liquid/ Water Mixtures: Measurements and Mechanism. *J Phys Chem B*. 2016;120(3):492–503.
19. Mclain SE, Soper AK. Investigations on the structure of dimethyl sulfoxide and acetone in aqueous solution. *J Chem Phys*. 2007;127(17):174515.
20. Gaylord Chemical. Replacing DMF with DMSO : Replacing DMF [Internet]. [cited 2020 Apr 21]. Available from: <https://www.gaylordchemical.com/innovation-center-2/using-superior-solvents/replace-dmf-with-dmso/%3Famp>
21. Gaylord Chemical. DMSO vs . NMP [Internet]. 2014 [cited 2018 Mar 26]. p. 1. Available from: <https://www.yumpu.com/en/document/read/12143673/dmso-vs-nmp-gaylord-chemical>
22. Riley DL, Walwyn DR, Edlin CD. An Improved Process for the Preparation of Tenofovir Disoproxil Fumarate. *Org Process Res Dev*. 2016;20(4):742–50.
23. Gao Y, Zhong J-L, Wu T-Z, Jin L-Y, Fu-Li Z. Synthesis and Structure Elucidation of ((*R*))-3-(2'-hydroxyprop-1-yl) adenine. *J Heterocycl Chem*. 2016;53(2):579–82.
24. Shukla MK, Leszczynski J. Tautomerism in nucleic acid bases and base pairs : a brief overview. *Wiley Interdiscip Rev Comput Mol Sci*. 2013;3(6):637–49.
25. Siah HSM, Gundersen LL. Synthetic strategies to 9-substituted 8-oxoadenines. *Synth Commun*. 2013;43(11):1469–76.
26. Rejnek J, Hanus M, Kabeláč M, Ryjáček F, Hobza P. Correlated ab initio study of nucleic acid bases and their tautomers in the gas phase, in a microhydrated environment and in aqueous solution. Part 4. Uracil and thymine. *Phys Chem Chem Phys*. 2005;7(9):2006–17.
27. Ripin DHB, Teager DS, Fortunak J, Basha SM, Bivins N, Boddy CN, et al. Process Improvements for the Manufacture of Tenofovir Disoproxil Fumarate at Commercial Scale. *Org Process Res Dev*. 2010;14(5):1194–201.
28. Sharma S, Lee JK. Acidity of Adenine and Adenine Derivatives and Biological Implications . A Computational and Experimental Gas-Phase Study. *J Org Chem*. 2002;67(24):8360–5.
29. Chavakula (*R*), Mutyala N, Chennupati S. Synthesis of ( *E* )-9-(Propen-1-yl)-9 H -adenine, a Mutagenic Impurity in Tenofovir Disoproxil Fumarate . *Org Prep Proced Int*. 2013;45(4):336–40.
30. Lambertucci C, Antonini I, Buccioni M, Dal Ben D, Kachare DD, Volpini (*R*), et al. 8-Bromo-9-alkyl adenine derivatives as tools for developing new adenosine A2A and A2B receptors ligands. *Bioorganic Med Chem*. 2009;17(7):2812–22.
31. Singh V, Fedeles BI, Essigmann JM. Role of tautomerism in RNA biochemistry. *Rna*. 2014;21(1):1–13.
32. Uniqsis Ltd. UNIQSIS Accessible flow chemistry [Internet]. 2020 [cited 2020 Jan 24]. Available from: <http://www.uniqsis.com/paAccesories.aspx>

## Chapter 4: Synthesis of tenofovir

### A. Synthesis and isolation of phosphonate propyl adenine (PPA).

The next step headed for the synthesis of the ARV drugs, TD **25** and TA **26**, was the addition of a crucial group to its activity: the organo-phosphonate group. The addition of the phosphonate transforms the nucleoside analogues into nucleotide analogues which are able to resist enzymatic attack (from e.g. esterases, phosphatases, etc.)<sup>1</sup> and in the case of HIV, it helps to by-pass the rate-limiting intracellular “initial phosphorylation” step thereby interrupting viral replication.<sup>1,2</sup>

The addition of a phosphate ester to the hydroxyl group of **28** occurs via a two-step process, with the initial step being an S<sub>N</sub>2 addition of a phosphonate ester to **28** by the displacement of the tosyl group of DESMP **37** followed by the hydrolysis of the ester group with TMSBr in the subsequent step to afford tenofovir **9** (scheme 4.1).



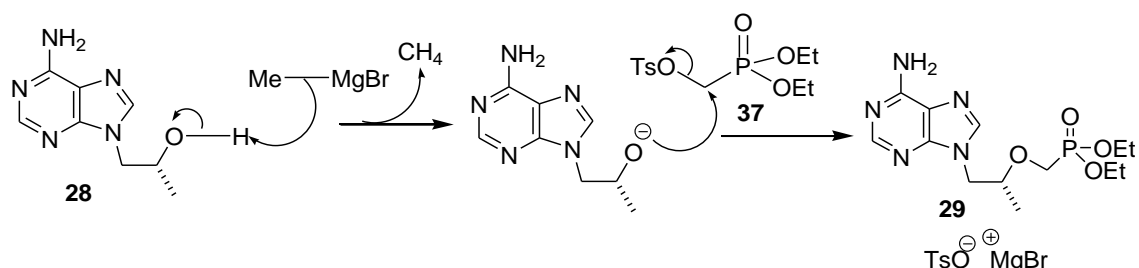
Scheme 4.1: Addition of the phosphonate ester to HPA and the hydrolysis thereof to form tenofovir.

#### 4.1) Previous challenges associated with isolating PPA.

The approach described above in scheme 4.1 has historically been associated with isolation and purification challenges in particular the phosphorylated product, PPA **29**, in most reports has to undergo an *in situ* hydrolysis to afford tenofovir **9**.<sup>2,3</sup> This is despite the fact that PPA **29** is characteristically contaminated with residual water which interferes with the TMSBr used in the hydrolysis step.

The process is also extremely restrictive in terms of the base that can be used for the initial S<sub>N</sub>2 displacement (scheme 4.2), with almost all high yielding reports making use of magnesium *tert*-butoxide (MTB). Unfortunately, the use of MTB complicates the process and a major difficulty faced is that the magnesium salt by-products ‘trap’ PPA **29** in a sticky hydrophobic salt cake which is difficult to process. The salt cake places a challenge in both the isolation of the product and also creates a huge stumbling block for translation of this synthetic step to flow. Another issue with the work-up was the challenging removal of the high boiling point polar aprotic solvents used for the reaction as well as the

similarity in the polarity of both **29** and the magnesium salts: they are both highly soluble in water and both poorly soluble in non-polar solvents such as dichloromethane, which posed a challenge for the efficient isolation of PPA **29**.



Scheme 4.2: Proposed reaction mechanism for the formation of PPA from HPA.

A study by Riley *et. al.*<sup>4</sup> attempted to solve the issue of the salt cake formation by looking into the use of alternative bases for step 2a. A series of bases, including MTB, were tested in three different solvents systems, *N*-methyl-2-pyrrolidone, dimethyl sulfoxide or DMSO/THF. The MTB gave an impressive conversion of 92% to PPA **29** while almost all other bases failed to show any conversion with the exception of PhMgBr and PhMgCl which afforded conversions of 6% and 28%, respectively.

These results led to the suspicion that the presence of both Mg and <sup>t</sup>BuOH played a vital role in the conversion of HPA **28** to PPA **29**. Upon addition of <sup>t</sup>BuOH to the PhMgBr/Cl bases, the conversion to PPA **29** increased significantly to a reported maximum of 78%.<sup>4</sup> The group made no postulation for the role of <sup>t</sup>BuOH but suggested that the Mg<sup>2+</sup> facilitated the S<sub>N</sub>2 reaction with HPA **28** by coordinating with the DESMP **37** oxygen atoms (figure 4.1).

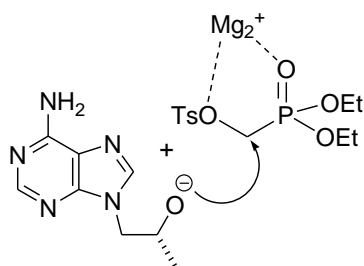


Figure 4.1: Proposed coordination of magnesium (II) salts with DESMP, as shown by Riley *et. al.*<sup>4</sup>

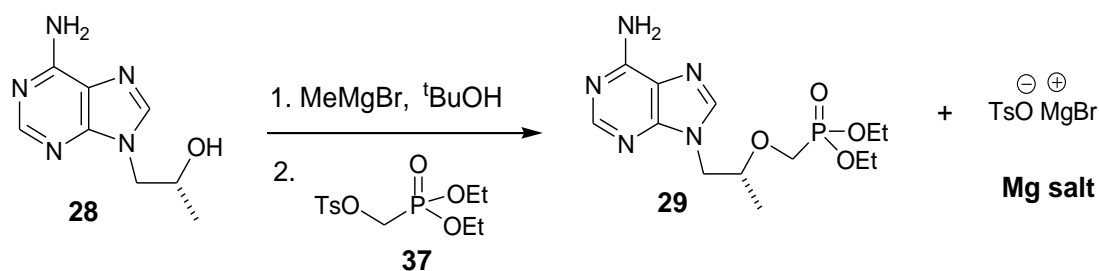
Owing to the failure to obtain an alternative non-magnesium base meant that the formation of the magnesium salt cake could not be avoided and so the work-up of the reaction was the next focus point for the group. The research group managed to develop a solvent free reaction mixture, doing away with the polar aprotic solvents; they then had the advantage of choosing their own solvent systems for the separation of the impurities from PPA **29**. Their obvious solvent choice was water to dissolve

the salts and an immiscible organic solvent to take in the organic compound, i.e. PPA **29**. Riley *et al* made use of continuous extraction for this first step.

#### 4.2) Validation of the Riley approach.

Riley *et al* dissolved the magnesium salt cake in water and extracted PPA **29** into chloroform via continuous extraction.<sup>4,5</sup> They reported that using chloroform as the extraction solvent was more efficient than its alternative, dichloromethane: The final yield of PPA **29** using chloroform for the continuous extraction was 85% as opposed to 63% when dichloromethane was used. This process was quite lengthy taking about twenty-four hours for the continuous extraction step alone. That being said, the group managed to successfully isolate PPA **29** and obtain an optimized isolated yield of 85%.

For our project, the optimized method obtained for the synthesis of PPA **29** would be validated as shown in scheme 4.3.

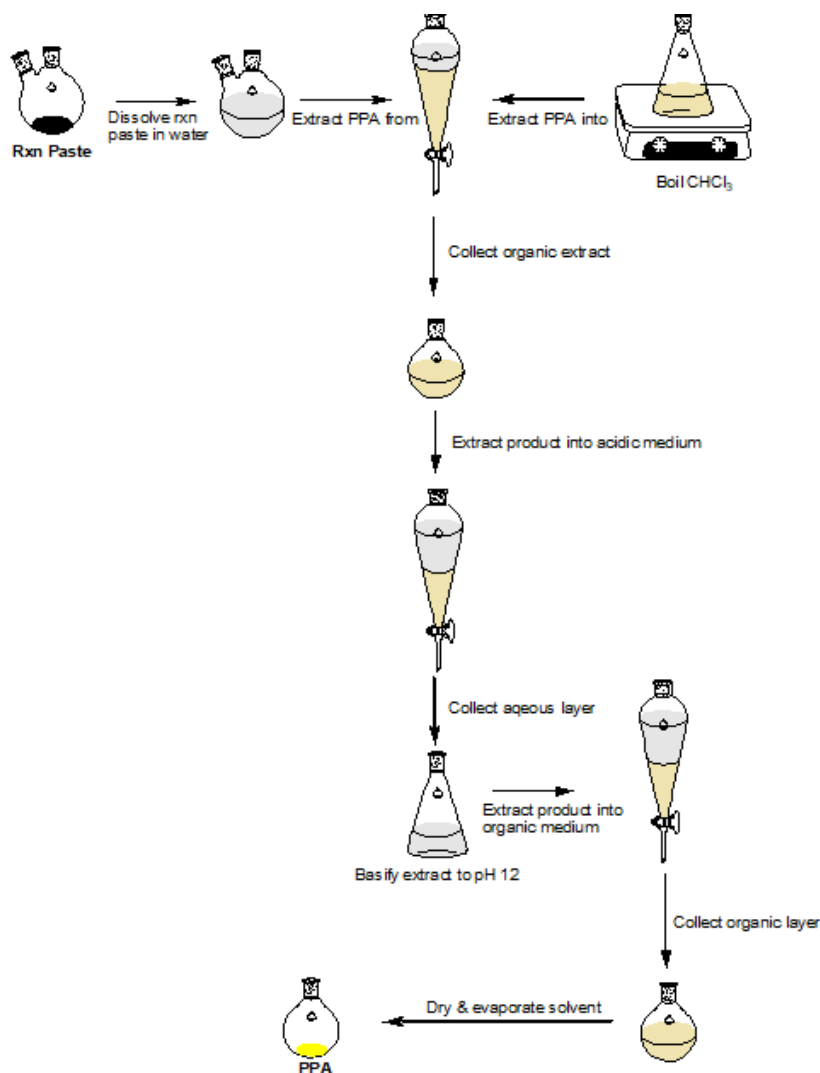


Scheme 4.3: Formation of PPA from HPA using the Grignard and <sup>t</sup>BuOH.

For the work-up, however, we employed a slightly shorter alternative to the continuous extractor.



We employed a liquid-liquid extraction using a standard separation funnel, with the reaction mixture being initially dissolved in water followed by extraction with hot/boiling chloroform. This brought the entire work-up time down to about four hours (scheme 4.4).



*Scheme 4.4: The work-up process for the isolation of PPA from the magnesium salt cake.*

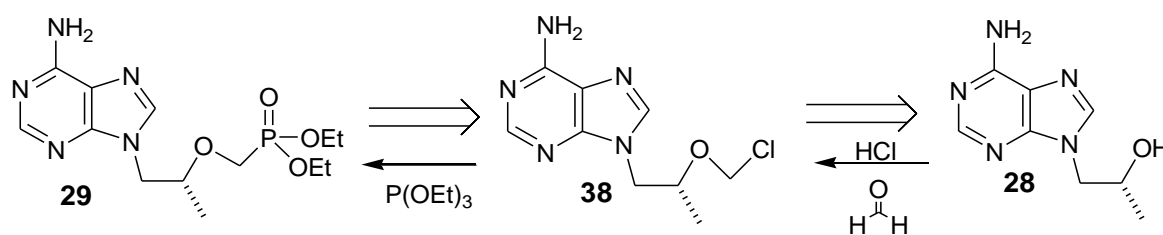
The initial step involved dissolving the sticky salt cake reaction mixture in water and extracting the organic compounds into hot chloroform, leaving behind any magnesium salts and unreacted HPA **28** in the aqueous layer. The procedure was less effective when dichloromethane was used and in order to push the otherwise highly water soluble PPA **29** into the organic solvent, chloroform was heated up requiring an organic:aqueous solvent ratio of about 10:1. The next step involved the separation of PPA **29** from DESMP **37** by acidic extraction, followed by basification of the acidic medium to release the

PPA **29** back into organic solvent, which in this case was dichloromethane (scheme 4.4). This afforded PPA **29** in a best yield of 70%.

Although impressive conversions and yields were obtained using this synthetic route (scheme 4.3) and work-up process (scheme 4.4), this step could in no way be translated to flow because of the thick sticky magnesium salt cake that forms. We had to face the fact that alternative routes for the production and isolation of PPA **29** had to be considered if we wanted to hold on to any hope of translating the step to flow.

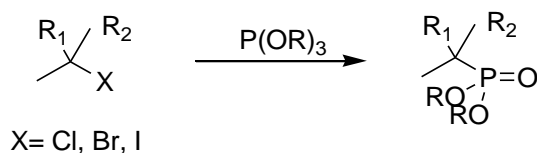
#### 4.3) Alternative approach to the synthesis of PPA.

A new synthetic approach was considered for the synthesis of PPA **29**, the key transformation of which focused on phosphate addition chemistry through an Arbuzov reaction. The proposed approach required the chloromethylation of alcohol **28** to the analogous chloro-analogue **38** thereafter an S<sub>N</sub>2 displacement via an Arbuzov reaction was envisaged (scheme 4.5).



Scheme 4.5: An alternative retrospective approach to the synthesis of PPA.

The Arbuzov is a widely used reaction that produces a wide range of phosphonates and phosphine oxides from just an alkyl halide and a trialkyl phosphite (scheme 4.6).<sup>6,7,8</sup> To add to that, there have been successful translations of the Arbuzov reactions to flow.<sup>9</sup> It has, however, been reported that the success of the reaction depends on the alkyl substituent used and the halide present<sup>10-11</sup>

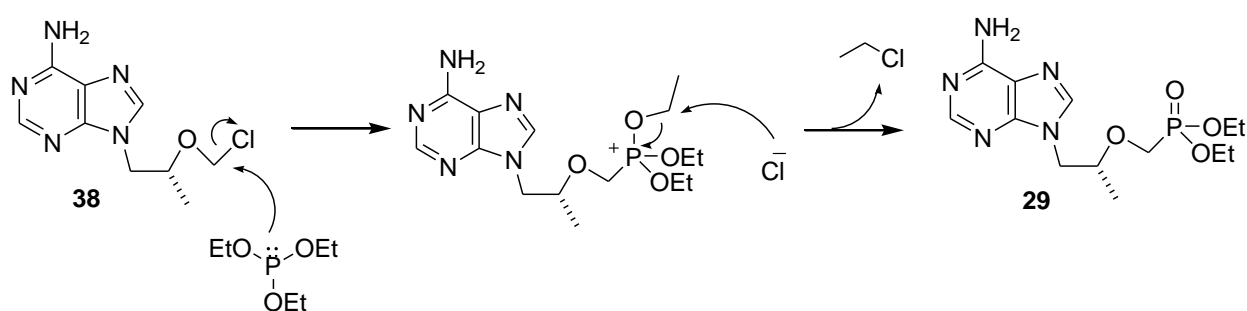


Scheme 4.6: A generic representation of an Arbuzov reaction.

This reaction dates back to over a century when an alkyl halide was reacted with a trivalent phospho-ester to form an alkyl phosphate (scheme 4.6) as reported by Arbuzov.<sup>12</sup> The novelty of the reaction allowed researchers to synthesize new organophosphates in just one step. There were, however, two main setbacks to this reaction: the first being the requirement of high temperature and the other

being the side reaction of the by-product alkyl halide with the organophosphate.<sup>7,8</sup> Attempts to curb this side reaction included using catalytic amounts of the reagent alkyl halide, this was helpful but affected the yield of the desired organophosphate drastically. Alternatively, the use of a Lewis acid aided in reducing the high temperatures to room temperature and also helped increase the yield of the reaction.

We considered the use of the Arbuzov reaction to add the phosphonate group to the nucleotide analogue (HPA **28**) in order to form PPA **29**. The Arbuzov reaction involves a nucleophilic attack of the phospho-ester on an electrophilic carbon bound to a halide (scheme 4.7). The release of an alkyl halide results in the formation of a new alkyl phosphate ester.

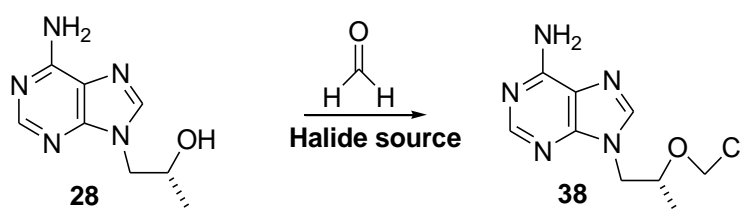


*scheme 4.7: Mechanistic synthesis of PPA from chloromethyl HPA via the Arbuzov route.*

To attempt the Arbuzov reaction we would need a preceding step which would involve the halo-methylation of the hydroxy group of HPA **28** (to form **38**). The methyl would have to be coupled to a good leaving group such as a halide, in order to accommodate the Arbuzov reaction which would substitute the halide for a phosphonate diethylester group, to form PPA **29**. This would have to be a chloromethylation step.

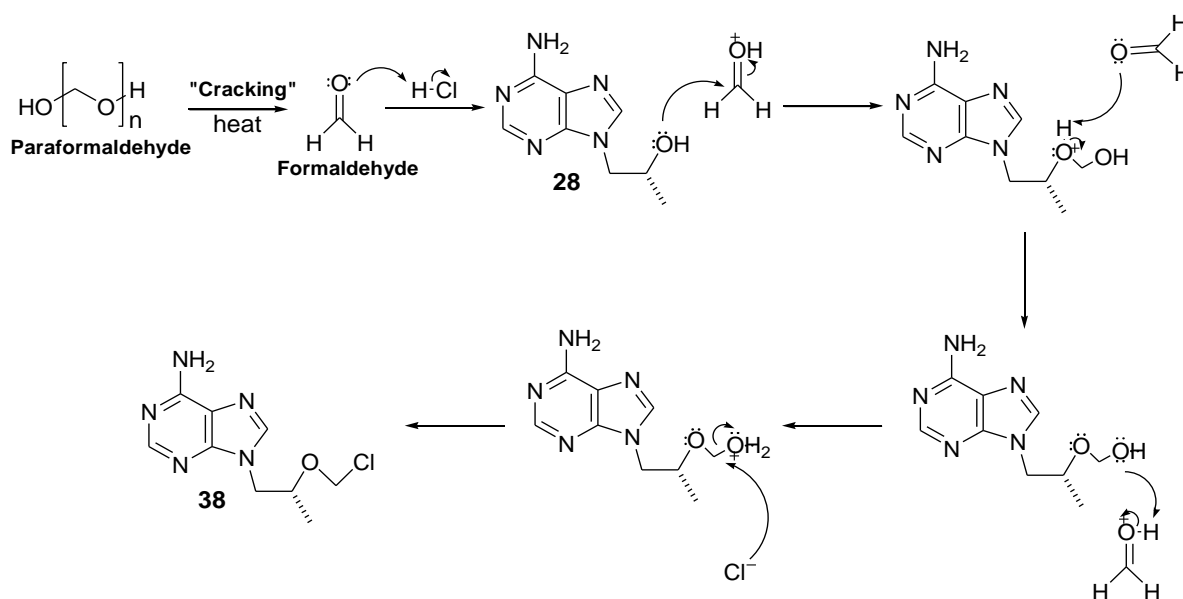
#### 4.3.1) Chloromethylation of HPA.

Chloromethylation involves the reaction of formaldehyde as a methyl source and hydrogen chloride gas as the halide source, together with an alcohol (scheme 4.8). Scheme 4.9 shows that the initial step is the “cracking” of the paraformaldehyde under heat in order to release the formaldehyde which then acts as a base, attacking the proton of the acid.



*scheme 4.8: Proposed reaction for the chloromethylation of HPA to form chloromethyl HPA.*

The electrophilic carbon of the now protonated formaldehyde is then attacked by the hydroxyl oxygen of **28** which adds a new C-OH bond to **28**. Water is then released and replaced by Cl (from the acid) to finally form chloromethyl HPA **38** (scheme 4.9). This reaction requires extreme reaction conditions to facilitate the cracking of paraformaldehyde to afford formaldehyde.



*Scheme 4.9: The mechanistic chloromethylation of HPA to form chloromethyl HPA.*

Investigation into halo-methylations revealed that much of the work performed made use of chlorine as the halogen of choice in the form of HCl (with more recent reports utilising TMSCl)<sup>13-14</sup> and formaldehyde as the methyl source.<sup>15-17</sup> We decided to employ a slightly modified experimental procedure from the Janicki *et al.*<sup>15</sup> and Wang *et al.*<sup>13</sup> research groups, with paraformaldehyde and **28**

stirring at room temperature in a round-bottom flask under inert atmosphere, while either HCl is bubbled through the reaction mixture or TMSCl is added to the round-bottom flask. The reaction could not be performed at temperatures lower than room temperature because of the limited solubility of HPA **28**. The choice of solvent, dimethylformamide, was also chosen based on the solubility of HPA **28**.

We initially performed several trials for the chloromethylation of **28** (scheme 4.8), the parameters of which are as indicated in table 4.1.

Table 4.1: The reaction parameters used for the halide methylation of HPA.

Trial	Halogen source	Reaction Vessel (RBF/Pressure Tube (PT))	Solvent	Time (hours)	Temperature (°C)
<b>1</b>	HCl (g)	RBF	DMF	3	RT
<b>2</b>		RBF	DMF	3	60
<b>3</b>		RBF	DMF	16	60
<b>4</b>		RBF	DMF	3	RT
<b>5</b>		RBF	DMF	3	50
<b>6</b>	TMSCl	PT	DMF	16	RT
<b>7</b>		RBF	DMF	20	RT
<b>8</b>		RBF	DCM	20	RT
<b>9</b>		RBF	DCM	48	50
<b>10</b>		PT	None	48	60
<b>11</b>		RBF	None	48	60
<b>12</b>	TMSBr	RBF	None	48	RT

Standard conditions: To HPA **28** (1 equiv) (dissolved in solvent) and paraformaldehyde (1.3 equiv), the halogen source (5 equiv) was added and the suspension was stirred at the temperature and time specified in the table.

We initially attempted to utilise a stream of anhydrous HCl as the chloride source, prepared by adding concentrated sulfuric acid in a dropwise fashion, into a round-bottom flask containing NaCl (figure 4.2).

The HCl gas generated was then transferred via a polyester pipe and bubbled into a second round-bottom flask containing the paraformaldehyde and HPA **28** (figure 4.2).

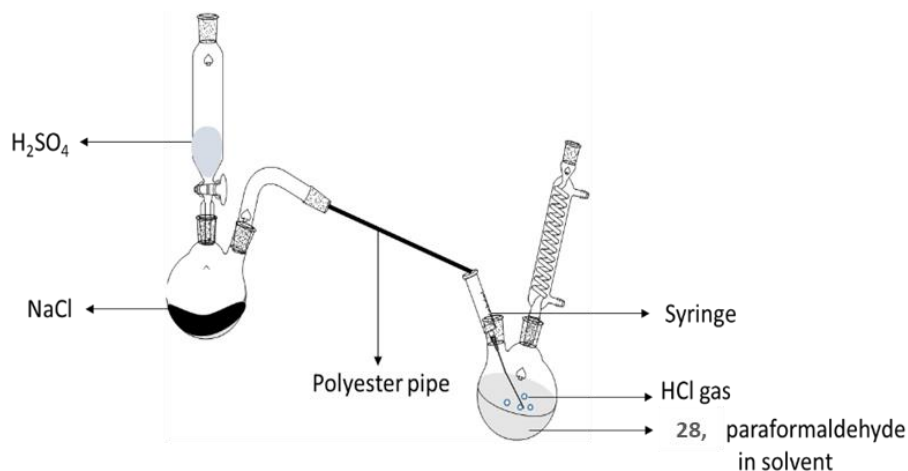


Figure 4.2: Representation of the chloromethylation laboratory set-up.

We had hoped that the HCl gas would facilitate both the cracking of the paraformaldehyde and act as the chloride source for the chloromethylation. The challenge with using gas was controlling the amount of gas entering the system and the duration of exposure. Additionally, for halide methylation, the use of gas has been reported to form chloro (chloromethoxy) methane as a side product which is known to be a highly carcinogenic compound, linked to lung cancer.<sup>18</sup> Unfortunately, under these conditions no chloromethylation was observed.

In trials 4-9 (table 4.1) we made use of TMSCl as the halogen source and paraformaldehyde as the formaldehyde source. We attempted the reactions in dimethylformamide or dichloromethane the latter of which has commonly been employed in chloromethylation reactions,<sup>18-20</sup> again we were unable to observe any of the desired chloromethylation. We also attempted the reaction under pressure using an ACE<sup>®</sup> pressure tube (trials 6 and 10) with the hopes that it would facilitate the “cracking” of the paraformaldehyde and prevent loss or escape of formaldehyde. In the case of trials 10 and 11 we performed the reactions under solvent free conditions. Once again, we were not able to observe any formation of the desired chloromethylated product. Finally, in trial 12 we employed the use of TMSBr under solvent free conditions in this case targeting the analogous bromo-methylated product. Unfortunately, we were still unable to isolate any of the desired material.

In all instances the progress of the reactions was monitored using TLC, however, for all trials there was limited consumption of HPA **28** noted and only trials 4 and 5 showed any macroscopic physical changes. Analysis of the <sup>1</sup>H NMR spectra of these reaction products all revealed peaks common to the starting material HPA **28** and no product formation peaks were observed. We also ran <sup>13</sup>C DEPT 135

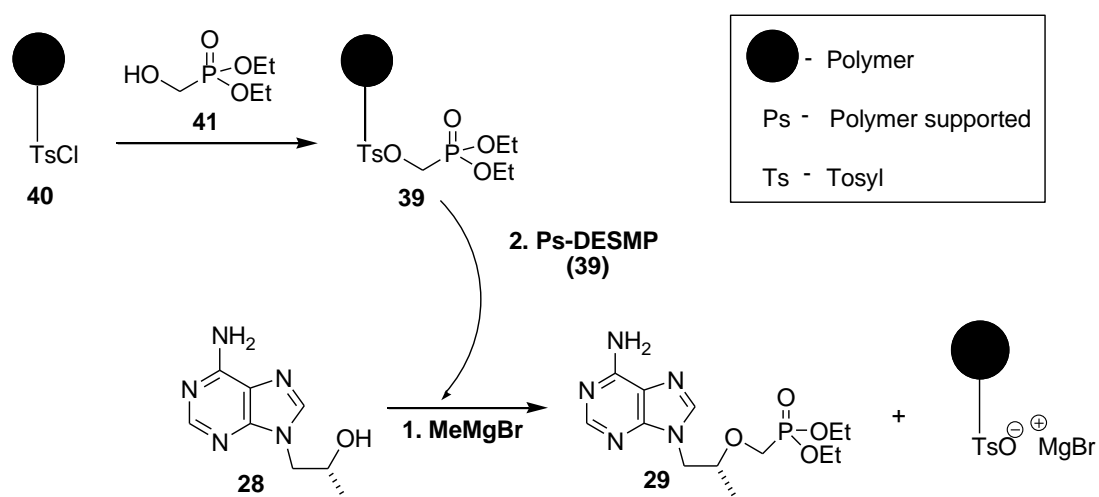
NMR but unfortunately it did not help us identify the product formed because only one unambiguous negative phase peak was observed, which only confirmed the presence of the propyl CH<sub>2</sub> group. A trial of the Arbuzov reaction (scheme 4.8 and scheme 4.9) was attempted in any case with the product from trial 4 but as expected this resulted in no product formation of PPA **29**. We performed no further optimization of the reaction and conclude the results of the chloromethylation as inconclusive.

At this point we decided to move on to an alternative approach employing polymer-supported reagents.

#### 4.4) Alternative approach to the isolation of PPA: Resin bound reagent (DESMP).

As mentioned in the previous chapters, resins are a “go-to” for flow systems. In this step particularly, the use of a resin/s would be expedient if it allowed for the by-products (particularly the magnesium by-products) to be selectively isolated, making the extraction of HPA **29** much simpler. Should this be successful, the synthetic route or work-up could potentially be translated to flow.

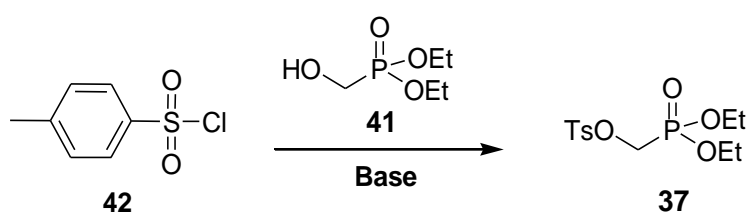
We envisaged the preparation of a novel polymer bound version of DESMP **39** using commercial polymer-supported tosyl chloride **40** as a logical feedstock. As the tosyl group is displaced in the S<sub>N</sub>2 displacement with HPA **28** we had hoped that upon reaction pure PPA **29** would be formed and released from the polymer support and that the resulting tosylate anion would capture the spent magnesium salts. PPA **29** could then easily be recovered post-reaction by simple solvent evaporation. (scheme 4.10).



Scheme 4.10: Proposed synthesis of PPA using polymer-supported DESMP.

The major challenge that the polymer bound reagent could pose was constrained access to the reactive sites of the molecule of interest. This is one of the main reasons why resin-bound reactions

in general have longer reaction times than the standard batch reactions. It becomes even more challenging when dealing with relatively large molecules, such as in this case HPA **28**, because the accessibility of the reactive sites becomes all the more constrained. Additional complications when working with polymer-supported reagents is that they often suffer from temperature sensitivity depending on the resin support, and under stirring conditions the polymer support tends to break down due to mechanical strain experienced. We initially sought to test the proposed synthetic approach using unsupported reagents (scheme 4.11) in order to gauge the possible reaction parameters needed.

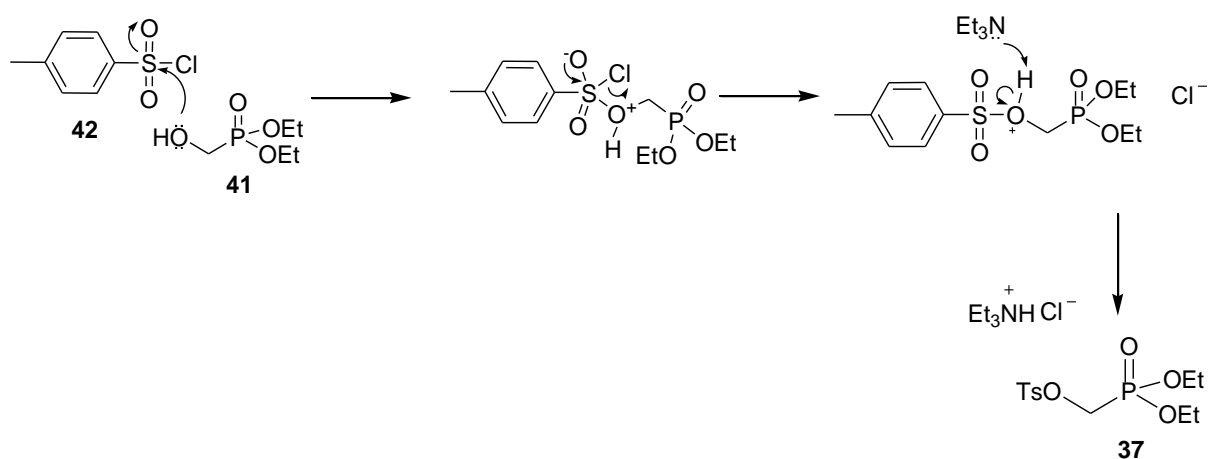


*Scheme 4.11: Formation of DESMP from TsCl in the presence of a base.*

The tosylation of a phosphonate ester is not a novel step and although the literature for the exact phosphate ester (DMP) **41** reacting with TsCl **42** was mostly patented work, literature with similar structures/substructures to DMP **41** were available. The common thread for the experimental methods reported was that the reaction is generally performed at ambient temperatures with an amine base and in most instances dichloromethane as the solvent of choice.<sup>20–24</sup>



The reaction required a base in order to facilitate the nucleophilic attack of the neutral alcohol oxygen of the DMP **41** on the electrophilic sulphur atom of TsCl **42** (resulting in the displacement of the Cl<sup>-</sup>). The charged OH is then deprotonated to form neutral tosylate. The amine base serves an additional role by assisting in the removal of HCl from the reaction solution (scheme 4.12).



*Scheme 4.12: Reaction mechanism for the tosylation of DMP to form DESMP in the presence of a base.*

We attempted the tosylation using a conventional set-up: In a round-bottom flask containing DMP **41** (2 equiv.) and Et<sub>3</sub>N (1 equiv.) in dichloromethane at room temperature, TsCl **42** (1 equiv.) was added and the reaction mixture was allowed to stir overnight at room temperature. A TLC was run and the formation of a new product was observed. The reaction was worked up and the white solid extracted from the organic layer was analysed using <sup>1</sup>H NMR spectroscopy. The spectrum (Figure A10, page 109) revealed that DESMP **37** was isolated, showing the loss of the hydroxyl proton around 5.90 ppm. Subsequently, two doublet peaks were found around the aromatic region, at 7.52 and 7.84 ppm, each integrated for two protons, showing the presence of the tosyl group. Alternatively, when less basic pyridine was used under the same reaction conditions as Et<sub>3</sub>N, it failed to give a conversion greater than 50%; no optimization was performed (but it was suspected that a greater equivalence ratio of pyridine: TsCl **42** would be needed as well as longer reaction time) because the success of this simple batch reaction was enough to attempt the reaction on polymer supported material.

The successful synthesis of DESMP **37**, prompted us to attempt the synthesis of the envisaged polymer-supported DESMP **39**. The attempted syntheses are summarised in table 4.2:

Table 4.2: Reaction parameters used in the trials of formation of Ps-DESMP from Ps-TsCl.

Trial	Base	Resin Swelling time (hours)	Reaction time (hours)	Reaction temperature (° C)
1	Et <sub>3</sub> N	2	20	RT
2	Pyridine			
3	Et <sub>3</sub> N	24	48	
4	Pyridine			
5	Et <sub>3</sub> N	24	20	80
6	Et <sub>3</sub> N ( +10% DMAP)	3	20	RT

Standard conditions: Ps-TsCl **40** (1 equiv) was allowed to swell in DCM for at least 2 hours. A mixture of DMP **41** (2 equiv) and base, Et<sub>3</sub>N (1 equiv) or pyridine (4 equiv), was added dropwise to the gently stirring reaction mixture at the set temperature for the reported time.

We used a similar set-up to the homogenized batch reaction trials where DMP **41** (1 equiv.) and Et<sub>3</sub>N (2 equiv.) were premixed after which time they were added to a gently swirling mixture of Ps-TsCl **40** (1 equiv.) in solvent at room temperature.

The polymer support was prepared by allowing the resin to swell (enhancing the accessibility to the functional groups within the polymer) in anhydrous dichloromethane for two to twenty-four hours in preparation for the tosylation reaction. For the initial trials 1 and 2 (table 4.2), the reaction parameters were matched with those used in the homogeneous batch synthesis of DESMP **37** with Et<sub>3</sub>N and pyridine used as bases and the reaction mixture allowed to swirl gently at room temperature overnight.

Alongside trials 1 and 2 we decided to tweak a few parameters in pursuit of the most suitable conditions for a resin system (also being mindful that we had not optimized the homogeneous batch synthesis). In trials 3 and 4 we stretched the “swelling” duration of the resin to a full day as well as the duration of the reaction to two days. This was done based on the suspicion that the reaction would require a longer time to complete than under homogenous conditions because the frequency of interactions between the reagents was less.

We also decided to gently heat one of the reaction mixtures (trial 5), keeping the other parameters the similar to trials 1 and 3, being curious to see if the increase in temperature would have any positive effect on the rate of the reaction. Finally, in the sixth round-bottom flask, we decided to attempt a base combination that Lai *et al* made use of,<sup>25</sup> employing the similar parameters as the research group

(with yields ranging from 80-90%), to see how the results with a polymer-supported reagent would affect the rate and success of the reaction.

Analysis of the reaction progression for each of the trials proved challenging: TLC could not provide any useful information because the Ps-TsCl **40** served as the limiting reagent (DMP **41** and the base was in excess) and as a result we were unable to precisely monitor the consumption of any of the non-polymer bound reagents. Fortunately, we were able to successfully run an NMR of the polymer support which allowed us to monitor the success of the reaction by comparing the spectra of the product polymer with that of the Ps-TsCl **40** and DMP **41**.

The NMR of the Ps-TsCl **40** was run before the product polymer. To obtain an  $^1\text{H}$  NMR of the solid phase, the Ps-TsCl **40** was placed in an NMR tube and a less dense deuterated solvent was added so that polymer would settle at the bottom of the tube (DMSO- $d_6$  was used for this purpose). The NMR instrument was "pre-shimmed" with a tube containing only solvent prior to running the NMR of our polymer sample. This allowed us to skip the shimming for our polymer sample, which would not have been possible with the solid phase-polymer, and run the  $^1\text{H}$  NMR scans (16) straight away. The same process was employed to obtain the  $^1\text{H}$  NMR spectra of our product polymer.

An  $^1\text{H}$  NMR of the Ps-TsCl **40** and DESMP **37** were obtained and used to compare each reaction polymer product within order to determine whether there had been a change to the resin's chemical make-up or not.

The  $^1\text{H}$  NMR data obtained for all the trials (1-6) produced unclear results. The peaks obtained could not conclusively be ruled as pure Ps-TsCl **40** peaks even though standard DMP **41** peaks were not observed. This led us to believe that there could possibly be a change to the chemical make-up of the polymer. The  $^{31}\text{P}$  NMR of DMP **41** was then run and compared to the product polymer's  $^{31}\text{P}$  NMR spectrum in order to identify if any new phosphorous compound peaks would be observed: All the  $^{31}\text{P}$  NMRs, surprisingly, only showed peaks corresponding to those of free DMP **41**. The inconsistency could not be clarified and so the results of each trial were inconclusive.

## ***B. Conclusion for the synthesis of PPA.***

After validation of the approach by Riley *et al.*<sup>4</sup>, we found that the formation of PPA **29** was successful, however, the work-up was lengthy, consuming over four hours and the route could not be translated to flow due to the formation of a salt cake.

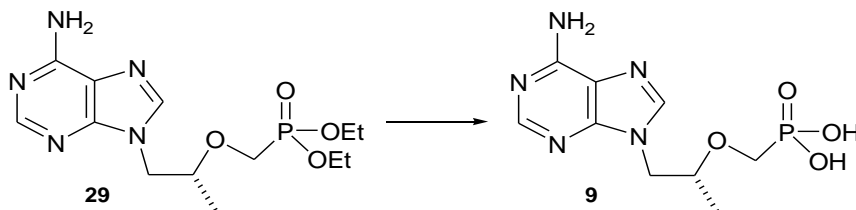
As a result, we elected to investigate two alternative routes which were designed to either remove the need for the troublesome magnesium base or improve the time-consuming down-stream processing and purification.

In the first approach a chloromethylation of HPA **28** followed by an Arbuzov type reaction was planned to access PPA **29**. Unfortunately, despite several attempts the required chloromethylation proved unsuccessful. In the second approach we elected to retain the original synthetic route of PPA **29** but planned on streamlining the work-up and purification through the synthesis and use of polymer-supported DESMP **39**. In this instance the approach was hypothesised to allow us to isolate pure PPA **29** while trapping the troublesome magnesium salts on the spent solid support. Unfortunately, although we were able to successfully prepare unsupported DESMP **37**, the results of the formation of the analogous polymer supported DESMP **39**, trials were inconclusive.

Overall, we elected to leave step 2a as a batch reaction wherein a Grignard reagent is used for the conversion of HPA **28** to PPA **29** (scheme 4.3) as described by Riley *et al.*<sup>4</sup> We adopted a similar albeit shorter work-up procedure (scheme 4.4) affording the desired PPA **29** in 70% yield in about four hours, in comparison the downstream processing by Riley *et al.*<sup>4</sup> afforded a higher overall yield 85% but in a significantly longer time (greater than twenty-four hours).

### C. Hydrolysis of PPA to form the prodrug, tenofovir.

Previously, we looked at the addition of a phosphonate ester group to HPA **28** to form PPA **29**, leaving one more step towards the synthesis of the active species itself, tenofovir **9** (scheme 4.13).



Scheme 4.13: Hydrolysis of the phosphonate esters of to form tenofovir.

Although a “one-pot” synthesis of PPA **29** from HPA **28** has been previously reported (scheme 4.1),<sup>3,2</sup> this was primarily driven by the difficulties associated with the isolation of PPA **29** which further complicated the hydrolysis. Most critically, direct telescoping introduced difficulties linked to the drying of PPA **29** arising from the hygroscopic magnesium salt cake that forms during stage 2a. Using our approach, however, we were able to synthesize and isolate PPA **29** in good yield and purity and as such we were interested in the hydrolysis of PPA **29** to form tenofovir **9**.

#### 4.5) Literature: The hydrolysis of a dialkyl phosphonate ester to a phosphonic acid.

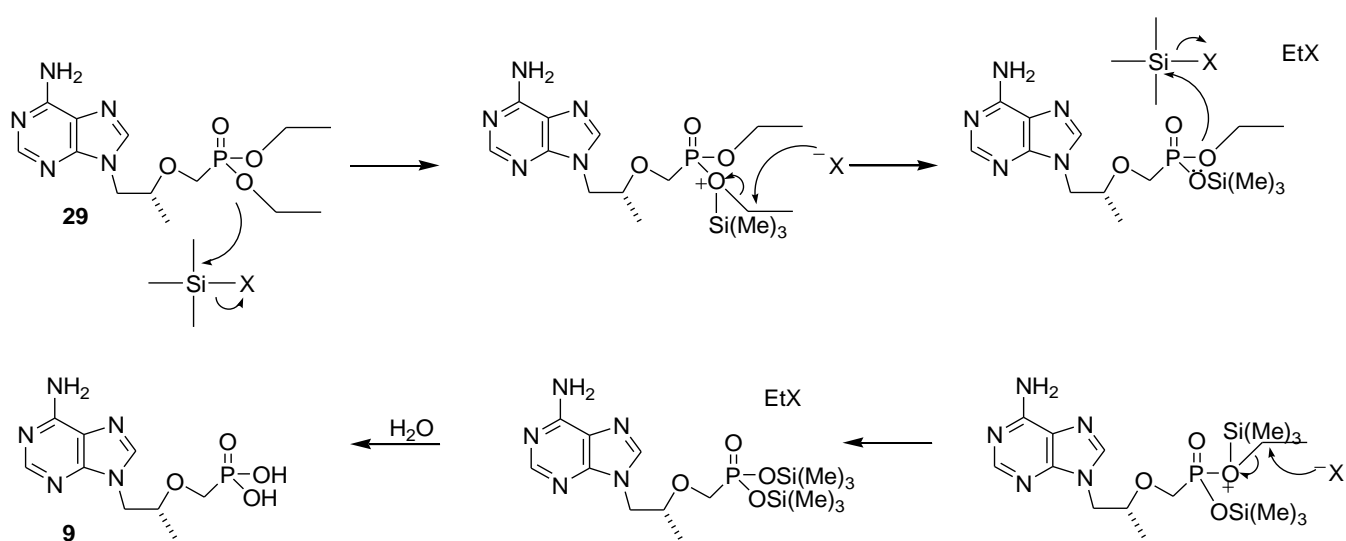
Theoretically we had two streams of options for the hydrolysis of the phosphonate ester: (i) an alkaline based hydrolysis and (ii) an acid-based hydrolysis. An alkaline hydrolysis of the phosphonate diester was not a feasible option as it typically fails to hydrolyze both esters, resulting in a monoester instead of a phosphonic acid.<sup>26</sup> An acid based hydrolysis of the phosphonate diester on the other hand is more commonly employed typically making use of either a Lewis acid (trimethylsilyl halides) or a mineral acid (hydrohalides). Although both acid groups are quite aggressive, trimethylsilyl (TMS) halides are most attractive as they selectively target phosphonate esters.<sup>27</sup> The use of the Lewis acids form silyl phosphate esters which are easily hydrolyzed in the presence of water.

Many reports described the use of TMSBr as the Lewis acid,<sup>28–32</sup> which although effective in its hydrolysis of the phosphonate ester, is expensive and difficult to handle. Its alternative, TMSCl, on the other hand, has been reported as less reactive and mainly used for deprotection of dimethyl phosphonate.<sup>27</sup> For this reason some of the reported trials conducted with TMSCl would have longer reactions times and elevated temperatures.<sup>2</sup> To overcome this issue, some studies implemented the addition of a nucleophilic halogen (e.g. NaI, LiI, NaBr etc.)<sup>29,4</sup> to accelerate the rate of hydrolysis of

phosphonate esters to phosphonic acids using TMSCl. They speculate that the halide facilitates the nucleophilic displacement of the phosphonic esters.<sup>29</sup>

Houghton *and co-workers* conducted a study that in part investigated the halogen salts that would best couple TMSCl and found that NaBr was the optimal salt of choice, with a rapid reaction rate at low temperature, ultimately affording quantitative conversions to the desired phosphonic acid.<sup>29</sup>

Gutierrez *et al.* took a different approach of optimization by looking at the reaction conditions that would best increase the effectiveness of TMSCl alone.<sup>27</sup> They decided to attempt the hydrolysis of several dialkyl phosphonates using TMSCl in chlorobenzene, under pressure (using a pressure tube). The results were not disappointing as they reported conversions of >98% in eight hours.



Scheme 4.14: The Mechanism of the hydrolysis of phosphonate ester of PPA, using TMSX. X represents a halide.

Scheme 4.14 shows the mechanism of hydrolysis by TMSX (X= Cl or Br) which involves the (i) activation of the phosphonate ester by silylation, which is followed by what has been determined to be the rate determining step, the (ii) displacement of the alkyl chain by a nucleophile. Thereafter hydrolysis of the silyl esters forms the phosphonic acid.<sup>28,29</sup>

The main objective of our studies was to validate the hydrolysis step and translate the batch procedure, using TMSCl to flow.

#### 4.6) Experimental: The hydrolysis of PPA to tenofovir in batch.

With positive results reported by Houghton *and co-workers* for the hydrolysis of a phosphonate diester using TMSCl and NaBr,<sup>30</sup> we decided to try the reactions ourselves with (i) TMSBr, (ii) TMSCl and NaBr, as well as a (iii) TMSX (X= Cl or Br) with no solvent system and/or no NaBr as attempted by Gutierrez *and co-workers*.<sup>27</sup> The details are recorded in table 4.3

Table 4.3: Reagents used for the hydrolysis of PPA to tenofovir, performed under pressure.

Trial	Hydrolysis Reagent	Solvent	Temperature (°C)	PPA Yield (%)	Conversion (%)
1	TMSBr	Acetonitrile	120	45	>98
2		No solvent		58	
3	TMSCl	Acetonitrile		N/A	<10
4		No solvent		N/A	
5	TMSCl + NaBr	Acetonitrile		<40	>70
6		DMF		<40	

Standard Conditions: PPA **29** (1 equiv.) with hydrolysis reagent (5 equiv.) (and 2 equiv. NaBr where applicable) and solvent were added to an ACE<sup>®</sup> pressure tube. The RM was left stirring at 120 °C for about 18 hours (overnight).

The parameters from all the trials, 1-6, were kept the same so as to be able to directly compare the efficiency of TMSBr and TMSCl as hydrolysis reagents (table 4.3). In each trial, all the reactants (PPA **29**, TMSCl/Br and NaBr /solvent where applicable) were added to a pressure tube and the RM was left to stir at 120 °C overnight. The results of trials 1-2 shown in table 4.3 reveal that TMSBr gave the best conversions (> 98%) and yields (> 45%) of the phosphonic acid (**9**), and also that the absence of solvent managed to result in a higher isolated yield (58%) than when acetonitrile was used. Acetonitrile,<sup>28,33</sup> worked comparably to similar systems reported in dimethylformamide, *N*-methyl-2-pyrrolidone,<sup>3,29</sup> and chlorobenzene,<sup>27</sup> in terms of conversions.

TMSCl, corresponding to Hampton *and co-workers'* speculation, could not successfully perform the nucleophilic displacement without the presence of NaBr (trials 3-4),<sup>34</sup> resulting in almost no conversion to tenofovir **9**. (Houghton *and co-workers*<sup>30</sup> did a more extensive study on the effects of the different nucleophiles and counter ions on the conversion of phosphonate esters to phosphonic acids and found that NaBr was the most effect environmentally and economically). Addition of NaBr to the system resulted in a significant improvement on the synthesis of tenofovir **9** (trials 5-6), even though the results did not quite match those of TMSBr (trials 1-2). Literature comparison indicated that TMSCl worked most efficiently at slightly higher temperatures than TMSBr, which can explain the poor conversions to tenofovir **9** even in the presence of NaBr.<sup>28,30,31</sup>

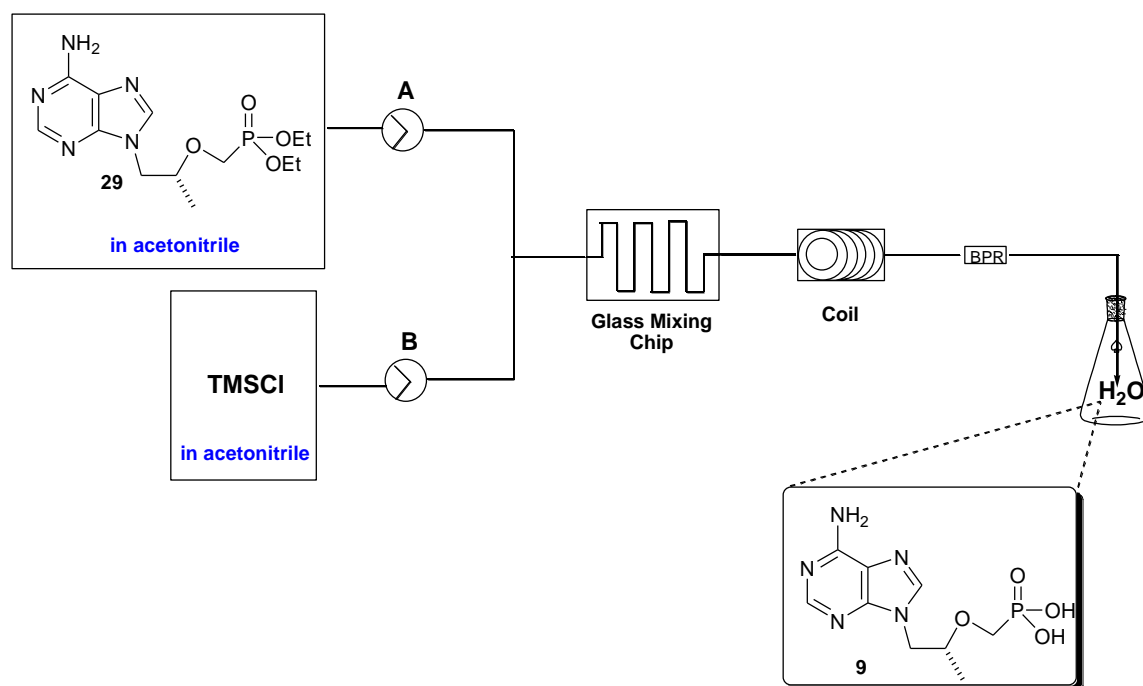
It is quite common to obtain low yields (trial 1-2, 5-6) when working with a relatively small scale (we used 0.5 mmol - 2 mmol PPA **29**) when the isolation of the product (in this case tenofovir **9**) involves precipitation; such as was the case for Baszczyński *et al* as well (reported yields ranging between 30%-53%).<sup>33</sup> Increasing the scale is usually a simple solution to this problem and would probably result in similar yields obtained by the likes of Kaiser *et al*, who reported yields ranging from 73-76%.<sup>31</sup>

Without investing any more time on the optimization of the hydrolysis in batch, we decided to move over to the main objective: attempting the hydrolysis reaction, using TMSCl, on flow.

#### 4.7a) Experimental: The hydrolysis of PPA to tenofovir using TMSCl; translation to flow.

The hydrolysis of the phosphonate ester (**29**) to its phosphonic acid (**9**) categorically required (i) high pressure-which is the environment found in a flow reactor, (ii) high temperature-which is easily controlled in flow and (iii) it needed enough contact time (as the long reaction times in batch indicated), which could be achieved using both a mixing chip and coil reactor as well as manipulating the flow rate.

To achieve these requirements we started with an initial simple set-up as illustrated by scheme 4.15.



Scheme 4.15: Flow set-up for trials attempting to convert PPA to PMPA; with PPA and TMSCl intercepting at the T-piece and mixing at the mixing chip.



We wanted to start off with the assumption that the high pressure, micro-scale flow system might be sufficient to drive the hydrolysis of PPA **29** using just TMSCl (without NaBr), hoping we would achieve similar results to what Gutierrez *and co-workers* did in high pressure and chlorobenzene.<sup>28</sup>

The simple flow set-up (scheme 4.15) had PPA **29** and TMSCl pumped into a T-mixer from two separate stock solutions, via pump A and B, respectively. The combined stream passed through a heated mixing chip (2 mL) to assist with the efficient mixing of the two reagents and then moved into a heated 5 mL coil reactor (steel or PEEK). The mixing chip was heated (the maximum temperature it could reach was 120 °C)<sup>35</sup> identical to the reactor coil, giving the reaction additional progress time. The stream leaving the coil reactor was pumped directed into an external work-up station containing water via a back pressure regulator.

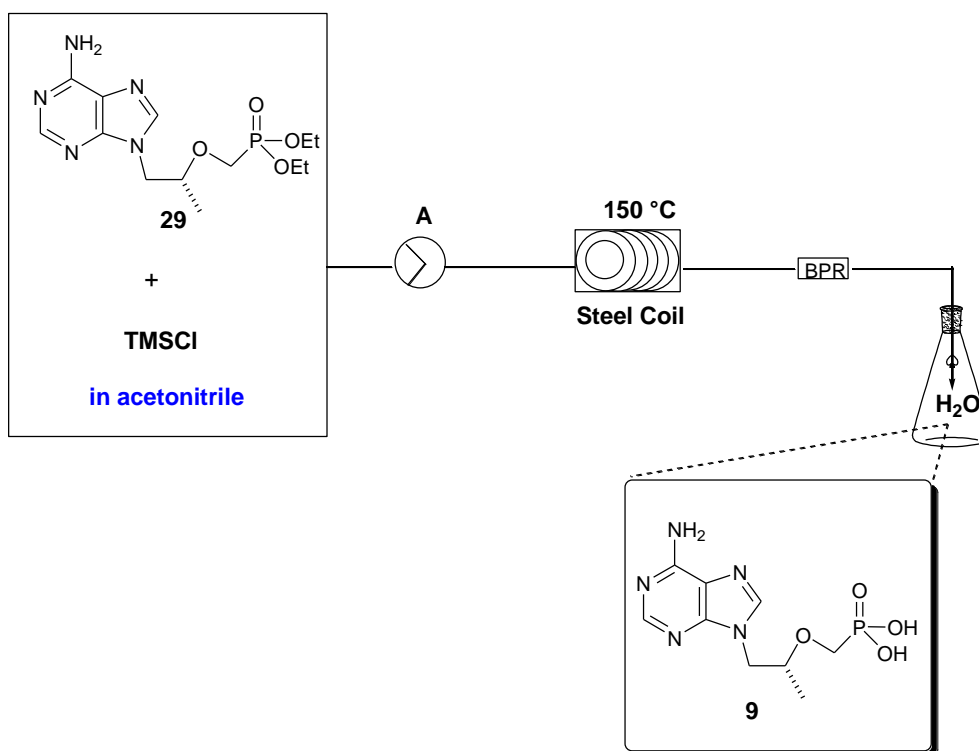
*Table 4.4: Parameters used for the trials performed under flow as shown in scheme 4.15, in attempt to convert PPA to tenofovir, using both a mixing chip and coil reactor.*

Trial	Concentration (M)		Flow Rate (mL/min)	Temperature (°C)		Residence Time (Hours:Minutes)
	PPA ( <b>29</b> )	TMSCl		Glass mixing chip (2 mL)	Coil (5 mL)	
<b>1</b>	0.30	1.6	0.500	120	120	02:23
<b>2</b>	0.15	0.79	0.100			04:43
<b>3</b>	0.30	1.6	0.110		150	04:15
<b>4</b>			0.080			05:40
<b>5</b>			0.060			06:36
<b>6</b>			0.040			07:33

The flow rate of the stream was started off fast at a rate of half a millilitre per minute (trial 1, table 4.4), all the way to trial 6 which was at 0.040 mL/min. The ratio of PPA **29** to TMSCl was kept the same as that in batch (1:5) and the concentration was the highest we achieved (trial 1, 3-6) without a lengthy optimization step. In trial 2 we attempted a more dilute concentration to evaluate if it would have any positive effect on the reaction progress but it proved unsuccessful.

From trial 3-6 we maintained a high temperature of 150 °C for the coil (and maximum 120°C for the glass mixing chip) while changing only the residence time (via flow rate) of the reagents to a point where we had just a little under a twentieth of a millilitre of PPA **29** and TMSCl moving through the flow system per minute that had a residence time of seven-and-a-half hours (trial 6, table 4.4). Despite these efforts to extend the residence/ reaction time, no conversion to tenofovir **9** was obtained.

Before we could admit defeat, we attempted a few trials that had both PPA **29** and TMSCl pre-mixed in the same stock solution before entering the flow system. We thought this would be good to eliminate possible technical issues, i.e. dispersion, that could likely play a hand at the unsuccessful synthesis of PPA **9** in a set-up like scheme 4.15. Scheme 4.16 shows this further simplified set-up.



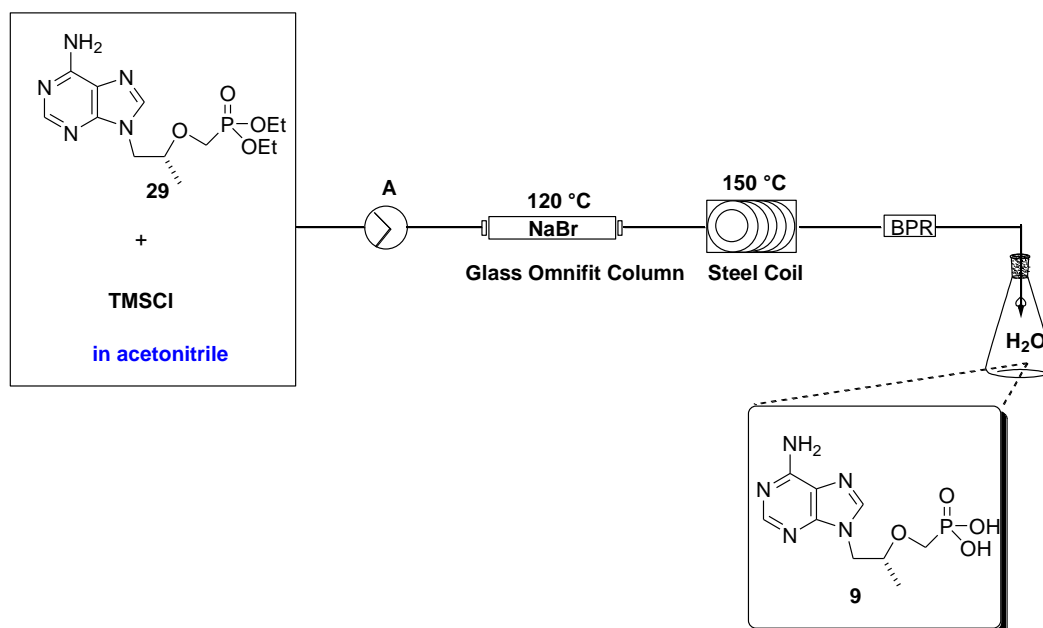
*Scheme 4.16: Flow set-up for trials attempting to convert PPA to tenofovir; with PPA and TMSCl pre-mixed before entering the flow system.*

Scheme 4.16 shows that we had PPA **29** and TMSCl pre-mix (eliminating the need for a mixing chip) before entering as a singular stream via pump A and into the coil reactor. The coil reactor was heated at 150 °C and a flow rate of 0.1 mL / min was programmed. None of the phosphonate ester (**29**) was converted to tenofovir **9** and we were satisfied to conclude that TMSCl alone was not sufficient for the hydrolysis, even in a high pressure flow system.

#### **4.7b) Experimental: The hydrolysis of PPA to tenofovir using TMSCl and NaBr; translation to flow.**

Although we initially attempted to avoid the use of NaBr in flow for the hydrolysis using TMSCl, it seemed as though its presence was necessary.

We decided to add solid NaBr to the flow system by packing the reagent in a glass column reactor as shown in scheme 4.17. This approach was employed as NaBr is completely insoluble in acetonitrile. The parameters used for the trials we ran are found on table 4.5.



Scheme 4.17: Flow set-up for trials attempting to convert PPA to tenofovir; with PPA and TMSCl pre-mixed before entering the flow system and flowing through a column bed of NaBr.

Table 4.5: Parameters used for the trials performed under flow in attempt to convert PPA to tenofovir, using both a column and coil reactor.

Trial	Concentration (M)		Flow Rate (mL / min)	Temperature (°C)	
	PPA (29)	TMSCl		Column (5.5 mL)	Coil (5 mL)
1	0.30	1.6	0.2	120	150
2			0.4		
3			0.8		
4			1.0		

Conditions: 1 equiv. PPA, **29** and 5 equiv. TMSCl were prepared in total volume of 7 mL anhydrous acetonitrile. (> 3.5 equiv.) NaBr was stacked to the brim of 5.5 mL the column reactor.

A stream of pre-mixed PPA **29** and TMSCl was let into the flow system via pump A, and passed through a bed of excess NaBr that was heated to 120 °C. The stream was then allowed to pass through a reactor coil at 150 °C. The outlet was once again passed through a back pressure regulator before being collected in a flask containing water. Only the flow rate was altered and TLC showed conversion of PPA **29** to tenofovir **9** was taking place at the flow rates from trial 1 and 2 (and also slightly at trial 3).

Although there were indications that there was progress in the hydrolysis of PPA **29** to tenofovir **9** on flow, we were unfortunately unable to investigate this reaction any further due to time constraints.

#### ***D. Conclusion for the synthesis of tenofovir.***

The hydrolysis of PPA **29** to tenofovir **9** requires unavoidable harsh conditions. Literature, however, seemed to favour the use of TMS halides, specifically TMSBr and TMSCl. Ideally TMSBr was the best reagent considering both reaction parameters and qualitative and quantitative production of phosphonic acid, however, practically it was at a disadvantage because it was both costly and difficult to handle.

We have seen, nevertheless, that TMSCl can offer satisfactory results as well when used in conjunction with a nucleophilic salt, NaBr, both in batch and flow. Although this step still needs optimization and quantitative analysis, we can speculate that hydrolysis can be achieved in flow using both TMSCl and NaBr.

## References

1. Barral K, Priet S, Sire J, Neyts J, Balzarini J, Canard B, et al. Synthesis, in vitro antiviral evaluation, and stability studies of novel  $\alpha$ -borano-nucleotide analogues of 9-[2-(phosphonomethoxy)ethyl]adenine and ((*R*))-9-[2-(phosphonomethoxy)propyl]adenine. *J Med Chem*. 2006;49(26):7799–806.
2. Roux L, Priet S, Payrot N, Weck C, Fournier M, Zoulim F, et al. Ester prodrugs of acyclic nucleoside thiophosphonates compared to phosphonates: Synthesis, antiviral activity and decomposition study. *Eur J Med Chem*. 2013;63:869–81.
3. Brown Ripin DH, Teager DS, Fortunak J, Basha SM, Bivins N, Boddy CN, et al. Process improvements for the manufacture of tenofovir disoproxil fumarate at commercial scale. *Org Process Res Dev*. 2010;14(5):1194–201.
4. Riley DL, Walwyn DR, Edlin CD. An Improved Process for the Preparation of Tenofovir Disoproxil Fumarate. *Org Process Res Dev*. 2016;20:742–50.
5. Goldberg MC, Delong L, Kahn L. Continuous Extraction of Organic Materials from Water. *Environ Sci Technol*. 1971;5(2):161–2.
6. Hacène K, Aouf Z, Souk TO, Zerrouki (*R*), Aouf N. A new family of 1,2,3-oxathiazolidine-2,2-dioxide phosphonate derivatives : Synthesis , characterization and anticancer evaluation. *Phosphorus, Sulfur, Silicon Relat Elem*. 2017;192(5):555–9.
7. Rajeshwaran GG, Nandakumar M, Sureshbabu (*R*), Mohanakrishnan AK. Lewis Acid-Mediated Michaelis - Arbuzov Reaction at Room Temperature : A Facile Preparation of Arylmethyl / Heteroarylmethyl Phosphonates. *Org Lett*. 2011;13(6):1270–3.
8. Kedrowski SMA, Dougherty DA. Room-Temperature Alternative to the Arbuzov Reaction : The Reductive Deoxygenation of Acyl Phosphonates. *Org Lett*. 2010;12(18):3990–3.
9. Jasiak A, Mielniczak G, Owsianik K, Koprowski M, Krasowska D, Drabowicz J. Solvent-Free Michaelis – Arbuzov Rearrangement under Flow Conditions . *J Org Chem*. 2019;84(5):2619–25.
10. Morgalyuk VP, Strelkova T V, Nifant EE, Valery K, Morgalyuk VP, Strelkova V, et al. New synthesis of trimethylsilyldiphenylphosphinite. *Phosphorus, Sulfur, Silicon Relat Elem*. 2016;191(11–12):1462–3.
11. Hägele G, Gerhard H. Michaelis – Arbuzov Reactions of Perhalogenated Cyclobutenes with Trialkyl Phosphites. *Phosphorus, Sulfur, Silicon Relat Elem*. 2015;190(12):2094–109.
12. Powell S, Kosolapo BGM, Powell S. Alkylation of Triethyl Phosphonoacetate and Related Esters. *J Am Chem Soc*. 1950;72(9):4198–200.
13. Wang Z, Tang J, Salomon CE, Dreis CD, Vince (*R*). Pharmacophore and structure – activity relationships of integrase inhibition within a dual inhibitor scaffold of HIV reverse transcriptase and integrase. *Bioorg Med Chem*. 2010;18(12):4202–11.
14. Renard P, Vayron P, Mioskowski C. Trimethylsilyl Halide-Promoted Michaelis-Arbuzov Rearrangement. *Org Lett*. 2003;5(10):1661–4.
15. Janicki SZ, Fairgrieve JM, Petillo PA. A facile , general approach to the synthesis of electrophilic acetone equivalents. *J Org Chem*. 1998;63(11):3694–700.
16. Zheng N, Tilve S, Oe T, Albelda SM. Synthesis of the stable isotope labeled antiviral nucleoside analog [8-<sup>13</sup>C–7, 9-<sup>15</sup>N2]-ganciclovir. *J Label Compd Radiopharm Off J Int Isot Soc*.

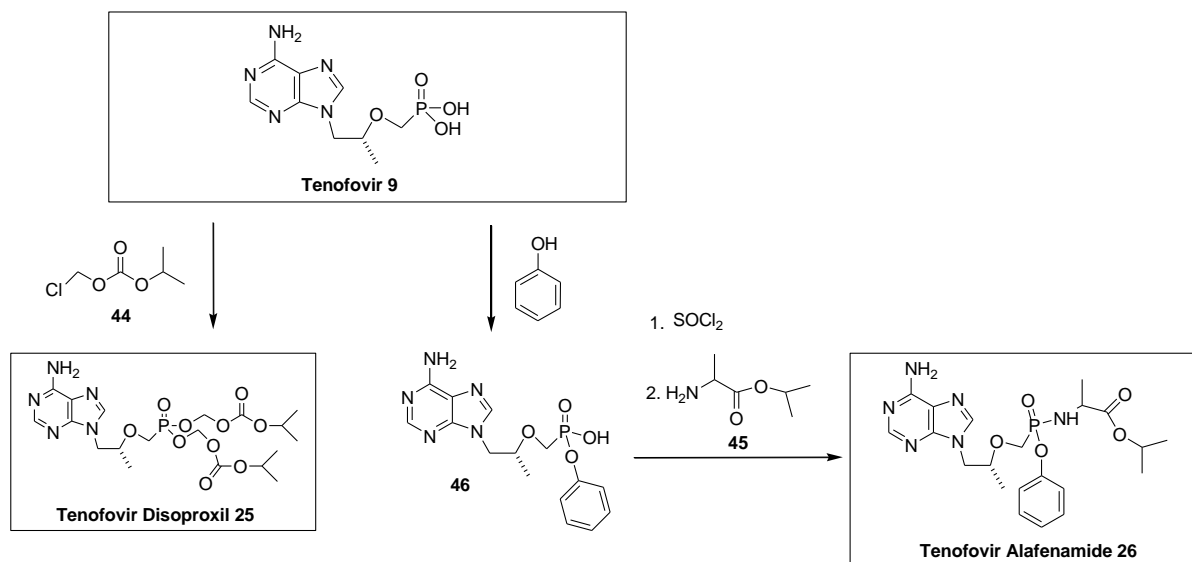
- 2006;49(13):1131–9.
17. Pernak J, Feder-kubis J. Synthesis and properties of chiral ammonium-based ionic liquids. *Chem Eur J*. 2005;11(15):4441–9.
  18. Arbuzov B, Vinokurova G. Reactions of bis (chloromethyl) ethers of glycols with sodium alkoxides. *Bull Acad Sci USSR, Div Chem Sci*. 1953;2(5):735–45.
  19. Anderson NG, Ciaramella BM, Feldman AF, Lust DA, Moniot JL, Moran L, et al. Process development for the preparation of a monopril intermediate by a trimethylsilyl-modified arbuzov reaction. *Org Process Res Dev*. 1997;1(3):211–6.
  20. Yamagishi T, Mori J, Haruki T, Yokomatsu T. A chemo-enzymatic synthesis of optically active 1, 1-diethoxyethyl ( aminomethyl ) phosphinates : useful chiral building blocks for phosphinyl dipeptide isosteres. *Tetrahedron: Asymmetry*. 2011;22(12):1358–63.
  21. Hwang J, Jung K. A Short Synthesis of a Novel Nucleoside Analog of Fosfomycin. *Bull Korean Chem Soc*. 2002;23(12):1848–50.
  22. Berger O, Gavara L, Montchamp J. Chemistry of the Versatile (Hydroxymethyl) phosphinyl P(O)CH<sub>2</sub>OH Functional Group. *Org Lett*. 2012;14(13):3404–7.
  23. Doboszewski B, Groaz E, Herdewijn P. Synthesis of Phosphonoglycine Backbone Units for the Development of Phosphono Peptide Nucleic Acids. *European J Org Chem*. 2013;2013(22):4804–15.
  24. Kong D-L, Li G-Z, Liu (R)-D. Synthesis and crystal structure of diethyl tosyloxybenzylphosphonate. *Asian J Chem*. 2014;26(7):2138–40.
  25. Lai G, Tan P, Ghoshal P. A one-pot method for the efficient conversion of aryl-and acyl-substituted methyl alcohols into chlorides. *Synth Commun*. 2003;33(10):1727–32.
  26. Ripin DHB, Teager DS, Fortunak J, Basha SM, Bivins N, Boddy CN, et al. Process Improvements for the Manufacture of Tenofovir Disoproxil Fumarate at Commercial Scale. *Org Process Res Dev*. 2010;14(5):1194–201.
  27. Jansa P, Baszczynski O, Prochazkova E, Dracinsky M, Janeba Z. Microwave-assisted hydrolysis of phosphonate diesters: an efficient protocol for the preparation of phosphonic acids. *Green Chem*. 2012;14(8):2282–8.
  28. Gutierrez AJ, Prisbe EJ, Rohloff JC, Gutierrez AJ, Prisbe EJ, Rohloff JC. DEALKYLATION OF PHOSPHONATE ESTERS WITH CHLOROTRIMETHYLSILANE. *Nucleosides, Nucleotides and Nucleic Acids*. 2001;20(4–7):1299–302.
  29. Blazewska K. McKenna Reaction - Which Oxygen Attacks Bromotrimethylsilane? *J Org Chem*. 2014;79(1):408–12.
  30. Houghton SR, Melton J, Fortunak J, Brown DH, Boddy CN. Rapid , mild method for phosphonate diester hydrolysis : development of a one-pot synthesis of tenofovir disoproxil fumarate from tenofovir diethyl ester. *Tetrahedron*. 2010;66(41):8137–44.
  31. Pos L, Kaiser MM, Hockovµ D, Wang T, Drac M, Edstein MD, et al. Synthesis and Evaluation of Novel Acyclic Nucleoside Phosphonates as Inhibitors of Plasmodium falciparum and Human 6-Oxopurine Phosphoribosyltransferases. *ChemMedChem*. 2015;10(10):1707–23.
  32. Baszczynski O, Jansa P, Klepetarova B, Holy A, Votruba I, de Clercq E, et al. Synthesis and antiviral activity of N9-[3-fluoro-2-(phosphonomethoxy) propyl] analogues derived from N6-substituted adenines and 2, 6-diaminopurines. *Bioorg Med Chem*. 2011;19(7):2114–24.

33. Schultze LM, Chapman HH, Dubree NJP, Jones RJ, Kent KM, Lee TT, et al. Practical Synthesis of Anti-retroviral Drug, PMPA. *Tetrahedron Lett.* 1998;39(14):1853–6.
34. Hampton A, Sasaki T, Paul B. Synthesis of 6'-cyano-6'-deoxyhomoadenosine-6'-phosphonic acid and its phosphoryl and pyrophosphoryl anhydrides and studies of their interactions with adenine nucleotide utilizing enzymes. *J Am Chem Soc.* 1973;95(13):4404–14.
35. Uniqsis Ltd. UNIQSIS Accessible flow chemistry [Internet]. 2020 [cited 2020 Jan 24]. Available from: <http://www.uniqsis.com/paAccessories.aspx>



## Chapter 5: The final steps towards the synthesis of TD and TA.

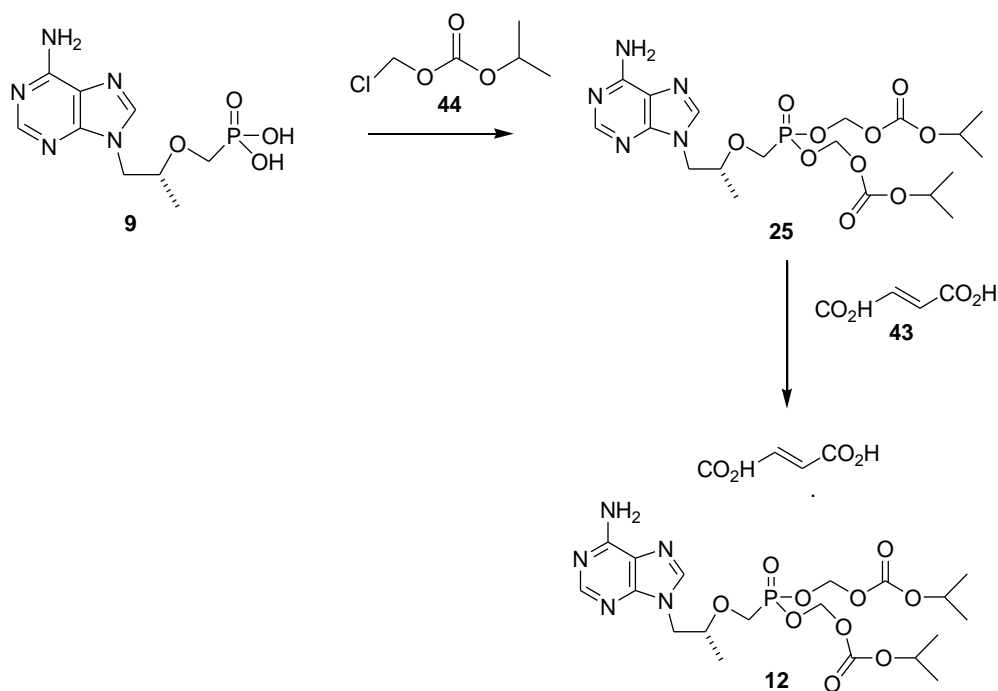
Following the successful synthesis of the active drug tenofovir **9**, the last few steps of the synthetic pathway diverged into the synthesis of the ARV drugs, TD **25** and TA **26** (scheme 5.1).



Scheme 5.1: Translation of tenofovir to ARV drugs, TD and TA.

### A. Synthesis of prodrug TD.

The synthesis of prodrug TDF **12**, is completed with an alkylative esterification of tenofovir **9**, to form the diester TD **25**, which is then treated with fumaric acid **43**, to crystallize out as TDF **12** (scheme 5.2).<sup>1</sup>



Scheme 5.2: Synthesis of TDF from tenofovir.

The base promoted alkylation is usually performed with trimethylamine and chloromethyl isopropylcarbonate, **44**, in a polar aprotic solvent, usually *N*-methyl-2-pyrrolidone. Interestingly, Stephen and co-workers suggested that an *in situ* production of TD **25** from PPA **29** was possible based on the favourable results they obtained from an *in situ* synthesis of TD **25** from tenofovir (PMPA) **9**.<sup>2</sup>

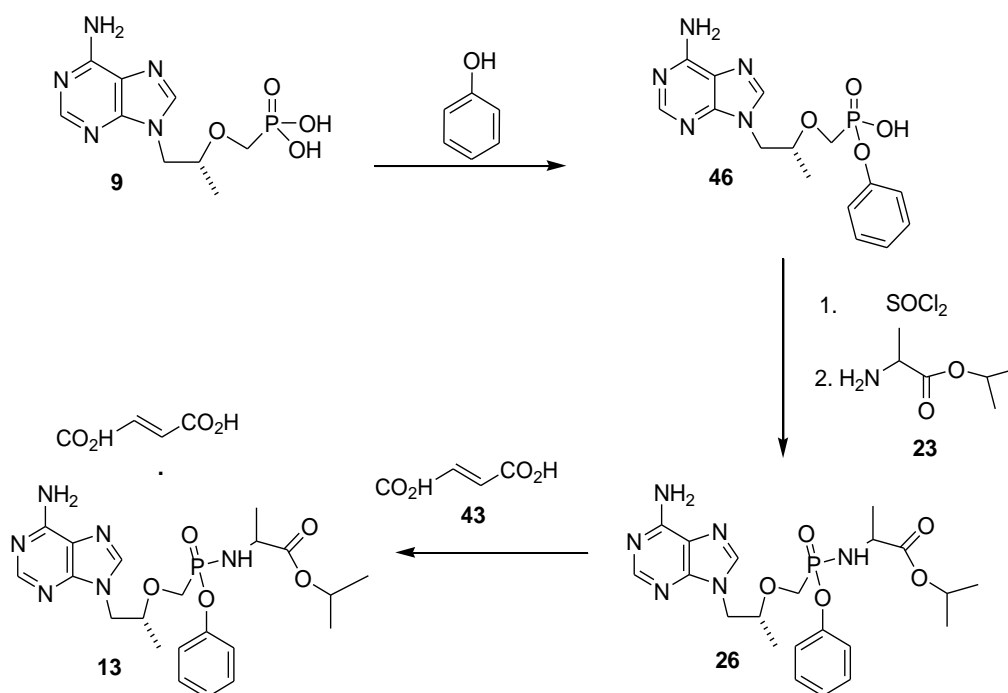
A common issue with this step is the solubility of PMPA **9**, which requires a polar aprotic solvent, heated in basic medium (similarly to the solubility issue we faced with HPA **28**).<sup>3</sup> We were however unable to investigate this due to time constraints and hence we replicated the procedure employed by Ripin and co-workers.<sup>3</sup>

The procedure involved the addition of trimethylamine (4 equiv.) and chloromethyl isopropylcarbonate (5 equiv.) to a round-bottom flask containing PMPA **9** (1 equiv.). The reaction mixture was stirred together at 60 °C for six hours. TD, **25** was isolated at 26% yield (unoptimized).

## B. Synthesis of prodrug TA.

TA **26** has three chiral centres: the 2-propyloxy centre and the alanine-amidate (*S*) chiral centre which are both controlled synthetically. The other chiral centre is that found on the phosphorous of TA **26** which isn't controlled synthetically and forms a 1:1 diastereomeric mixture.<sup>4,5</sup> Chapman and co-workers,<sup>4</sup> managed to successfully separate the two diastereoisomers for analysis using Simulated Moving Bed (SMB) chromatography while Yang and co-workers claim to have found a more traditional and economically friendly route for isolation of the diastereoisomers by using resolving agents.<sup>6</sup> The separation of the diastereoisomers did, however, not form part of the scope of our research as we focused mainly on producing TA and not necessarily isolating the active diastereoisomer.

For the synthesis of TA **26**, from PMPA **9**, two separate steps are required (scheme 5.3). The first is an esterification between PMPA **9** and phenol, using a coupling agent, e.g DCC (dicyclohexyl carbodiimide),<sup>6</sup> followed by the addition of isopropyl L-alanine **45** to form TA **26**. TA **26** is then isolated as a salt by addition of fumaric acid, **43**<sup>7</sup>



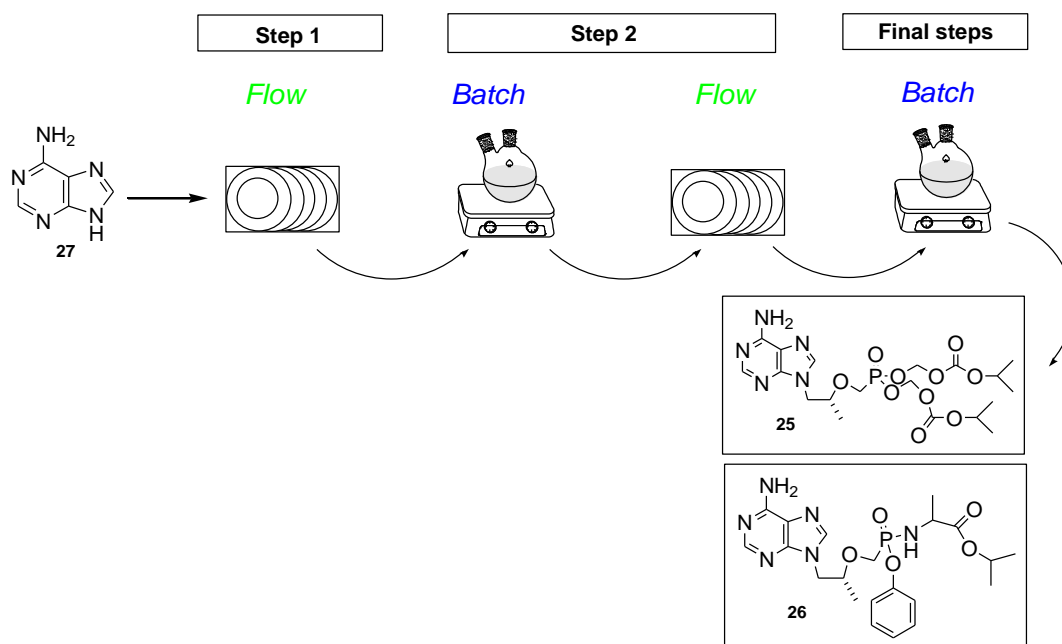
Scheme 5.3: Synthesis of TAF from tenofovir.

The procedure recorded by Chapman and co-workers was followed in which PMPA **9** (1 equiv.) was coupled to phenol (2 equiv.) using alternative coupling agent, CDI (1,1'-Carbonyldiimidazole) (1.6 equiv.).<sup>8</sup> The collected product, **46**, (1 equiv.) was activated using thionyl chloride (2.4 equiv.) and isopropyl L-alanine **45**, (2.4 equiv.) with triethylamine (3.0 equiv.) was added. The reaction ran for

about three hours and the resulted in crude product was collected as an oil. Analysis of NMR spectra did not provide proof of TA **26**, but rather showed presence of phenol-PMPA **46** and possibly other unknown impurities. We were unable to investigate this any further due to time constraints.

### C. Final Conclusion towards the synthesis of TD and TA.

We attempted to validate known approaches for the synthesis of TD **25** and TA **26**,<sup>3,7</sup> and although the given procedures were not attempted on flow or optimized in batch due to time constraints, the production of TD **25** was successful. Unfortunately, in our hands we were unable to isolate TA **26**.



Scheme 5.4: Summary of the synthetic pathway for the synthesis of TD and TA.

Looking at the overall view of the pathway (scheme 5.4), the initial step, which was the alkylation of adenine **27** with ((*R*))-propylene carbonate **33**, was successfully translated to flow with work-up aided by use of an immobilized catch-and-release reagent, Amberlyst 15<sup>®</sup> **36**. Step 2b, which was the hydrolysis of PPA **29** to tenofovir **9**, was also translated to flow using TMSX (X= Cl or Br).

The steps that remained as batch reactions had issues that hindered translation to flow, particularly precipitation for step 2a and time constraints for step 3. These issues could possibly be resolved with further investigation and optimizations that we were unable to explore

Overall, a semi-continuous pathway was established for the synthesis of prodrug, TD **25** and precursor to TA **26**, phenol-PMPA **46**.

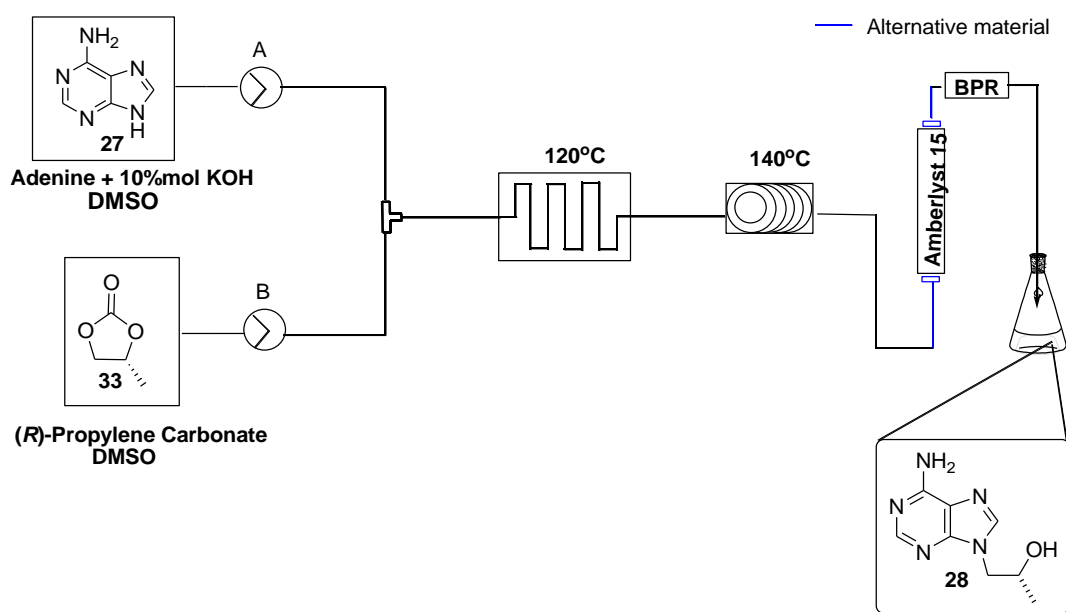
## References

1. Brown Ripin DH, Teager DS, Fortunak J, Basha SM, Bivins N, Boddy CN, et al. Process improvements for the manufacture of tenofovir disoproxil fumarate at commercial scale. *Org Process Res Dev.* 2010;14(5):1194–201.
2. Houghton SR, Melton J, Fortunak J, Ripin DHB, Boddy CN. Rapid , mild method for phosphonate diester hydrolysis : development of a one-pot synthesis of tenofovir disoproxil fumarate from tenofovir diethyl ester. *Tetrahedron.* 2010;66(41):8137–44.
3. Chapman H, Kernan M, Rohloff J, Sparacino M, Terhorst T. PURIFICATION OF PMPA AMIDATE PRODRUGS BY SMB CHROMATOGRAPHY AND X-RAY CRYSTALLOGRAPHY OF THE DIASTEREOMERICALLY PURE GS-7340. *Nucleosides, Nucleotides and Nucleic Acids.* 2007;7770(20):1085–90.
4. Schultze LM, Chapman HH, Dubree NJP, Jones RJ, Kent KM, Lee TT, et al. Practical Synthesis of Anti-retroviral Drug, PMPA. *Tetrahedron Lett.* 1998;39(14):1853–6.
5. Yang B, Xie H, Ran K, Gan Y. Efficient Synthesis and Resolution of Tenofovir Alafenamide. *Lett Org Chem.* 2018;15:10–4.
6. Chapman H, Kernan M, Prisbe E, Rohloff J, Sparacino M, Terhorst T. PRACTICAL SYNTHESIS , SEPARATION , AND STEREOCHEMICAL ASSIGNMENT OF THE PMPA PRO-DRUG GS-7340. *Nucleosides, Nucleotides and Nucleic Acids.* 2007;7770(20):621–8.

## Chapter 6: Future Work

### 6.1) Synthetic Step 1.

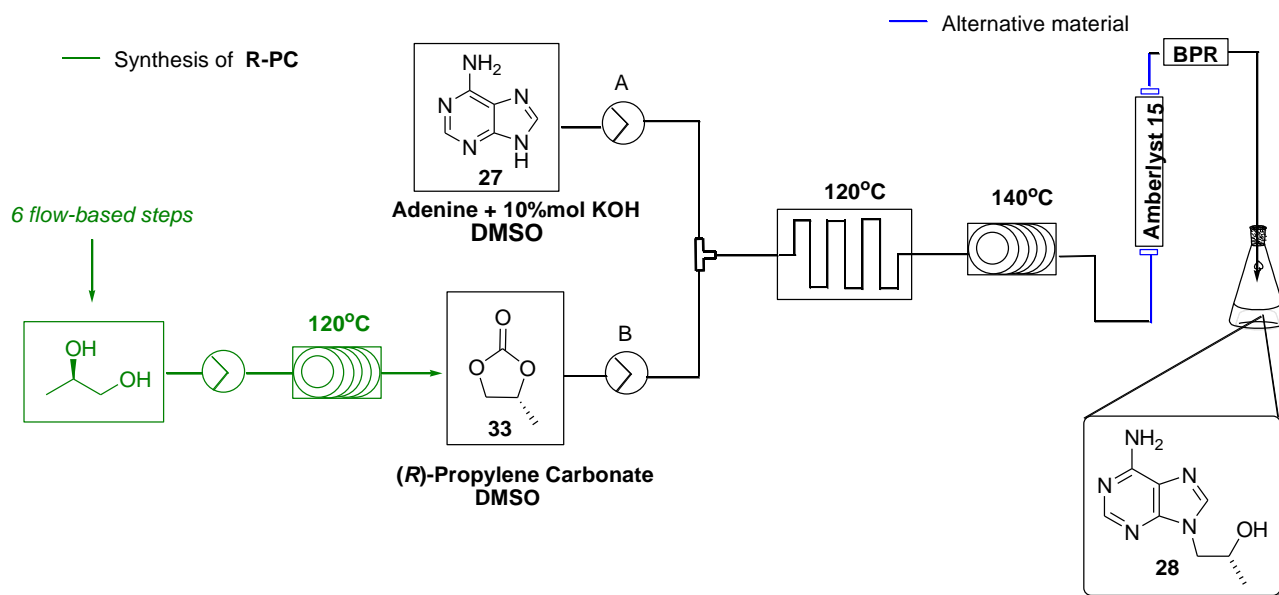
The successful conversion of adenine **27** to HPA, **28**, on flow was impressive. The main issue was the work-up which we were unable to translate to flow because of the unsuitability of the solvent, dimethyl sulfoxide, with the PEEK material fittings of the glass column. It would be interesting to investigate how well the work-up integrates with the synthesis if suitable material (perhaps steel, Teflon, etc.) fittings for the glass column could be sourced (scheme 6.1). If positive results could be obtained it would push an even more compelling case for the flow synthesis of HPA, **28**, as compared to the batch synthesis.



Scheme 6.1: Proposed in-line work-up with Amberlyst 15<sup>®</sup> in glass column fitted with alternative, DMSO-compatible material, fittings.

Suveges and co-workers<sup>1</sup> recently published an article that detailed a continuous flow synthesis of an important intermediate for the synthesis of tenofovir **9**, ((R))-propylene carbonate **33**. The entire strategy took seven steps reaction sequence, with the starting material as glycerol, a “cheap and renewable raw material”, as reported by the team<sup>1</sup>. They concluded that their results show reduced steps and increased conversion rates.

It might be worth investigating, for industry purposes, the incorporation of the work done by Suveges and co-workers to our synthetic pathway to evaluate if there is any economic benefit to adding some, if not all, of the steps proposed by Suveges and co-workers (scheme 6.2).



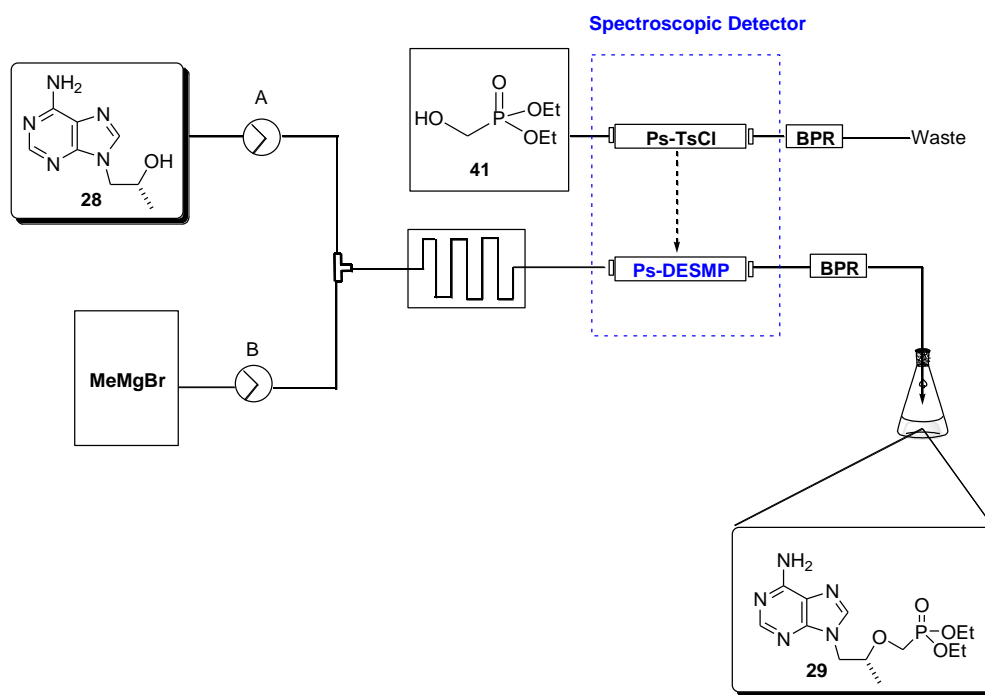
Scheme 6.2: Proposed employment of the flow synthesis of ((R))-propylene carbonate using Suveges et al<sup>1</sup> method to our flow synthesis of HPA, including our proposed in-line workup.

## 6.2) Synthetic Step 2.

To date there hasn't been a reported method for the synthesis of Ps-DESMP **39** and moreover, most of the work reported for the synthesis of DESMP **37** is patent work (research conducted by Martin LJ and co-workers reported the use of Ps-TsCl **40** on flow at temperatures as high as 110 °C but only has a scavenger for diamines<sup>2</sup>).



It could be worth attempting the trials of Ps-TsCl **40** to Ps-DESMP **39** again, but this time using flow in hopes that the manipulation of the parameters (such as temperature and flow rate) under flow conditions could successfully convert Ps-TsCl **40** to Ps-DESMP **39** (scheme 6.3).

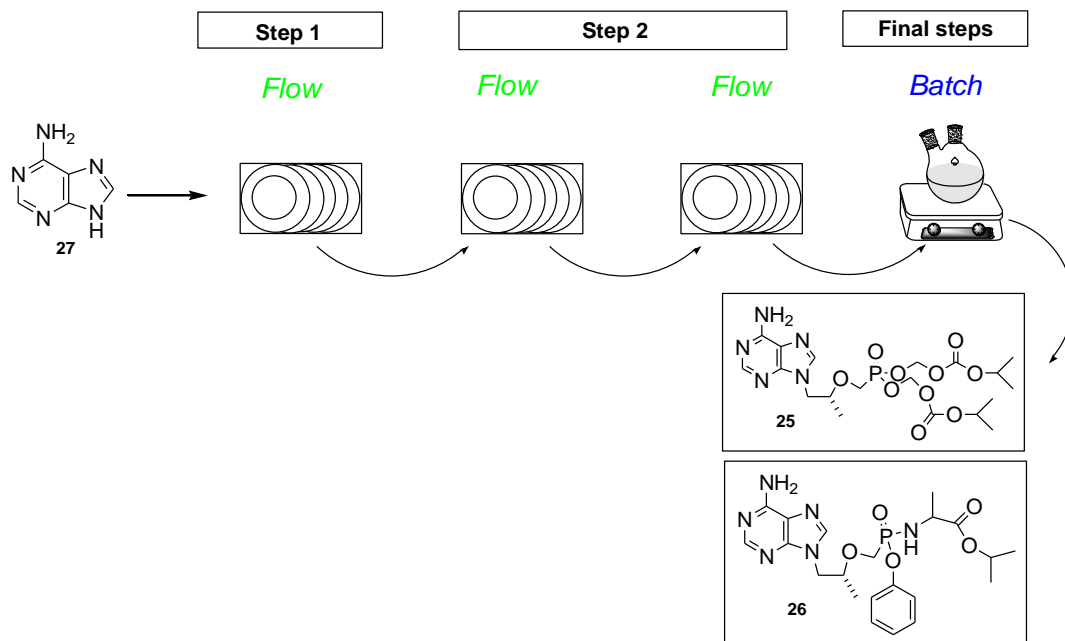


*Scheme 6.3: A simplified representation of a flow set-up for the synthesis of Ps-DESMP from Ps-TsCl and conversion of HPA to PPA with a spectroscopy detector included.*

With attempts on flow, we would also get an opportunity to overcome another major setback we had encountered, which is the monitoring of the reaction progress. Monitoring of reactions is not a new concept to flow and particularly for resin bound reagents. This could be done by adding an in-line spectroscopic analysis, such as fluorescence spectroscopy<sup>3</sup> as suggested by Yue and co-workers who go into detail on how to integrate spectroscopic detection to microreactors.

Needless to say that the success of the production of Ps-DESMP **39** would catapult this step of the tenofovir synthetic pathway into a new level of ease and environmental friendliness (the Ps-DESMP **39** would act as both a reagent and a scavenger of Grignard by-product as shown in chapter 4, scheme 4.10).

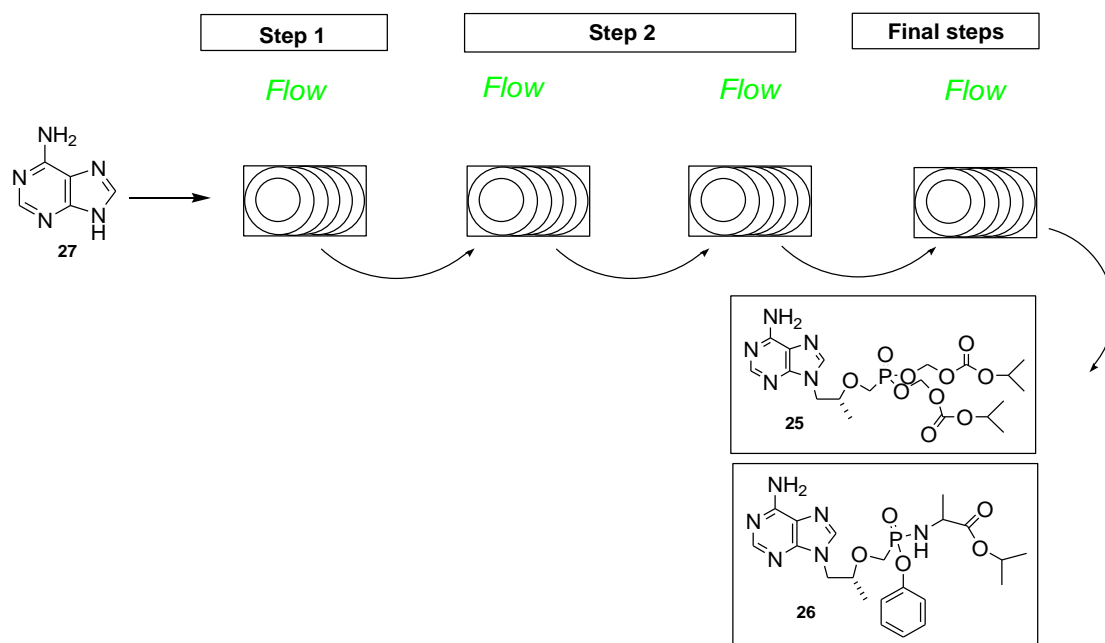
Any more work done for step 2 of the synthetic pathway would be to optimize the parameters already obtained in our research, to obtain the best conversion and yielding parameters. Assuming the success of the suggested implementations above, we could in the near future obtain a continuous flow based synthesis of active drug, tenofovir **9** (scheme 6.4).



*Scheme 6.4: Summary of a prospective synthetic pathway for the synthesis of TA and TD, with continuous flow reaching the up to the synthesis of tenofovir.*

### 6.3) Final synthetic steps.

The long term goal would be to investigate the feasibility of the translation of the final steps towards the synthesis of TD **25** and TA **26** to flow. If successful, we would end up with a completely (staged) continuous flow synthesis of ARV drugs, TD **25** and TA **26** (scheme 6.5).



Scheme 6.5: Summary of a prospective fully continuous (at least 5 stages) synthetic pathway for the synthesis of TA and TD.

## References

1. Suveges NS, Rodriguez AA, Diederichs CC, Souza SP De, Leão RAC, Miranda LSM, et al. Continuous-Flow Synthesis of ((*R*))-Propylene Carbonate : An Important Intermediate in the Synthesis of Tenofovir. *European J Org Chem.* 2018;2018(23):2931–8.
2. Martin LJ, Marzinzik AL, Ley S V, Baxendale (*R*). Safe and reliable synthesis of diazoketones and quinoxalines in a continuous flow reactor. *Org Lett.* 2011;13(2):320–3.
3. Yue J, Schouten JC, Nijhuis TA. Integration of Microreactors with Spectroscopic Detection for Online Reaction Monitoring and Catalyst Characterization. *Ind Eng Chem Res.* 2012;51(45):14583–609.

## Chapter 7: Experimental descriptions

### General

#### Preparation of anhydrous solvents

- Tetrahydrofuran (THF) and diethyl ether were pre-dried over sodium wire, and distilled from sodium metal wire and benzophenone.
- Acetonitrile, dichloromethane, and *tert*-butanol were distilled from calcium hydride.
- *N,N*-dimethylformamide (DMF), dimethyl sulfoxide (DMSO) and *N*-methyl-2-pyrrolidone (NMP) were distilled from, and stored over 4 Å molecular sieves.

#### Techniques

- All reactions were performed under an inert atmosphere (either nitrogen or argon) using either a standard manifold line connected to the gas cylinder or via a balloon containing the inert gas.
- The vessels were either oven dried overnight or flame dried while under vacuum and were allowed to cool to room temperature under the inert atmosphere.

#### Special Instruments

- All flow reactions were performed on a Uniqsis “FlowSyn™ Multi-X” flow reactor with Uniqsis FlowSyn™ accessories and consumables.

#### Spectroscopic data

##### Nuclear Magnetic Resonance (NMR)

The  $^1\text{H}$ ,  $^{13}\text{C}$  and  $^{31}\text{P}$  NMR were recorded on a Bruker Avance-300 at 300.13 MHz. Chemical shifts are reported in parts per million (ppm) relative to tetramethylsilane as internal standard.  $^1\text{H}$  NMR solvent DMSO- $\text{d}_6$  was referenced on the chemical shift 2.50 ppm and  $\text{CDCl}_3\text{-d}$  on the chemical shift 7.24 ppm.  $^{13}\text{C}$  NMR solvent DMSO- $\text{d}_6$  was referenced on the chemical shift 39.5 ppm and  $\text{CDCl}_3\text{-d}$  on the chemical shift 77.2 ppm. The  $^1\text{H}$  NMR chemical shifts are reported as follows: value (splitting pattern, number of hydrogens, assignment).  $^{13}\text{C}$  NMR chemical shifts are reported: value (assignment) and  $^{31}\text{P}$  NMR chemical shifts as: value. Abbreviations used: s = singlet, d = doublet, dd = double doublet, m = multiplet.

##### Infrared (IR)

Infrared spectra were obtained on a Bruker Vector 22 spectrometer, or a Varian 800FTIR spectrometer (Scimitar Series). The absorptions are reported on the wavenumber ( $\text{cm}^{-1}$ ) scale, in the range 400-4000  $\text{cm}^{-1}$ . The signals are reported: value (relative intensity, assignment). Abbreviations used in quoting spectra are: s = strong, m = medium.

#### Disclaimers

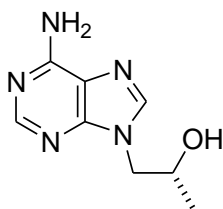
- *Nomenclature and numbering of compounds*

The compounds prepared during the course of this project are named in the following sections according to systematic nomenclature. However, the numbering system (and abbreviations) used to illustrate the diagrams of these compounds is one implemented for convenience and is not meant to reflect systematic numbering of these compounds. Common names of reagents may also be employed for convenience.

- Reactions in “batch” refer to reactions performed using standard laboratory glassware.
- Reactions on “flow” refer to reactions performed on the flow reactor specified under “special instruments”.
- All experiments labelled “attempt” were either inconclusive or concluded to be unsuccessful.
- The number of trials for each experiment / attempt is not specified.

### ***Experimental for chapter 3: Step 1***

#### ***Synthesis of ((R))-9-(2-Hydroxypropyl)adenine (HPA 28).....(Batch)***



#### ***Trituration work-up***

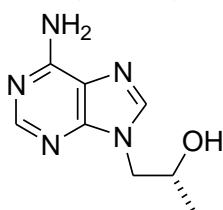
Adenine **27** (1.0 g, 7.4 mmol) and potassium hydroxide (0.042 g, 0.74 mmol, 0.1 equiv.) were mixed with anhydrous DMSO (10 mL) and stirred for 15 minutes at room temperature. ((R))-propylene carbonate **33** (0.84 mL, 9.8 mmol, 1.32 equiv.) was added dropwise to the reaction mixture over 2 minutes. The resulting mixture was heated to 120 °C and held at that temperature for 3.5 hours. A clear yellow solution resulted, and the reaction mixture was cooled to 70 °C. Ethanol (30 mL) was added dropwise to the reaction mixture over 10 minutes, and precipitation of product was observed. The reaction mixture was further cooled to ~5 °C and held at this temperature for 1 hour. The product was isolated by filtration, and the white solid was washed with chilled ethanol (10 mL). The resulting solid was dried under vacuum affording **HPA 28** as a white powder (0.89 g, 62% yield). <sup>1</sup>H NMR (300 MHz, DMSO-d<sub>6</sub>) δ 8.09 (s, 1H, Ar-H), 8.00 (s, 1H, Ar-H), 7.14 (s broad, 2H, NH<sub>2</sub>), 4.99 (s broad, 1H, OH), 4.00 (m, 3H, CH<sub>2</sub>CH, CH<sub>2</sub>CH), 1.02 (d, 3H, CH<sub>3</sub>CH). <sup>13</sup>C NMR (75 MHz, DMSO-d<sub>6</sub>) δ 155.99 (C2) 152.34 (C8) 149.79 (C6) 141.56 (C4) 118.62 (C5) 64.70 (CH) 50.19 (CH<sub>2</sub>) 20.93 (CH<sub>3</sub>). FTIR 3409 (s broad, OH) 3136 (m, NH) cm<sup>-1</sup>.

#### ***Catch-and-release work-up***

Adenine **27** (1.0 g, 7.4 mmol) and potassium hydroxide (0.042 g, 0.74 mmol, 0.1 equiv.) were mixed with anhydrous DMSO (10 mL) and stirred for 15 minutes at room temperature. ((R))-propylene

carbonate **33** (0.84 mL, 9.8 mmol, 1.32 equiv.) was added dropwise to the reaction mixture over 2 minutes. The resulting mixture was heated to 120 °C and held at that temperature for 3.5 hours. The clear yellow solution was left to cool and then added to an Erlenmeyer flask containing 5.0 g Amberlyst 15® **36** resin, followed by gentle stirring at room temperature overnight. The liquor was then filtered in vacuo and the resin was washed with 7 mL 2N methanolic ammonia. The liquor was collected and solvent removed via rotary evaporation in vacuo to produce an off-white solid compound. **HPA 28** (1.1 g, 77%). <sup>1</sup>H NMR (300 MHz, DMSO-d<sub>6</sub>) δ 8.09 (s, 1H, Ar-H), 8.00 (s, 1H, Ar-H), 7.13 (s broad, 2H, NH<sub>2</sub>), 4.99 (s broad, 1H, OH), 4.00 (m, 3H, CH<sub>2</sub>CH, CH<sub>2</sub>CH), 1.01 (d, 3H, CH<sub>3</sub>CH). <sup>13</sup>C NMR (75 MHz DMSO-d<sub>6</sub>) δ 155.99 (C2) 152.34 (C8) 149.79 (C6) 141.56 (C4) 118.62 (C5) 64.70 (CH) 50.19 (CH<sub>2</sub>) 20.93 (CH<sub>3</sub>)

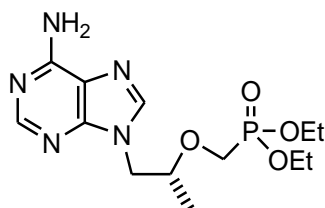
**Synthesis of ((R))-9-(2-Hydroxypropyl)adenine (HPA 28).....(Flow)**



Using the flow reactor, there were two streams driven by pump A and pump B, respectively. Stream A consisted of adenine **27** (1.0 g, 7.4 mmol), potassium hydroxide (0.04 g, 0.74 mmol, 0.1 equiv.) and anhydrous DMSO (15 mL), heated at 140°C to dissolve adenine **27**. Stream B consisted of ((R))-propylene carbonate **33** (0.84 mL, 9.8 mmol, 1.32 equiv.) and anhydrous DMSO (15 mL), also heated at 140°C to avoid significant viscosity differences between the two streams. Once adenine **27** was dissolved, 7 mL of each solution was pumped from the stock vessels, into the loops, at the same rate (0.2 mL/min) and mixed together at the 2 mL mixing chip for 70 minutes, at 140°C. The mixture was released into a 5mL coil for another 70 minutes at 140°C and finally ejected out of the reactor via the back-pressure regulator, into a stirring solution of Amberlyst 15® **36** (3.88 g in 5 mL DMSO) and left to stir at room temperature overnight. The DMSO solution was filtered out and discarded. The resin was washed with 15 mL of 2 N methanolic ammonia and the methanol liquor was removed by evaporating in vacuo to afford an off-white solid, **HPA 28** (1.2 g, 84% yield). <sup>1</sup>H NMR (300 MHz, DMSO-d<sub>6</sub>) δ 8.09 (s, 1H, Ar-H), 8.00 (s, 1H, Ar-H), 7.14 (s broad, 2H, NH<sub>2</sub>), 5.01 (s broad, 1H, OH), 4.04 (m, 3H, CH<sub>2</sub>CH, CH<sub>2</sub>CH), 1.02 (d, 3H, CHCH<sub>3</sub>).

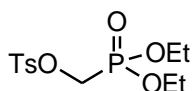
### Experimental for chapter 4: Step 2a

#### Synthesis of ((R))-diethyl (((1-(6-amino-9H-purin-9-yl)propan-2-yl)oxy)methyl)phosphonate (PPA 29).....(Batch)



A mixture of **HPA 28** (1.0 g, 5.18 mmol), *tert*-butanol (0.5 mL, 5.2 mmol, 1 equiv.) and anhydrous cyclohexane (5 mL) were charged to a 2-necked round-bottom flask that was cooled to 0°C. Methyl magnesium bromide (3.4 M in methylated THF, 1.7 mL, 5.7 mmol, 1.1 equiv.) was added dropwise to the suspension kept at 0°C, inertly, and the reaction mixture was left to stir for 30 minutes. Following this was the dropwise addition of commercial DESMP **37** (3.2 mL, 12.5 mmol, 2.5 equiv.) to the stirring reaction mixture and then heating the mixture to 75°C and leaving it there for about an hour. The round-bottom flask was then opened up in order to boil off the cyclohexane for about 3 hours. The sticky residue was taken up in water, gravity filtered, and concentrated to about 20 mL. This aliquot was extracted with hot chloroform (200 mL x2) and the organic layer was evaporated in vacuo. The yellow oil was taken up in 30 mL dichloromethane and extracted with 2 M hydrochloric acid (15 mL x 3), followed by basifying the aqueous layer to pH 11 with ammonium hydroxide (25%). The basified aliquot was further extracted with dichloromethane (50 mL x2) and the organic layer was dried using sodium sulphate, gravity filtered and evaporated in vacuo to afford a yellow oil which was placed under reduced pressure to give a white solid, **PPA 29** (1.07g, 60% yield) <sup>1</sup>H NMR (300 MHz, DMSO-d<sub>6</sub>) δ 8.14 (s, 1H, Ar-H), 8.05 (s, 1H, Ar-H), 7.24 (s broad, 2H, NH<sub>2</sub>), 4.29-3.79 (m, 9H, NCH<sub>2</sub>CH, NCH<sub>2</sub>CH, OCH<sub>2</sub>P, OCH<sub>2</sub>CH<sub>3</sub>), 1.17-1.08 (m, 9H, CHCH<sub>3</sub>, OCH<sub>2</sub>CH<sub>3</sub>). <sup>13</sup>C NMR (75 MHz, DMSO-d<sub>6</sub>) δ 156.39 (C2) 152.84 (C8) 150.22 (C6) 141.78 (C4) 118.81 (C5) 76.00, 63.17, 62.13, 61.00, 47.21(NCH<sub>2</sub>) 17.11, 16.66, 16.56 <sup>31</sup>P NMR (121 MHz, DMSO-d<sub>6</sub>) δ 21.20.

#### Synthesis of Diethyl (tosyloxy) methylphosphonate (DESMP 37).....(Batch)



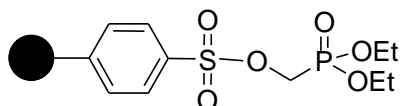
Tosyl chloride, **42** (0.20 g, 1 mmol) was dissolved in 0.5 mL anhydrous dichloromethane. To this, pyridine (0.08 mL, 1 mmol, 1 equiv.), was added and the reaction mixture was stirred at room temperature for about 10 minutes. An additional 0.5 mL anhydrous dichloromethane was added to form a clear reaction mixture, followed by the dropwise addition of DMP **41** (0.3 mL, 2 mmol, 2 equiv.) dissolved in 6 mL anhydrous dichloromethane. The clear reaction mixture was left to stir at room temperature overnight. The crude product was washed with 2 M HCl (5 mL x2) and the organic layer



dried with Na<sub>2</sub>SO<sub>4</sub> and dichloromethane was evaporated in vacuo to afford a yellow oil, **DESMP 37** <sup>1</sup>H NMR (300 MHz, DMSO-d<sub>6</sub>)δ 7.84 (d, 2H, Ar-H), 7.52 (d, 2H, Ar-H), 4.38 (d, 2H, OCH<sub>2</sub>P), 4.01 (m, 4H, OCH<sub>2</sub>CH<sub>3</sub>), 2.43 (d, 3H, CHCH<sub>3</sub>), 1.18 (m, 6H, CHCH<sub>3</sub>).

**Alternate:** Triethylamine (0.14 mL, 1 mmol, 1 equiv.) used in place of pyridine and crude product was washed with water (5 mL x 2) instead of HCl. **DESMP 37** <sup>1</sup>H NMR (300 MHz, DMSO-d<sub>6</sub>)δ 7.84 (d, 2H, Ar-H), 7.52 (d, 2H, Ar-H), 4.38 (d, 2H, OCH<sub>2</sub>P), 4.01 (m, 4H, OCH<sub>2</sub>CH<sub>3</sub>), 2.43 (d, 3H, CHCH<sub>3</sub>), 1.18 (m, 6H, CHCH<sub>3</sub>).

**Synthesis of polymer-supported diethyl (tosyloxy) methylphosphonate (Ps-DESMP, 39).....(Batch)**



Attempt 1

In a round-bottom-flask containing Ps-TsCl **40** (0.28 g, 0.5 mmol) and DMP **41** (0.075 mL, 0.5 mmol, 1 equiv.) in 2.5 mL anhydrous dichloromethane at 0 °C, triethylamine (0.15 mL, 1 mmol, 2 equiv.) in 1 mL anhydrous dichloromethane was added dropwise to the gently stirring reaction mixture. The reaction mixture was taken out of the ice bath and left to increase to room temperature before it was left stirring overnight. The solid emulsion was taken up in 5 mL of dichloromethane and washed with water (5 mL x 2). Dichloromethane was then evaporated in vacuo, leaving behind an orange solid/polymer.

**Alternate:** The equivalents of DMP **41** and triethylamine were altered. DMP **41** (0.15 mL, 1 mmol, 2 equiv.) and triethylamine (0.075 mL, 0.5 mmol, 1 equiv.). The reaction was carried out at room temperature throughout.

Attempt 2

Ps-TsCl **40** (0.29 g, 0.5 mmol) was left in 2 mL anhydrous dichloromethane for about an hour at room temperature. The polymer swelled up and an additional 2 mL anhydrous dichloromethane was added. DMP **41** (0.15 mL, 1 mmol, 2 equiv.) was added to the polymer emulsion and triethylamine (0.075 mL, 0.5 mmol, 1 equiv.) in 1 mL anhydrous dichloromethane followed in a dropwise fashion. The reaction mixture was gently stirred at room temperature, overnight. The solvent was removed in vacuo and 5 mL of dichloromethane was added. The emulsion was washed with water (5 mL x 2). Dichloromethane was then evaporated in vacuo, leaving behind an orange solid/polymer.

Attempt 3

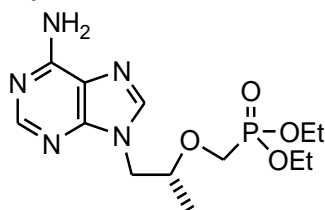
Ps-TsCl **40** (0.29 g, 0.5 mmol) was left in 2 mL anhydrous dichloromethane for about an hour at room temperature. The polymer swelled up and an additional 1 mL anhydrous dichloromethane was added. Triethylamine (0.075 mL, 0.5 mmol, 1 equiv.) in 1 mL anhydrous dichloromethane was added dropwise

to the polymer, and followed by the dropwise addition of DMP **41** (0.15 mL, 1 mmol, 2 equiv.). The reaction mixture was gently stirred at room temperature, overnight. The solvent was removed in vacuo and 5 mL of dichloromethane was added. The emulsion was washed with water (5 mL x 2). Dichloromethane was then evaporated in vacuo, leaving behind an orange solid/polymer.

#### Attempt 4

Ps-TsCl **40** (0.59 g, 1 mmol) was left in 4 mL dichloromethane overnight, at room temperature. The polymer swelled up and an additional 2 mL dichloromethane was added. DMP **41** (0.3 mL, 2 mmol, 2 equiv.) was added to the polymer emulsion and triethylamine (0.15 mL, 1 mmol, 1 equiv.) with DMAP (0.013 g, 0.1 mmol, 0.1 equiv.) in 2 mL dichloromethane followed in a dropwise fashion. The reaction mixture was gently stirred at room temperature, overnight. The solvent was removed in vacuo and 5 mL of dichloromethane was added. The emulsion was washed with water (5 mL x 2). Dichloromethane was then evaporated in vacuo, leaving behind an orange solid/polymer.

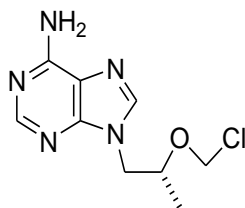
#### **Synthesis of PPA 29 from Ps-DESMP 39 product.....(Batch)**



#### Attempt 1

HPA **28** (0.050 g, 0.26 mmol), *tert*-butanol (0.025 mL, 0.26 mmol, equiv.) and 0.25 mL anhydrous cyclohexane were added to a round-bottom-flask. MeMgBr (3.4 M in methylated THF, 0.1 mL, 0.27 mmol, 1.1 equiv.) was added dropwise and stirred at room temperature for about 15 minutes. The Ps-DESMP **39** "product" obtained from attempt 2 was mixed with 5 mL dichloromethane and the emulsion was added to the reaction mixture. The reaction mixture was heated to 75 °C and left stirring for 2 hours. The solvent was left to evaporate overnight at the same temperature. An orange, "fluffy", solid was obtained and this was washed with water (10 mL x 2). The solid was dried in vacuo and taken up in 10 mL dichloromethane and 5 mL water. This was extracted with 2 M HCl (10 mL x 2) and the pH of the aqueous phase was taken to 10 using 25% ammonium hydroxide. The aqueous phase was extracted with dichloromethane (20 mL x 2) and the organic phase dried with Na<sub>2</sub>SO<sub>4</sub> and dried in vacuo.

**Synthesis of 9-(((R))-2-(chloromethoxy)propyl)-9H-purin-6-amine (chloromethyl HPA 38) ....(Batch)**



**Attempt 1**

**General:** To a round-bottom-flask containing **HPA 28** (0.29 g, 1.5 mmol) dissolved in 8 mL anhydrous dimethylformamide, paraformaldehyde (0.057, 1.8 mmol, 1 equiv.) was added. To this, TMSCl (1 mL, 8 mmol, 5 equiv.) was added dropwise and the reaction mixture was left to stir at room temperature for 2 hours. An additional overnight (another trial lasted up to 48 hours) stir resulted when the starting material was still present on TLC. The reaction mixture was also heated to 60 °C. DMF was evaporated off and the residue was washed with ethanol and dried in vacuo.

**Alternate 1:** Instead of a round-bottom-flask, an ACE® pressure vessel was used.

**Alternate 2:** dichloromethane used in the place of DMF as possible source of Cl<sup>-</sup>

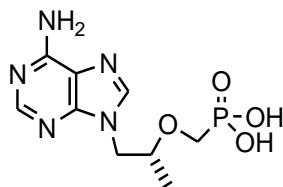
**Alternate 3:** 1,1,2,2-tetrachloroethane used in the place of DMF as possible source of Cl<sup>-</sup>

**Attempt 2**

The setup presented in *figure 2.3.1* in chapter 4 was employed. To a round-bottom-flask containing **HPA, 28** (0.59 g, 3 mmol) and paraformaldehyde (0.072 g, 3.6 mmol, 1 equiv.) in 25 mL dimethylformamide, HCl gas produced from H<sub>2</sub>SO<sub>4</sub> (98%, 2 mL, 36 mmol) and NaCl (2.1 g, 36 mmol), was bubbled into the solution for 10 minutes as the reaction mixture was stirring at room temperature. The reaction mixture was then left to stir for 3 hours, heated briefly at 60 °C in attempt to dissolve paraformaldehyde, and then left overnight at room temperature. DMF was evaporated off and the residue was washed with ethanol and dried in vacuo.

**Experimental chapter 4: Step 2b**

**Synthesis of ((R))-(((Adenin-9-yl)propan-2-oxy)methyl) phosphonic Acid, (PMPA 9) .....(Batch)**



To an ACE® pressure tube, **PPA 29** (0.20 g, 0.58 mmol) and TMSBr (0.38 mL, 2.9 mmol, 5 equiv.) were added and stirred together overnight at 120 °C. A yellow precipitate formed and was taken up in 10 mL water and extracted with 10 mL x 2 ethyl acetate. The aqueous phase was collected and placed in an ice bath, followed by a dropwise addition of a 10% NaOH solution until a pH 3 was reached. The

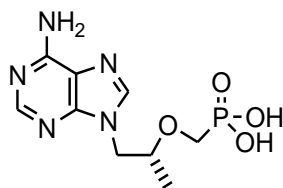
clear solution turned murky and was left to stir vigorously in the ice bath until the product crushed out. The precipitate liquor was gravity filtered and solid was dried to form a white solid, **PMPA 9** (0.097 g, 58% yield) <sup>1</sup>H NMR (300 MHz, CDCl<sub>3</sub>-d) δ 8.16 (s, 1H, Ar-H), 8.15 (s, 1H, Ar-H), 7.31 (s broad, 2H, NH<sub>2</sub>), 4.20-3.60 (m, 5H, NCH<sub>2</sub>CH, NCH<sub>2</sub>CH, OCH<sub>2</sub>P), 1.03 (d, 3H, CHCH<sub>3</sub>). <sup>13</sup>C NMR (75 MHz, DMSO-d<sub>6</sub>) δ 155.78 (C2) 152.29 (C8) 150.11 (C6) 142.85 (C4) 118.56 (C5) 75.73 (NCH<sub>2</sub>) 17.44 <sup>31</sup>P NMR (121 MHz, DMSO-d<sub>6</sub>) δ 16.57.

**Alternate 1:** Anhydrous acetonitrile (0.6 mL) was added to the reaction mixture and removed once the reaction was complete. The remainder of the work up was identical to the general procedure. A white solid was the product, **PMPA 9** (0.075 g, 45% yield)

**Alternate 2:** TMSCl (0.31 mL, 2.5 mmol, 5 equiv.) was used in the place of TMSBr for both general and alternate 1. No product formed.

**Alternate 3:** TMSCl (0.31 mL, 2.5 mmol, 5 equiv.), NaBr (0.26 g, 2.5 mmol 5 equiv.) and 0.6 mL DMF (or acetonitrile) replaced TMSBr in the general method. The same procedure was followed as in the general method. **PMPA 9** was isolated as a white solid (0.017 g- 0.11 g, 10%-68%)

**Synthesis of ((R))-(((Adenin-9-yl)propan-2-oxy)methyl) phosphonic Acid (PMPA 9) .....(Flow)**



Using a flow reactor, stream A, containing **PPA 29** (0.30 g, 0.87 mmol) in 6 mL anhydrous acetonitrile and stream B, TMSBr (0.6 mL, 4.5 mmol, 5 equiv.) in 6 mL anhydrous acetonitrile, were pumped into the reactor via pump A and B respectively, through the loops into a glass mixing chip heated at 120 °C at a rate of 0.1 mL/min. The combined stream moved into a 2 mL PEEK coil, heated to 120 °C and the eventually the reaction mixture bypassed the BPR and was collected in a flask containing 2 mL water. The aqueous liquor was extracted with 2 mL x 2 ethyl acetate and the aqueous phase was collected and placed in an ice bath, followed by a dropwise addition of a 10% NaOH solution until a pH 3 was reached. The clear solution turned murky and was left to stir vigorously in the ice bath until the product crushed out. The precipitate liquor was gravity filtered and solid was dried to form a white solid, **PMPA 9**. <sup>1</sup>H NMR (300 MHz, DMSO-d<sub>6</sub>)δ 8.16 (s, 1H, Ar-H), 8.15 (s, 1H, Ar-H), 7.31 (s broad, 2H, NH<sub>2</sub>), 4.20-3.60 (m, 5H, NCH<sub>2</sub>CH, NCH<sub>2</sub>CH, OCH<sub>2</sub>P), 1.03 (d, 3H, CHCH<sub>3</sub>). <sup>13</sup>C NMR (75 MHz, DMSO-d<sub>6</sub>) δ 155.78 (C2) 152.29 (C8) 150.11 (C6) 142.85 (C4) 118.56 (C5) 75.73 (NCH<sub>2</sub>) 17.44 <sup>31</sup>P NMR (121 MHz, DMSO-d<sub>6</sub>) δ 16.57.

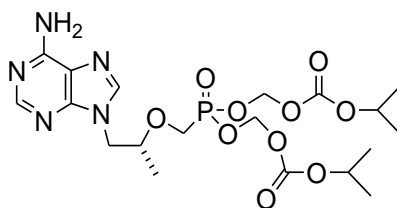
**Alternate 1:** TMSCl used in the place of TMSBr. No product formed

**Alternate 2:** TMSCl used in the place of TMSBr. Stream A and B were combined to form one stock solution: **PPA 29** and TMSCl in 7 mL anhydrous acetonitrile. No product formed

**Alternate 3:** TMSCl used in the place of TMSBr. Stream A and B were combined to form one stock solution: **PPA 29** and TMSCl in 7 mL anhydrous acetonitrile. Additionally, a glass column containing NaBr (5.5 mL fully packed) was added in place of the glass mixing chip. No product formed

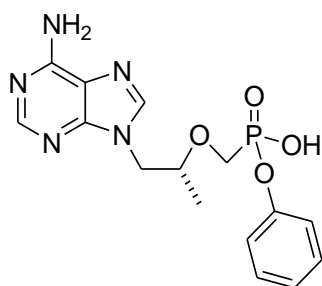
**Experimental for chapter 5: Final steps**

**Synthesis of Tenofovir diisoproxil (TD 25) .....(Batch)**



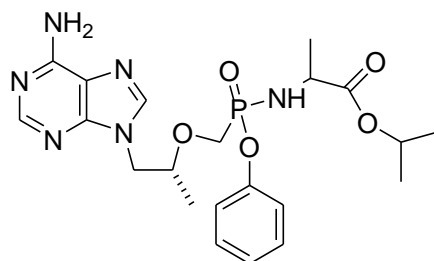
**PMPA 9** (0.50 g, 1.8 mmol) in was dried in vacuo for about 2 days. 2 mL anhydrous NMP and 1.5 mL anhydrous cyclohexane were added and cyclohexane was removed using rotary evaporation. Another 1.5 mL anhydrous cyclohexane was added and the process was repeated. Triethylamine (1 mL, 7.2 mmol, 4 equiv.) and CMIC (replacement for TBAB) (1.2 mL, 9 mmol, 5 equiv.) were added to the solution and the reaction mixture was left to stir at 65 °C for 6 hours. The sticky brown solid reaction mixture was allowed to cool to room temperature and washed in cyclohexane (2 mL x 2). The cyclohexane was removed via rotary evaporation. To the resultant orange emulsion, ethyl acetate (5 mL x 2) and water (2.5 mL x 2) were added and the mixture was left to stir vigorously for 15 minutes. The two solvent phases were separated and the ethyl acetate phase was collected. The organic layer was washed further with water (5 °C, 3 mL x 3) and 10% NaCl solution (3 mL x 1) and dried with Na<sub>2</sub>SO<sub>4</sub>, gravity filtered and concentrated in vacuo to afford a yellow oil which when cooled to 5 °C formed a sticky, yellow solid, **TD 25** (0.24 g, 26% yield)<sup>1</sup>H NMR (300 MHz, DMSO-d<sub>6</sub>) δ 8.26 (s, 1H, Ar-H), 7.84 (s, 1H, Ar-H), 7.20 (s broad, 2H, NH<sub>2</sub>), 6.84 (s broad, OCH<sub>2</sub>O), 4.30-3.53 (m, NCH<sub>2</sub>CH, NCH<sub>2</sub>CH, OCH<sub>2</sub>P, OCHCH<sub>3</sub>), 0.97 (d, OCHCH<sub>3</sub>), 0.92 (d, CHCH<sub>3</sub>).

**Synthesis of phenyl hydrogen (((R))-1-(6-amino-9H-purin-9-yl)propan-2-yloxy)methylphosphonate (phenol-PMPA 46) .....(Batch)**



To a round-bottom flask containing **PMPA 9** (0.088 g, 0.3 mmol ) phenol (0.058 g, 0.6mmol, 2 equiv.) and anhydrous NMP (2 mL) were added and the reaction mixture was heated to about 85°C. Triethylamine (0.054 mL, 3.8 mmol, 1.3 equiv.) was added which resulted in a completely dissolved reaction mixture. To this, CDI (0.083 g, 0.5 mmol, 1.6 equiv.) dissolved in NMP (0.8 mL) was added dropwise over a period of 15 minutes to the reaction mixture and this was allowed to continue stirring overnight. A thick brown solution was observed which was taken to pH 13 using 50% NaOH solution and extracted with ethyl acetate (7 mL x 3). The aqueous layer was then taken to pH 3 using 32% HCl to obtain a precipitated white powder. The white powder was washed with methanol and dried in vacuo and **phenol-PMPA 46** <sup>1</sup>H NMR (300 MHz, DMSO-d<sub>6</sub>) δ 8.17 (s, 1H, Ar-H), 8.16 (s, 1H, Ar-H), 7.44 (s broad, 5H, Ar-H), 7.42 (s broad, 2H, NH<sub>2</sub>), 4.31-3.60 (m, 5H, NCH<sub>2</sub>CH, NCH<sub>2</sub>CH, OCH<sub>2</sub>P), 1.02 (d, 3H, CHCH<sub>3</sub>).

**Synthesis of Tenofovir Alafenamide (TA 26).....(Batch)**



L-isopropyl alanine HCl (0.19 g,) dissolved in 0.7 mL anhydrous THF was added to a round-bottom-flask containing DABU (0.095 g) dissolved in 0.3 mL anhydrous THF. A white solid precipitated out and this was gravity filtered and washed with anhydrous THF. The liquor was taken up and solvent removed in vacuo to afford a clear oil, L- isopropyl alanine (0.075g,% yield)

0.42 mL anhydrous acetonitrile and SOCl<sub>2</sub> (0.1 mL, 1.4 mmol) were added to a round-bottom-flask containing **phenol- PMPA 46** dried in vacuo overnight. The reaction mixture was heated to 80 °C and left to stir for about 2 hours. The sticky brown residue was taken up in 5 mL anhydrous dichloromethane and placed in a xylene- dry ice bath to achieve a temperature of about – 20 °C. L- isopropyl-alanine, prepared as described previously, dissolved in 0.5 mL anhydrous dichloromethane was added to the reaction mixture which was left to stir for about an hour. 0.1 mL triethylamine was

slowly added under the same conditions and the reaction mixture was then allowed to gradually warm up to room temperature. The reaction mixture was washed with 10%  $\text{NaH}_2\text{PO}_4$  (2 mL x 2) and the organic layer was collected, and dried in vacuo to produce an orange oil, (0.035 g yield).

# APPENDIX A: A summarized collection of the project's NMR spectra.

## Experimental chapter 3: Synthesis of HPA

001BK001\_Analysis-DMSO

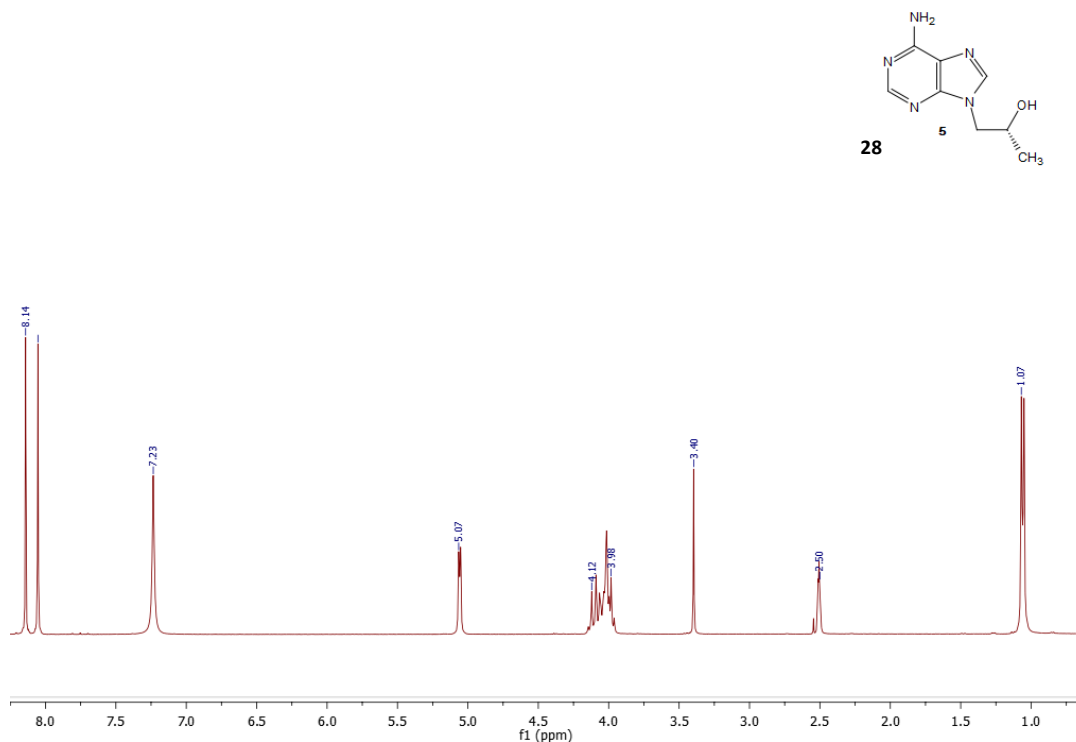


Figure A1: <sup>1</sup>H NMR spectrum of pure N-9 HPA in DMSO-d<sub>6</sub>.

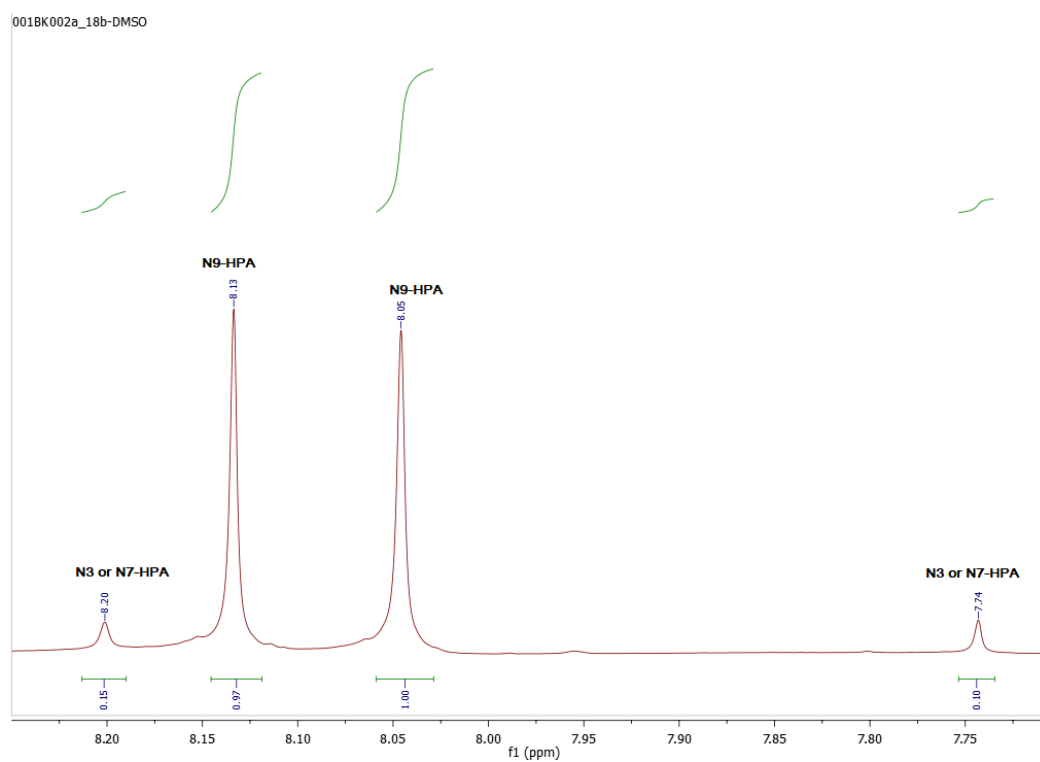


Figure A2: <sup>1</sup>H NMR spectrum (aromatic region) of HPA, including allocation of regioisomers. (DMF- reaction solvent and EtOH trituration work-up) in DMSO-d<sub>6</sub>.



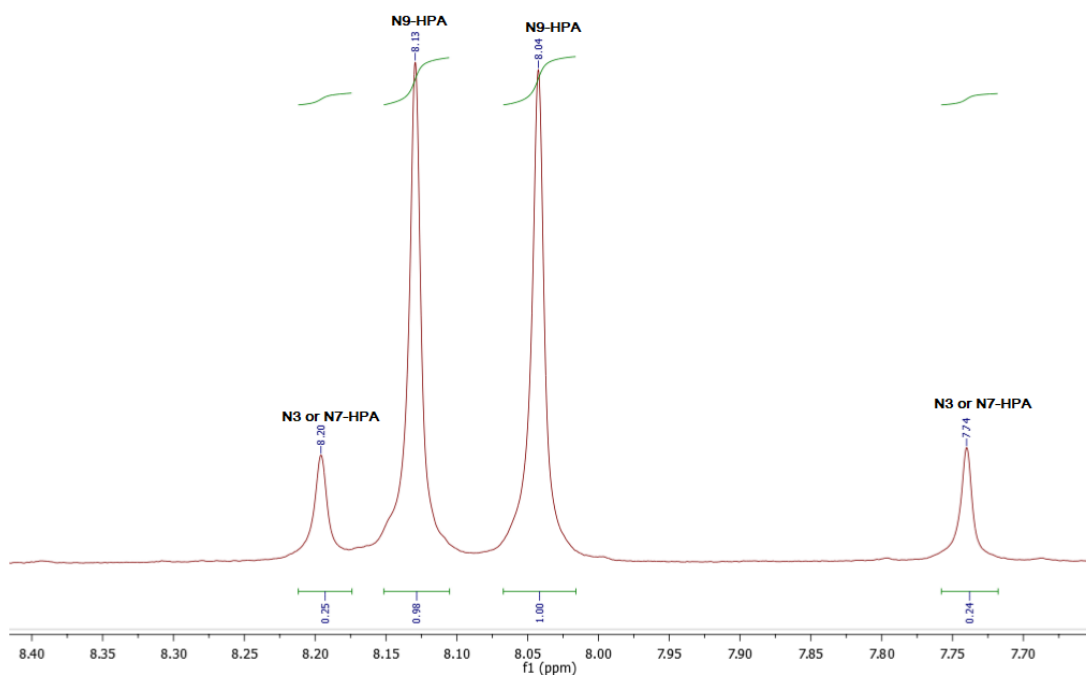


Figure A3:  $^1\text{H}$  NMR spectrum (aromatic region) of HPA, including allocation of regioisomers. (reaction solvent -DMSO- and trituration work-up -toluene) in  $\text{DMSO-d}_6$ .

#### Experimental chapter 4: Synthesis of PPA

001BK003f-CDCl3

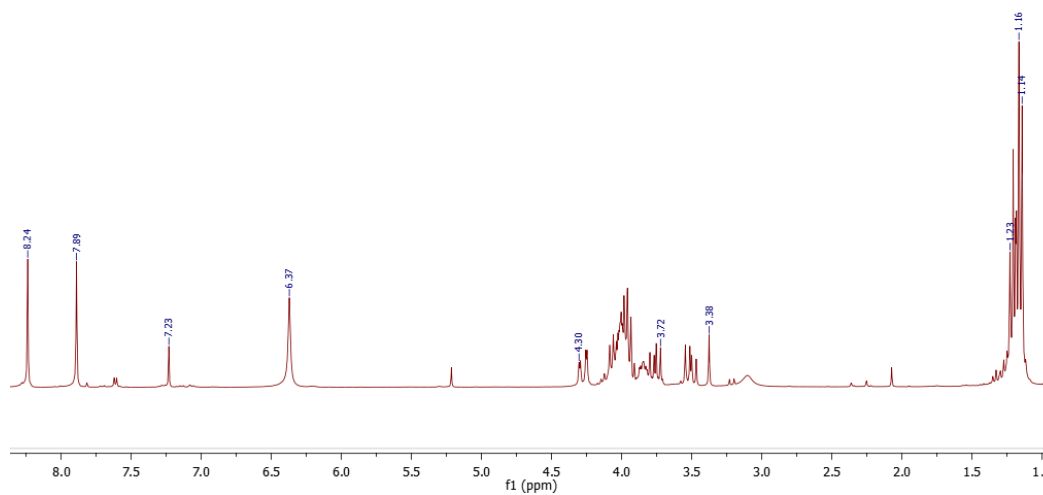
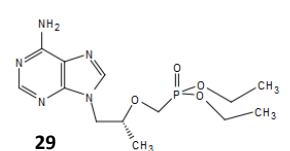


Figure A4:  $^1\text{H}$  NMR spectrum of PPA in  $\text{DMSO-d}_6$ .

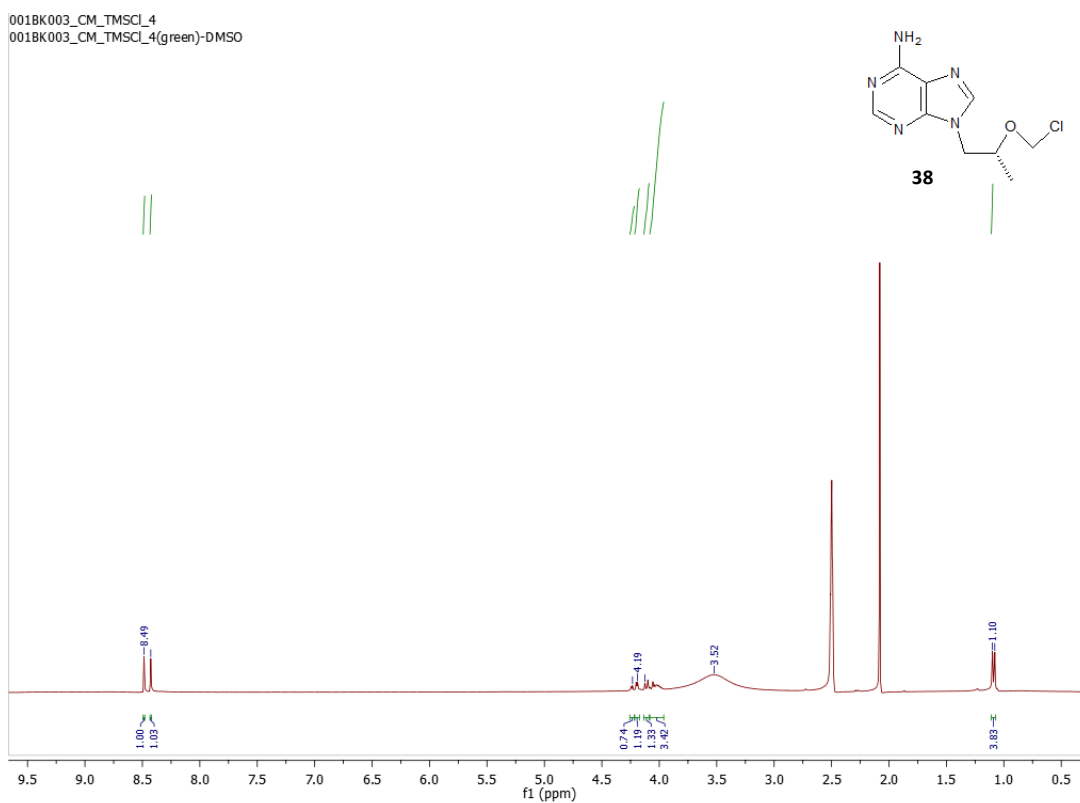


Figure A5:  $^1\text{H}$  NMR spectrum of attempt 1 product of chloromethyl HPA in  $\text{DMSO-d}_6$ .

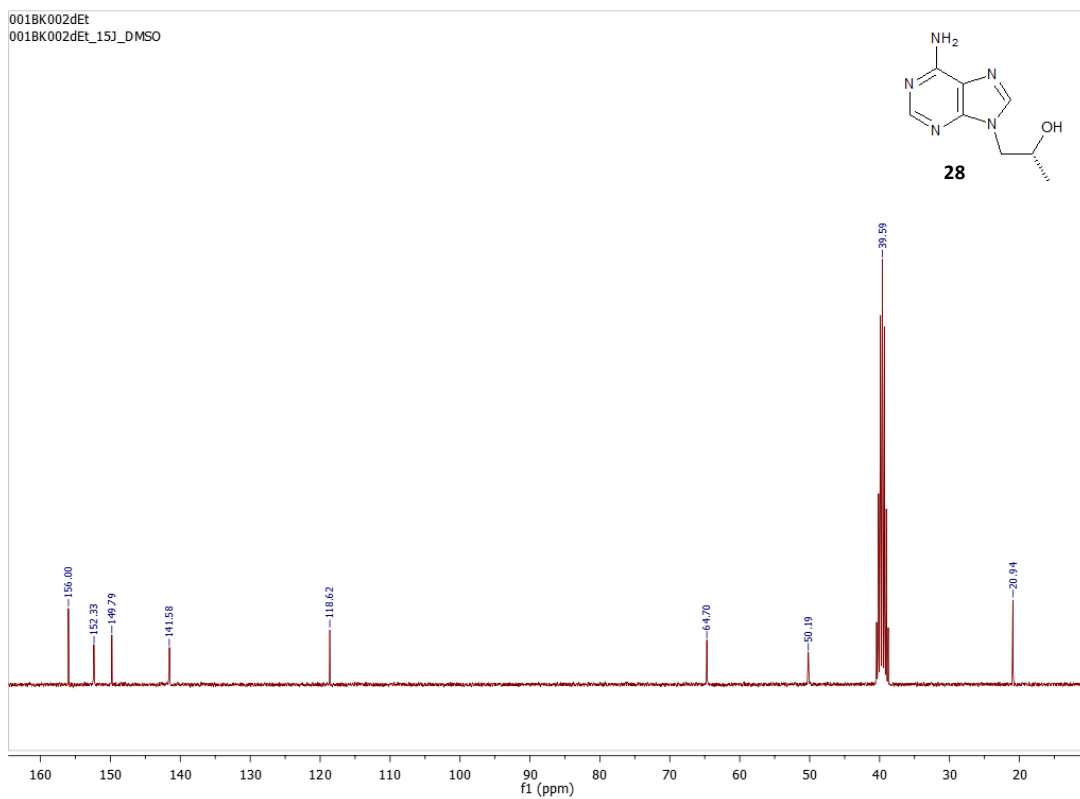


Figure A6:  $^{13}\text{C}$  NMR spectrum of HPA in  $\text{DMSO-d}_6$ .

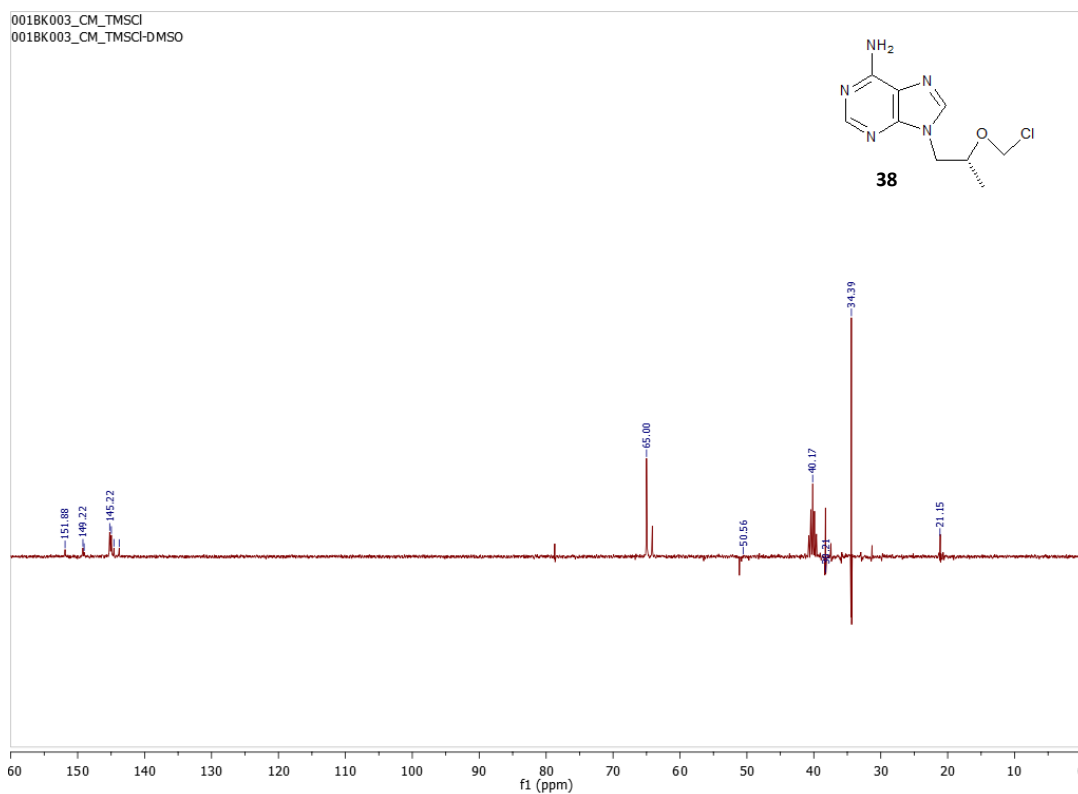


Figure A7:  $^{13}\text{C}$  DEPT 135 NMR spectrum of attempt 1 product of chloromethyl HPA in  $\text{DMSO-d}_6$ .

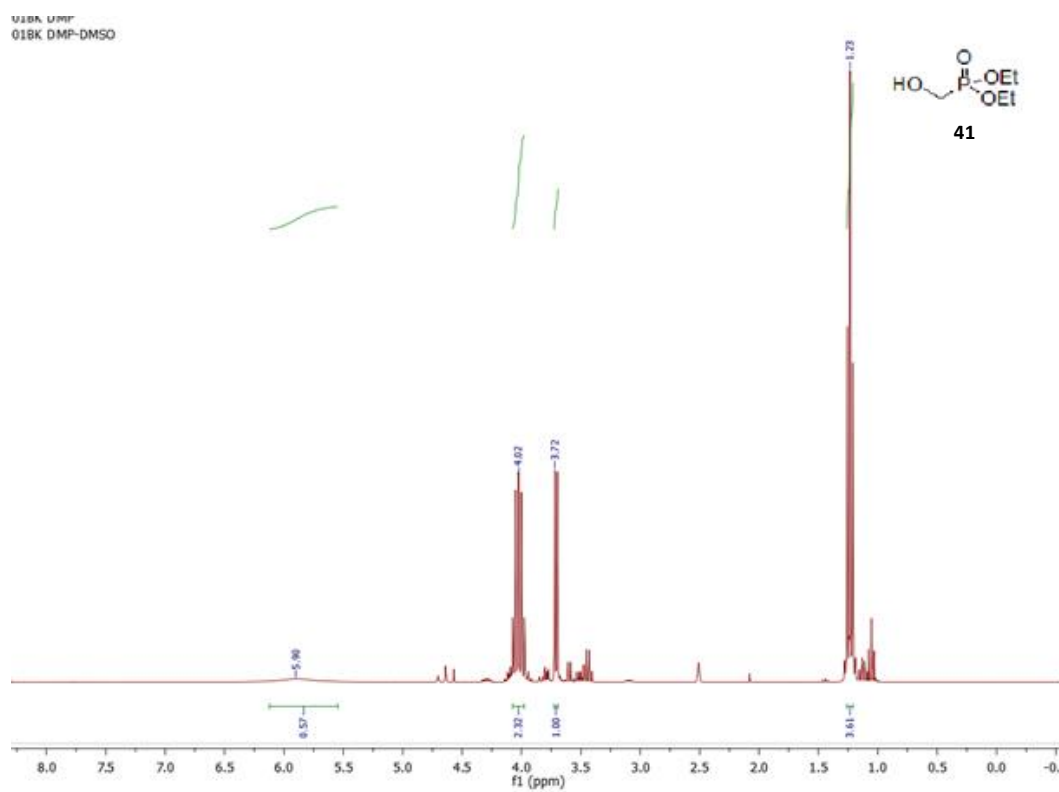


Figure A8:  $^1\text{H}$  NMR spectrum of DMP in  $\text{DMSO-d}_6$ .

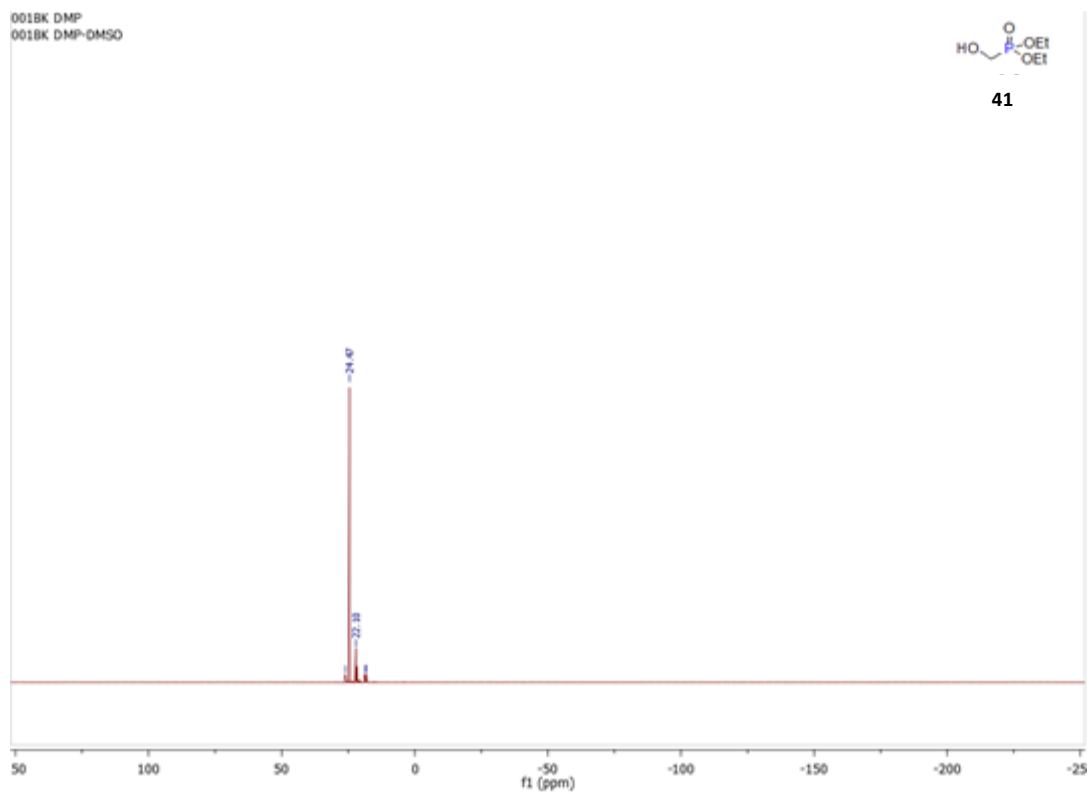


Figure A9:  $^{31}\text{P}$  NMR spectrum of DMP in  $\text{DMSO-d}_6$ .

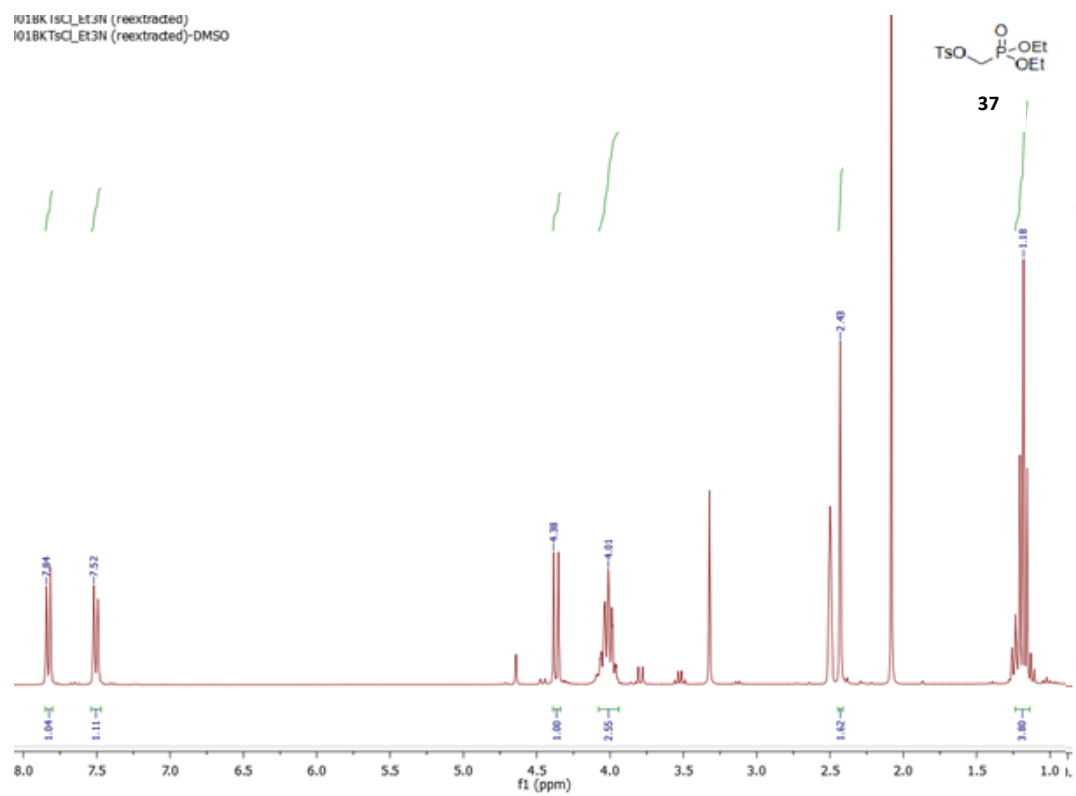


Figure A10:  $^1\text{H}$  NMR spectra of DESMP synthesized using  $\text{Et}_3\text{N}$ , in  $\text{DMSO-d}_6$ .

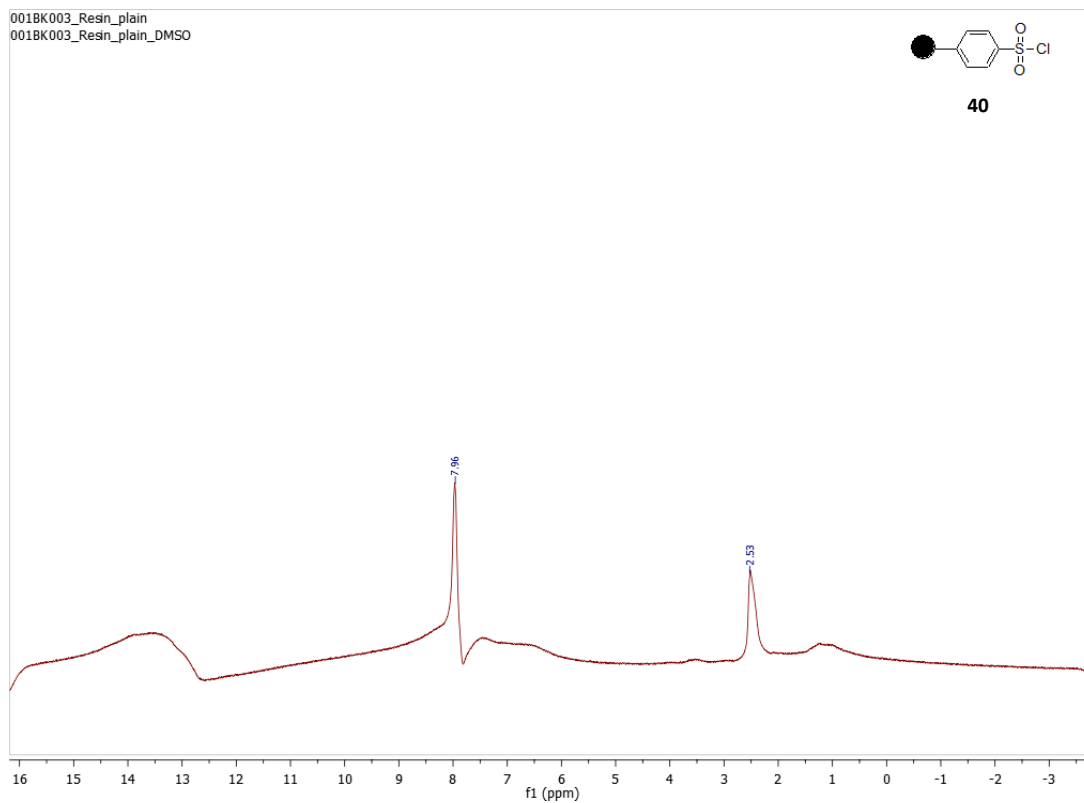


Figure A11:  $^1\text{H}$  NMR spectrum of Ps-TsCl in  $\text{DMSO-d}_6$ .

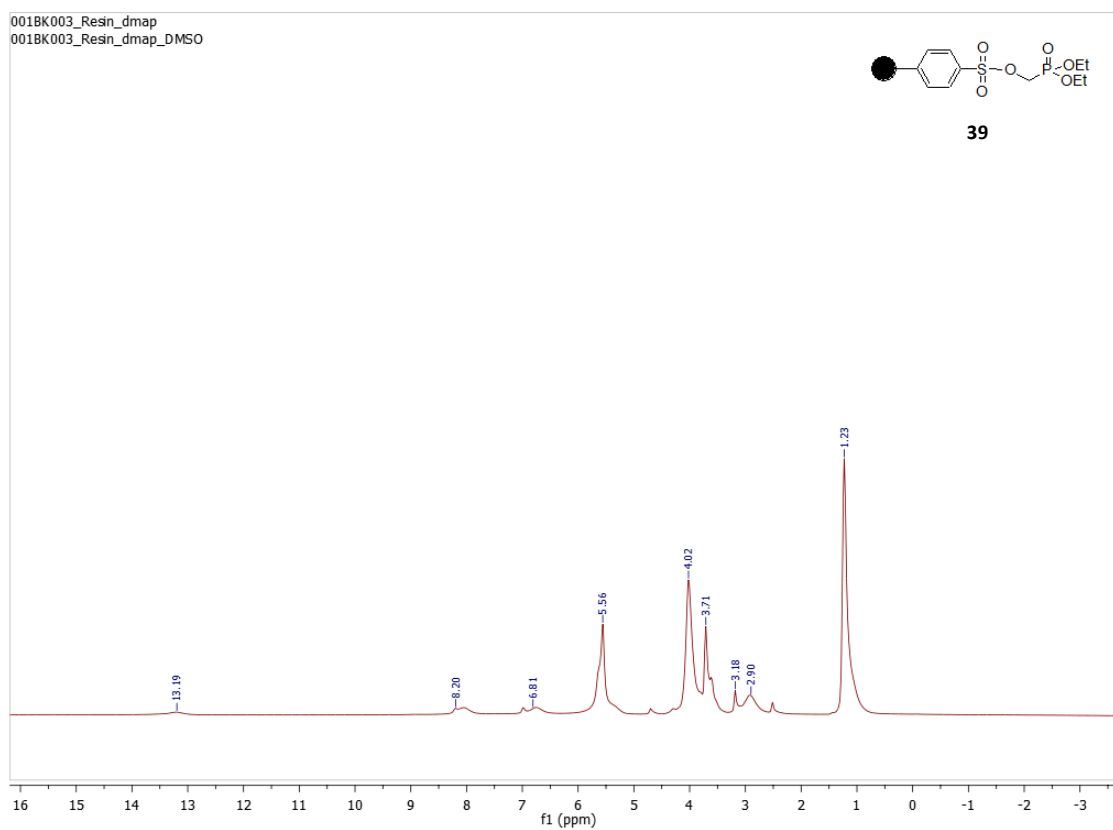


Figure A12:  $^1\text{H}$  NMR spectrum of attempt 4 polymer of Ps-DESMP in  $\text{DMSO-d}_6$ .

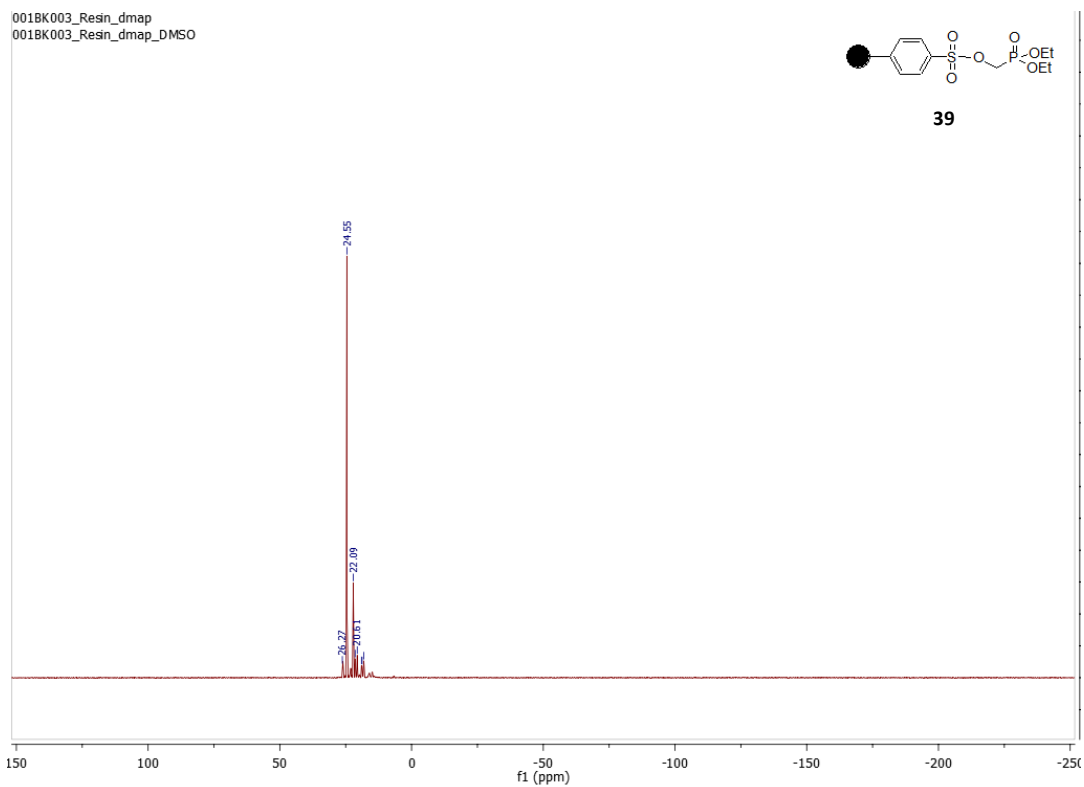


Figure A13:  $^{31}\text{P}$  NMR spectra of attempt 4 polymer of Ps-DESMP in  $\text{DMSO-d}_6$ .

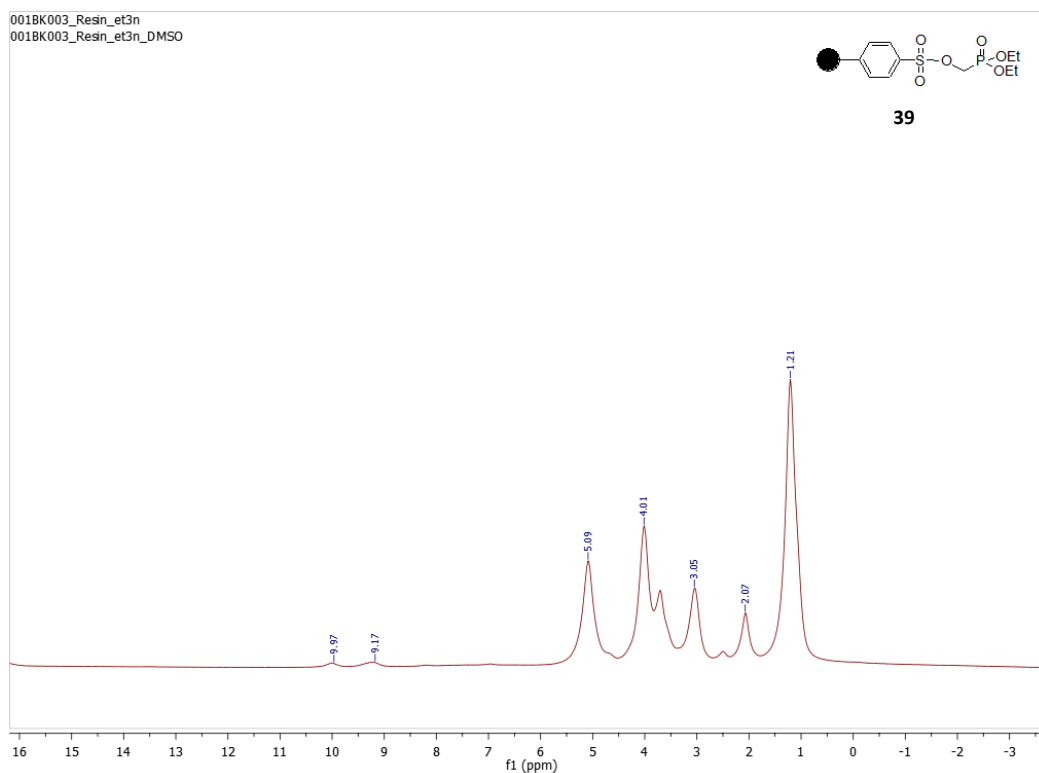


Figure A14:  $^1\text{H}$  NMR spectra of attempt 3 polymer of Ps-DESMP in  $\text{DMSO-d}_6$ .

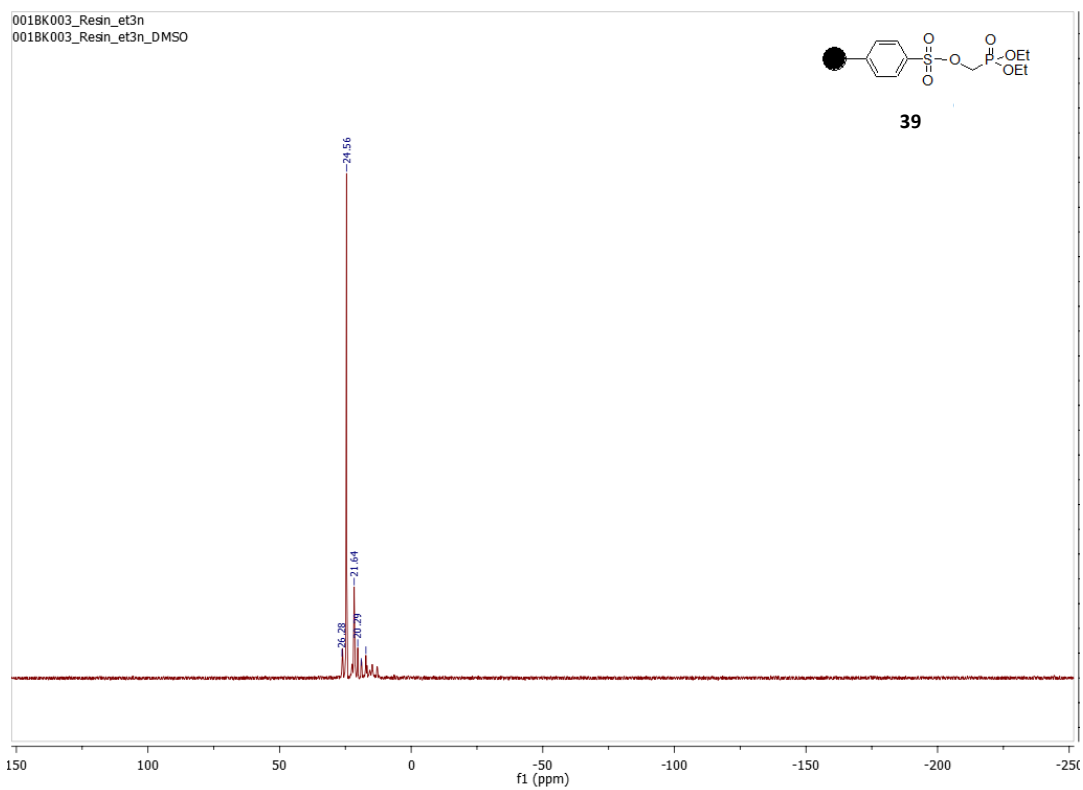


Figure A15:  $^{31}\text{P}$  NMR spectra of attempt 3 polymer of Ps-DESMP in  $\text{DMSO-d}_6$ .

#### Experimental chapter 4: Synthesis of tenofovir, PMPA.

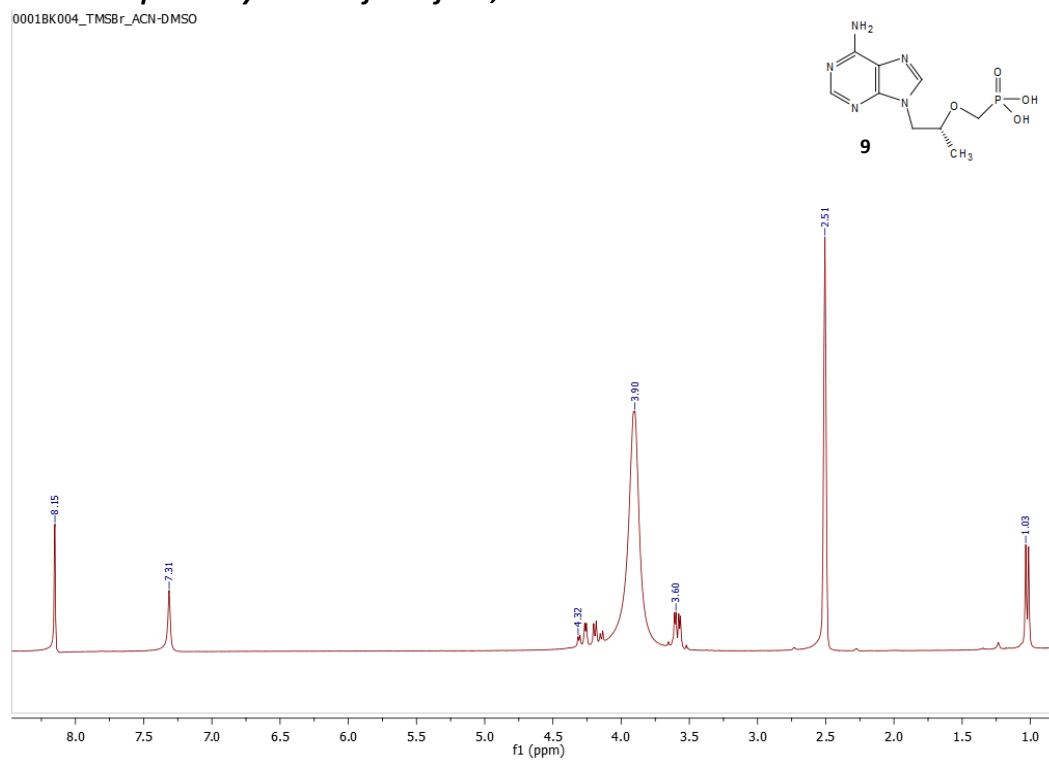


Figure A16:  $^1\text{H}$  NMR spectrum of tenofovir, PMPA in  $\text{DMSO-d}_6$ .

## Experimental chapter 5: Synthesis of TD 25

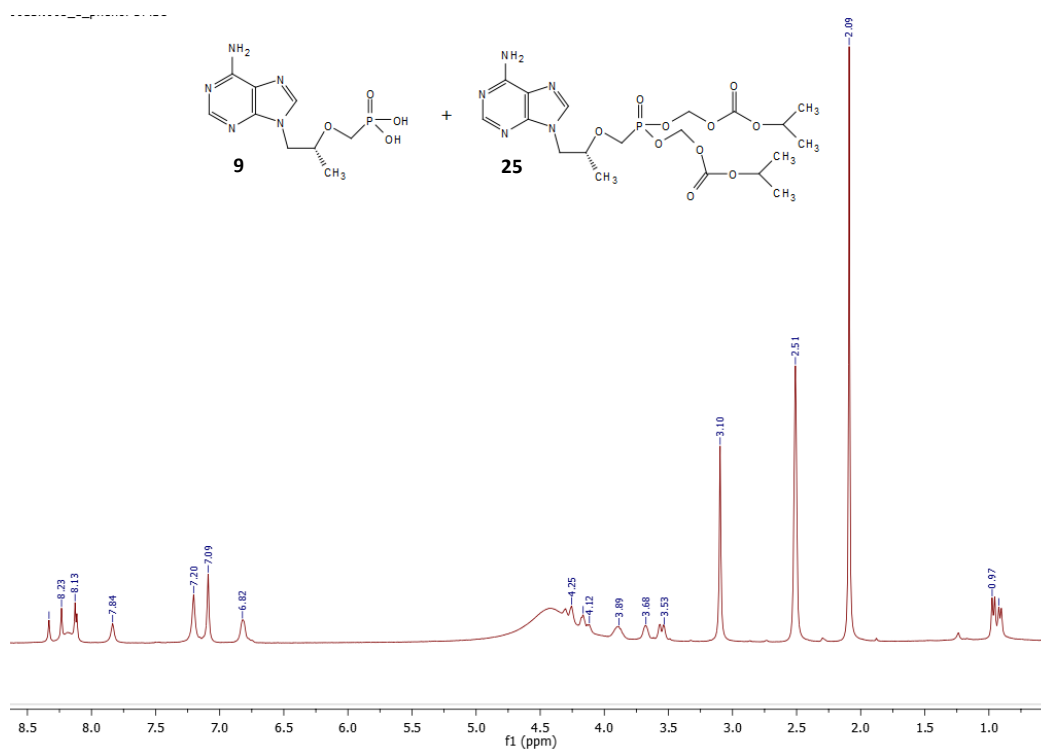


Figure A17:  $^1\text{H}$  NMR spectrum of TD in  $\text{DMSO-d}_6$ .

## Experimental chapter 5: Synthesis of phenol-PMPA 46

11BK\_TAF\_phenol\_PMPA (cream)\_DMSO

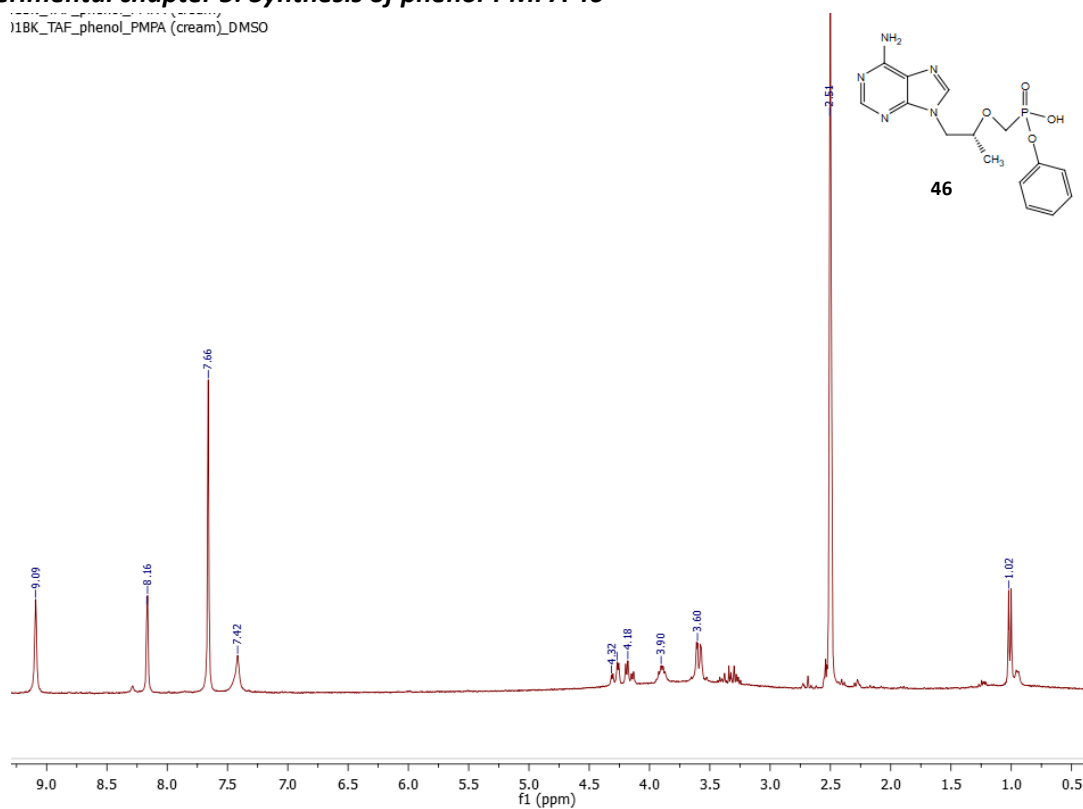


Figure A18:  $^1\text{H}$  NMR spectrum of phenol-PMPA in  $\text{DMSO-d}_6$ .



## Experimental chapter 5: Synthesis of TA 26

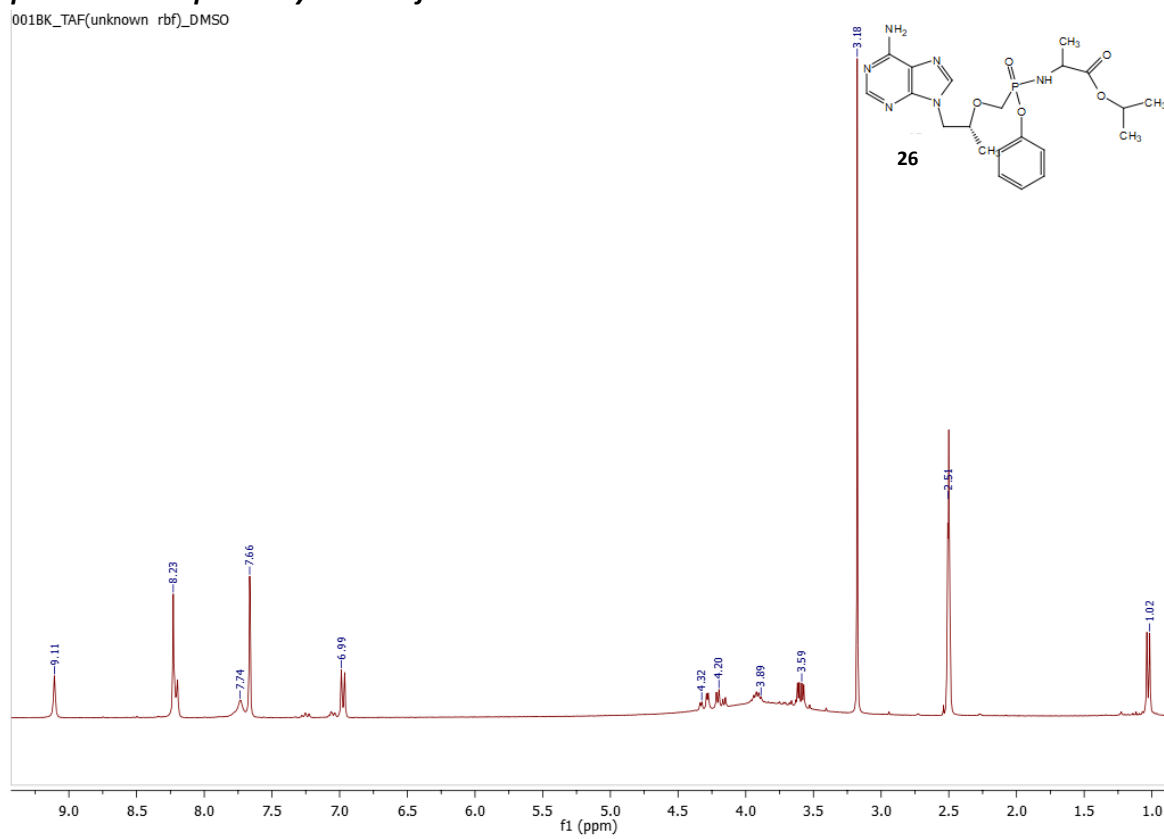


Figure A.19:  $^1\text{H}$  NMR spectrum of TA attempt product in  $\text{DMSO-d}_6$ .